BUDAPEST UNIVERSITY OF TECHNOLOGY AND ECONOMICS
DEPARTMENT OF ORGANIC CHEMISTRY AND TECHNOLOGY
GEORGE A. OLAH DOCTORAL SCHOOL

Development of integrated continuous pharmaceutical technologies

Integrált folyamatos gyógyszertechnológiák fejlesztése

Ph.D. Thesis

Author: András Domokos

Supervisor:	Co-supervisor:
Dr. Zsombor K. Nagy	Dr. Zsolt Rapi
associate professor	senior lecturer

2020

Table of contents

Acknowledgements

First of all, I would like to express my deepest gratitude to my supervisor, Dr. Zsombor Kristóf Nagy and my co-supervisor, Dr. Zsolt Rapi for the constant assistance in my work and for the useful advices they shared with me. Furthermore, I am thoroughly grateful to Dr. Attila Balogh for the guidance during the first period of my work, which helped me to always strive for the highest standards. I also would like to thank prof. György Marosi for always keeping his door open for suggestions and memorable conversations.

I am extremely thankful to prof. Zoltán K. Nagy for supervising and arranging my internship at Purdue University. Moreover, I am grateful to Dr. Botond Szilágyi, Emőke Szilágyi, Iben Østergaard, Dr. Yiqing Claire Liu and the entire CryPTSys Research Group for the assistance and welcoming environment during my stay in the U.S. Additionally, I would like to thank Paul Firth and Simon Coleman from Alconbury Weston Ltd. for the technical support during this period.

I also have to thank the following people who helped me during my work: Brigitta Nagy, Éva Kiserdei, Tamás Igricz, László Simon, Balázs Farkas, Dr. Attila Farkas, Martin Gyürkés, Edina Szabó, Bence Szabó, Dr. Balázs Démuth, Dorián Galata, dr. Gergő Fülöp, Dr. István Csontos, Kornélia Tacsi, Dr. Hajnalka Pataki, Enikő Borbás, Dániel Vadas, Lajos Madarász, Gyula Nyerges, Zoltán Nyiri, Máté Mihalovits, Dr. Róbert Örkényi, Dr. Béla Mátravölgyi, Dr. Tibor Casian, Kata Fügedi, Levente Ződi and Dániel Dénes. Furthermore, I am grateful to all the members of the Firepharma Research Group, to my professors and colleagues at the Department of Organic Chemistry and Technology.

Here I would like to grab the opportunity to record my thanks to Tempus Közalapítvány and the National Research, Development and Innovation Fund of Hungary for their generous financial support.

Last but not least, I highly appreciate the permanent support and motivation that I have been receiving from my family and my wife.

Abbreviations

16-DPA – 16-dehydropregnenolone acetate
ACN – acetonitrile
AcOH – acetic acid
ACS – American Chemical Society
ASA – acetylsalicylic acid
Ac_2O – acetic anhydride
API – active pharmaceutical ingredient
ASD – amorphous solid dispersion
ATR – attenuated total reflectance
AV – acceptance value
BPR – back pressure regulator
CAR – carvedilol
CD – cyclodextrin
CD_3OD – deuterated methanol
CFC – continuous filtration carousel
CFD – continuous filter dryer
cGMP – current good manufacturing practice
CIP – clean-in-place
CM – continuous manufacturing
CMA – critical material attribute
CMS – continuous model system
CPP – critical process parameter
CQA – critical quality attribute
CU – content uniformity
DMF – *N,N*-dimethylformamide
DMSO – dimethyl sulfoxide
D43 - De Brouckere mean moment diameter
DoE – design of experiments
DSC – differential scanning calorimetry
EMA – European Medicines Agency
ES – electrospinning
ESI – electrospray ionization
EtOAc – ethyl acetate
EtOH – ethanol
FDA – Food and Drug Administration
FTIR – Fourier-transform infrared spectroscopy
GA – genetic algorithm
GC – gas chromatography
GCI – Green Chemistry Institute
H_2SO_4 – sulfuric acid
H_3PO_4 – phosphoric acid

HCl – hydrochloric acid

HCOOH – formic acid

HPβCD – (2-hydroxypropyl)-β-cyclodextrin

HPLC – high performance liquid chromatography

HPMC – (hydroxypropyl)methyl cellulose

HVDC – high-voltage direct current

ICH – International Council for Harmonization

ID – internal diameter

IUPAC – International Union of Pure and Applied Chemistry

LV – latent variable

MCC – microcrystalline cellulose

MeOH – methanol

MIT – Massachusetts Institute of Technology

MS – mass spectrometry

MSMPR – mixed suspension mixed product removal

NIR – near infrared

NMR – nuclear magnetic resonance

OD – outer diameter

ODW – orally dissolving web

PACT – process analytical controlled technology

PAT – process analytical technology

PFR – plug flow reactor

PhAT – pharmaceutical area testing

PLS – partial least squares

PSD – particle size distribution

PTFE - polytetrafluoroethylene

PVPK30 – polyvinylpyrrolidone K30

QbD – quality by design

QbT – quality by testing

RMSEC – root mean squared error of calibration

RMSECV – root mean squared of cross-validation

RP-HPLC – reversed phase HPLC

RSD – relative standard deviation

SA – salicylic acid

SEM – scanning electron microscopy

UV – ultraviolet

XRPD – X-ray powder diffraction

Thesis findings

1. Acetylsalicylic acid (ASA) was synthesized in continuous flow reactors for the first time. Design of experiment studies were conducted in order to optimize the two synthetic steps: *i.e.* the acetylation of salicylic acid (SA) and the quenching of impurities. By applying the allocated optimal conditions high yield and purity was achieved (>95% ASA and <3% SA). The second, quenching step was optimized both with and without a dissolved polymer excipient, thus the final reaction mixture was ready for direct further processing using either electrospinning or continuous crystallization. [I, XIV, XVI, XVII, XIX]

2. Electrospinning (ES) was applied as an advanced solvent removal tool for the direct processing of a flow reaction mixture for the first time. By applying high voltage on the metal ES spinneret connected to the flow chemistry microreactors, the volatile components evaporated, and the API was embedded into amorphous nanofibers. This way the direct work-up of the reaction mixture was accomplished, and no solid-liquid separation was required before formulation. With appropriate air ventilation the amount of residual solvents could be reduced below the regulatory limits. [I, XIV, XVI, XVII, XIX]

3. We developed and applied an apparatus for the controlled collection of the electrospun product and for the continuous end-to-end production of an orally dissolving web (ODW) formulation. The acetylsalicylic acid-loaded fibers – produced directly from the flow reaction mixture – were collected on the surface of a water-soluble carrier film. The formed double-layered strip was conveyed further to a cutter mechanism and was cut into smaller dosage units ready for patient administration. The good content uniformity and low residual moisture content of the ODWs was confirmed during longer, 8-hour long operations of the system. [I, XIV, XVI, XVII, XIX]

4. The applicability of the developed continuous system was extended to the production of an ODW formulation containing a poorly water-soluble compound, carvedilol (CAR). ES of CAR-loaded nanofibers was optimized to obtain a stable process. The fibers were collected on the surface of a modified pullulan carrier: citric acid was incorporated into the film to act as pH modifier during dissolution tests. The immediate dissolution and disintegration of the created ODW formulation was confirmed under conditions modelling the oral cavity. The 4-hour long continuous production of CAR-loaded ODWs showed appropriate content

uniformity and the residual solvent content of the fibers complied to the regulatory requirements when secondary drying was applied on room temperature. [II]

5. A "Mixed Suspension Mixed Product Removal" (MSMPR) continuous crystallization equipment was directly connected to a Continuous Filtration Carousel (CFC) device for the first time. Stable continuous operation was achieved within the integrated system after the two combined steps were optimized together, and free-flowing crystalline product with excellent quality was obtained at the end of the process. [III, IV, XV]

6. The effect of critical crystallization process parameters on the filtered product quality was determined for the first time in an integrated continuous crystallization-filtration system. We found that only the temperature affected the yield and the particle size of the filtered product, while both residence time and temperature had an impact on the moisture content. The size of the acetylsalicylic acid crystals did not affect the filtration procedure of the used continuous filtration carousel device. The crystals could be dried appropriately to obtain a crystal powder with good flowability, applicable in the following continuous downstream processes. [III, IV, XV]

7. A continuously filtered pharmaceutical material was further processed to continuous blending with microcrystalline cellulose, and to the production of conventional compressed tablets for the first time. The blending efficiency was monitored by an in-line NIR probe. The produced tablets showed very low variation in content uniformity based on at-line NIR and off-line HPLC measurements. Thus, the end-to-end manufacturing of the most widespread compressed tablet dosage form was accomplished for the first time on a proof-of concept level. [IV, XV]

Új tudományos eredmények

1. Elsőként valósítottuk meg az acetilszalicilsav szintézisét folyamatos áramlásos reaktorokban. A szalicilsav acetilezését és a keletkezett szennyezők elbontását kísérlettervezéssel optimalizáltuk. A meghatározott optimális paramétereket alkalmazva nagy hozammal és tisztasággal kaptuk a terméket (>95% acetilszalicilsav, <3% szalicilsav). A második, megbontási lépést polimer segédanyag jelenlétében és anélkül is optimalizáltuk, így a végső reakcióelegy alkalmas volt különböző feldolgozási lépésekhez történő közvetlen kapcsolásra, úgymint elektrosztatikus szálképzés vagy folyamatos kristályosítás. [I, XIV, XVI, XVII, XIX]

2. Elsőként alkalmaztuk az elektrosztatikus szálképzést mint új típusú oldószer eltávolítási módszert egy áramlásos reakcióelegy közvetlen feldolgozására. A szálképzés szórófejére nagyfeszültséget kapcsolva az illékony komponensek elpárologtak, és a hatóanyag amorf formában a nanoszálas hordozóba ágyazódott. Így a reakcióelegy közvetlen feldolgozását további szilárd-folyadék elválasztási lépés nélkül sikerült megvalósítani. Megfelelő mennyiségű légáramot biztosítva a szálak maradékoldószer-tartalmát határérték alá tudtuk csökkenteni. [I, XIV, XVI, XVII, XIX]

3. Sikeresen kifejlesztettünk és alkalmaztunk egy folyamatos gyártóberendezést a szálképzett termék folyamatos gyűjtésére és egy, a szájüregben azonnal oldódó gyógyszerforma folyamatos, „end-to-end" gyártására. Az áramlásos reakcióelegyből közvetlenül előállított acetilszalicilsav-tartalmú szálakat egy vízoldható hordozó film felületén gyűjtöttük. Az előállított kétrétegű szalagot egy vágómechanizmus közvetlen gyógyszerformaként alkalmazható kisebb egységekre vágta. Az előállított készítmény megfelelő hatóanyag-tartalmának egységességét és a szálak kis maradékoldószer-tartalmát hosszabb, 8 órás kísérletek során igazoltuk. [I, XIV, XVI, XVII, XIX]

4. A kifejlesztett folyamatos gyártóberendezés alkalmazhatóságát kiterjesztettük egy rossz vízoldhatóságú hatóanyag, a carvedilol formulálására. A carvedilol-tartalmú nanoszálak előállításának optimalizálásával egy stabilan működtethető folyamatot kaptunk. A szálakat módosított pullulán-alapú hordozón gyűjtöttük: citromsavat kevertünk a filmbe, mely a kioldódásvizsgálatok során pH-módosítóként funkcionált. A kialakított carvedilol-tartalmú készítmény azonnali szétesését és kioldódását igazoltuk a szájüreget modellező körülmények között. A termék 4 órás gyártása során a hatóanyag-tartalom megfelelő

egységességét tapasztaltuk, és a szálak maradékoldószer-tartalma is megfelelt szobahőmérsékletű másodlagos szárítást követően a hatósági előírásoknak. [II]

5. Elsőként kapcsoltuk össze közvetlen módon egy hatóanyag folyamatos kristályosítását és szűrését egy „Mixed Suspension Mixed Product Removal (MSMPR) kristályosító és egy „Continuous Filtration Carousel" (CFC) berendezést alkalmazva. A közvetlenül kapcsolt két lépés együttes optimalizálását követően stabil működést sikerült elérni, és kiváló minőségű, jó folyóképességű kristályos terméket kaptunk a folyamat végén. [III, IV, XV]

6. Elsőként határoztuk meg egy folyamatos kristályosítás kritikus paramétereinek hatását a hozzákapcsolt folyamatos szűrés termékének minőségére egy integrált folyamatos kristályosító-szűrő rendszerben. Megállapítottuk, hogy a szűrt termék kihozatalát és szemcseméretét elsősorban a hőmérséklet, míg nedvességtartalmát a hőmérséklet és a tartózkodási idő együttesen befolyásolja. A kísérletek során az acetilszalicilsav kristályok mérete nem volt hatással a szűrési folyamatra. A folyamatos szűrés során a kristályokat megfelelő mértékben sikerült megszárítani ahhoz, hogy jó folyási tulajdonságú szilárd terméket kapjunk, ami felhasználható a további feldolgozási lépésekben. [III, IV, XV]

7. Elsőként valósítottuk meg egy folyamatosan kristályosított és szűrt hatóanyag folyamatos homogenizálását és tablettázását. A homogenizálást in-line követtük egy NIR-szondával. Az előállított tabletták hatóanyag-tartalma kis ingadozást mutatott az at-line NIR-spektroszkópiásan és off-line HPLC-vel történt vizsgálatokban. Összességében elsőként igazoltuk a gyógyszeriparban legelterjedtebb gyógyszerforma, a préselt tabletta folyamatos „end-to-end" gyártásának megvalósíthatóságát. [IV, XV]

1 Introduction

Innovation in the pharmaceutical industry has been limited to the research and development of new drug products, meanwhile the structure of the production has not changed in decades and relies on batchwise technologies to date. As it has already been demonstrated in several other industrial sectors, continuous manufacturing (CM) has many advantages over batch processes. Faster, cheaper and more flexible production can be developed with a significantly higher level of quality assurance.

In the recent years the main regulatory agencies recognized the need for a change in drug production and started to promote continuous technologies and encourage pharmaceutical companies to develop and adapt such processes. As a result, by today extensive research is being conducted in the various fields of pharmaceutical technologies from drug substance to drug product manufacturing. Many published papers can be found in the literature dealing with synthetic steps carried out in flow reactors, crystallizations implemented in a continuous manner, and on the formulation side continuous filtration, drying, granulation and blending have all been studied to a lesser or greater extent. Moreover, besides the modification of these traditional processes to continuous operation novel, intrinsically continuous technologies are being studied as well.

In order to entirely exploit all the advantages of CM, the processes developed mainly separately need to be connected to form end-to-end systems from the raw materials to the final dosage forms. According to the number of publications, even the integration of two technological steps is a challenging task. The development of end-to-end systems requires deep process understanding and holistic approach towards process development and optimization.

Our objectives were the development of various continuous pharmaceutical technologies and the examination of these individual processes. It was intended to accomplish the integration of the separated steps, and the evaluation of the challenges arisen from the direct connection. Novel, industrially not yet utilized techniques, such as electrospinning was aimed to be applied as part of a CM system. By coupling the separate technological steps, the main goal was to create end-to-end continuous systems for the production of final dosage forms starting from raw materials, which has not been published in the literature yet.

2 Literature review

2.1 Challenges of the 21st century in pharmaceutical manufacturing

By the end of the 20th century, most of the largest industrial sectors built the production lines based on assembly-line, continuous technologies [1]. This could be observed in the electronic, automobile, food and petrochemical industry as well. In contrast, the pharmaceutical production still relies mainly on traditional batch processes. The facilities are designed for the large-scale batch production of "blockbuster" drugs using large volume centralized batch manufacturing plants [2].

This approach divides the manufacturing process into many separate steps which are clearly isolated in space and time [3]. The two main sections of drug production, *i.e.* synthesis (drug substance manufacturing) and formulation (drug product manufacturing) are often located even in different countries [4]. This elongates supply chains drastically and the transportation of materials between facilities can take even weeks [2,5,6]. During the manufacturing process samples are taken from each produced batch, which are carried to the separate laboratory to conduct in-process-control measurements before moving the material to the next unit [7]. Since the production of a pharmaceutical product can take up to 10-20 steps, this cumbersome procedure together with the long supply chains often results in 12-24 months of production time for the entire process [1,2,5].

Pharmaceuticals are manufactured in a "campaign-like" manner, meaning that a given intermediate is prepared in successive batches, collecting a certain amount of material together before moving to the next step [2,8]. This manufacturing practice requires the factories to maintain substantial storage capacity, which seriously raises the cost of the production and thus of the product [2,5]. Additionally, storing large amounts of hazardous, potentially active pharmaceutical intermediates increases the safety issues of the manufacturing process [9].

Scale-up is always a great challenge during the development of batch technologies, as a process developed and optimized in laboratory can change dramatically when carried to pilot- or to operational-scale. However, during drug development usually there is no time for thorough re-optimization on large-scale, since ensuring adequate supply for the clinical trials is the priority [10]. Thus, usually the first operating procedure is accepted for industrial-scale operation and submitted to regulatory approval. After reaching the market, any modifications

aiming the improvement of production efficiency must go through the time- and money-consuming approval procedure again [11].

The greatest drawback of the batch-based structure of the pharmaceutical manufacturing is presumably the currently common practice of quality assurance. In the case of drug products ensuring consistent quality is of utmost importance, which is intended to be achieved by strict regulatory control [4]. The applied practice is the Quality by Testing (QbT) method, which consists of the analysis of samples taken from the raw materials, the intermediates after each step and the final products [12,13]. If any of the measured parameters is out of the regulatory-approved specifications, the entire batch must be reprocessed or discarded causing significant delays and extra costs [7]. The fluctuations are intended to be minimized by the tightly controlled process parameters instead of deeper process understanding and finding the root causes of the deviations [4].

The presented structure of the drug production makes the pharmaceutical industry slow and highly inflexible, unable to give quick answers to the changes in demand [14]. This poses a potential public health threat as the root causes of numerous reported drug shortages can be traced back to the problems of current manufacturing strategy of the industry [15,16]. Furthermore, recent trends in drug product development show that less and less blockbusters can be brought to the market, and the cost of new pharmaceutical research and development outpaced market growth [3,5,9,17]. There is an increasing need for a more agile, robust and efficient manufacturing structure in order to keep up with changes in market demand, to reduce costs, and to produce pharmaceuticals more reliably with improved quality [14].

2.2 The advantages of continuous manufacturing

As it has already been shown in other industrial sectors, by replacing the batch processes to continuous technologies significant improvements can be accomplished in the production [1]. Unlike batchwise manufacturing, in the case of continuous processes the raw materials and the product are continuously fed into and discharged from the equipment. All the materials are continuously flowing through the system eliminating the idle time between the different technological steps [14]. After a start-up period, continuous processes converge into a steady state, during which the process parameters are constant in time [4]. Monitoring and control of these variables on a fixed setpoint over time is much easier than that of the continuously changing batch operations. Therefore, by the development of appropriate analytical methods even constant product quality can be attained [4]. In the case of an error the deficient product

section can be traced back accurately and discarding the entire amount of material is no longer necessary [18].

Continuous technologies are usually developed as a whole, integrating the consecutive steps into one system [19]. Such a system in the pharmaceutical industry would result in a drastically different and improved production strategy [9]. By connecting the currently separated manufacturing sections, such as the synthesis and formulation, the elongated supply chains could be cut down [3,6]. As materials could flow directly to the next step, the huge and expensive inventory capacity maintained for storing the intermediates becomes unnecessary, and factory footprint can be reduced as well [14]. Because of the high-level automation and the lack of termination between the technological steps human intervention can be minimized, reducing the toxicity and safety issues of traditional batch manufacturing (*e.g.* the production of anticancer drugs and hormones is safe only in severe protective equipment) [20].

The productivity can be increased simply by operating the system for longer, facilitating to provide rapid response for sudden changes in demand [9,21]. There is no need for classical scale-up procedure, since it is enough to utilize parallel processing lines of the equipment used in laboratory, which accelerates the whole drug development process and reducing the time required to reach the market [9]. In the case of continuous technologies process optimization is usually faster and easier, which means that a more understood and optimized process can be submitted for regulatory approval. Additionally, according to studies in the literature, the investment and operating costs of continuous technologies are lower, and the expenses can be reduced even by 40% [22].

2.3   The first steps toward continuous pharmaceutical manufacturing

The necessity to improve the efficiency of current batch-based drug manufacturing drew the attention of the industry, the academia and the regulatory agencies to continuous technologies. The vision of a faster, cheaper, more flexible and robust production initiated the paradigm shift of the frozen-in pharmaceutical industry [23,24].

In 2005 the American Chemical Society (ACS) Green Chemistry Institute (GCI) and several global pharmaceutical corporations, such as Novartis, Pfizer, Roche, Sanofi, Eli Lilly, Johnson & Johnson and others founded the ACS GCI Roundtable [25]. This roundtable defined "continuous processing" as one of its research priorities [26,27]. The U.S. Food and Drug Administration (FDA) issued the first framework about promoting the application of Process Analytical Technologies (PAT) in 2004 [28]. These novel analytical techniques are suitable for

real-time process monitoring, with which better process understanding and improved product quality can be accomplished [29]. In the following years, several further guidelines were launched by the FDA [30], the International Council for Harmonization (ICH) [31–35] and also by the European Medicines Agency (EMA) [36] in the topic of quality improvement through the development and adaption of continuous technologies and by applying the Quality by Design (QbD) approach for quality assurance instead of QbT [7,37]. Recently the FDA declared CM as one of the most important tool in the modernization of the pharmaceutical industry [38].

According to the guidelines, unlike applying QbT, quality should be designed into the product [7,37]. Pharmaceutical Quality by Design (QbD) means a systematic approach towards development, starting with defining the critical quality attributes (CQAs) of the product, identifying the critical material attributes (CMAs) of the starting materials and the critical process parameters (CPPs) as well. By linking CMAs and CPPs to the CQAs it is possible to understand how the product quality is affected by changing the process parameters and the material attributes. As a result, an operating space of parameters can be defined, and within this processing region the same product quality can be produced.

By today nearly all the major innovator pharmaceutical companies are working on continuous technologies [18]. As a result, six drug products were released on the market which are produced at least partially by regulatory-approved continuous technologies: Vertex's Orkambi® and Symdeko®, Johnson & Johnson's Prezista®, Eli Lilly's Verzenio®, Pfizer's Daurismo® and Chinoin's Severin® (Figure 1) [8,39]. Much effort was required to achieve this progress, however, there is clearly a large room for improvement. Obviously, the movement towards CM is a long and costly journey, which requires extensive research [40]. It is necessary to evaluate the applicability of existing technologies in a continuous manner, and to develop novel continuous processes not yet utilized [18]. Moreover, changing the current mind set and training of CM experts also takes a long time.
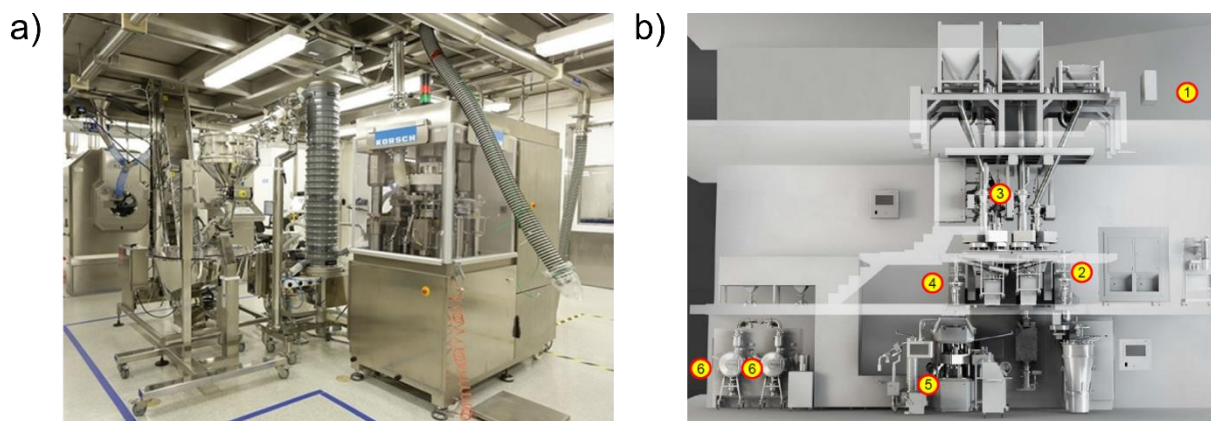
Figure 1. Examples of regulatory-approved continuous pharmaceutical production lines for the production of (a) Prezista® by Johnson & Johnson's [41] and (b) Orkambi® by Vertex [42]. The parts of Vertex's facility: 1. At-line NIR incoming material attributes; 2. NIR blend potency; 3. Granule properties (3a. NIR granule uniformity, moisture; 3b. Laser diffraction particle size); 4. NIR final blend, potency and moisture; 5. Tablet properties (5a. Raman API form and identification; 5b. Weight, thickness, hardness); 6. Raman film coat thickness.

There is a growing body of literature of continuous pharmaceutical manufacturing, covering the entire production line. Considerable research has been conducted for example in the field of flow chemistry [43], continuous crystallization or continuous blending and tableting [19]. However, beside examining the different continuous processes, connecting the individual steps is a much greater challenge [44]. In order to exploit all the described advantages of CM, the separated technological processes must be integrated into one continuous production line to form an end-to-end system from the raw materials to the final dosage forms. According to the literature, significantly less publications deal with continuous technologies in which at least two consecutive steps are coupled in any way. Moreover, the development of end-to-end continuous systems from the raw materials to the end products is presented only by a handful of papers. This also might be the result of the currently separated synthetic and formulation section, as scientists and experts usually do not have expertise in both fields. It is clearly visible, that a complete change in mind set is required for a more integrated development approach towards continuous technologies [4,8].

2.4   Recent progress in continuous pharmaceutical technologies

The following sections aim to present the progress accomplished to date in the various areas of continuous pharmaceutical manufacturing. First, the flow chemical transformations and multi-step syntheses of APIs will be discussed, followed by continuous crystallization and filtration. After these, the continuous blending and tableting of pharmaceuticals will be

presented. Emphasis will be put on published examples when more than one consecutive technological steps were integrated in a continuous manner to show the progress accomplished towards end-to-end pharmaceutical manufacturing. A few techniques from a usual pharmaceutical manufacturing line, such as granulation, milling and drying is left out of this review, as no experimental work has been conducted using these techniques in the field of end-to-end manufacturing. However, several well-organized and up-to-date studies focus on these research areas [45–48].

2.4.1   Multi-step flow synthesis of pharmaceuticals

2.4.1.1   Principles of flow chemistry

The multi-step synthesis of complex organic molecules from simple precursors is one of the greatest achievement as well as one of the greatest challenge of the synthetic organic chemistry [49]. The traditional batchwise synthetic route consists of a series of batch reactions with work-up procedures, purification and isolation after each step (Figure 2a). Although this approach is the basis of all modern syntheses, such a procedure is usually time-consuming and wasteful.
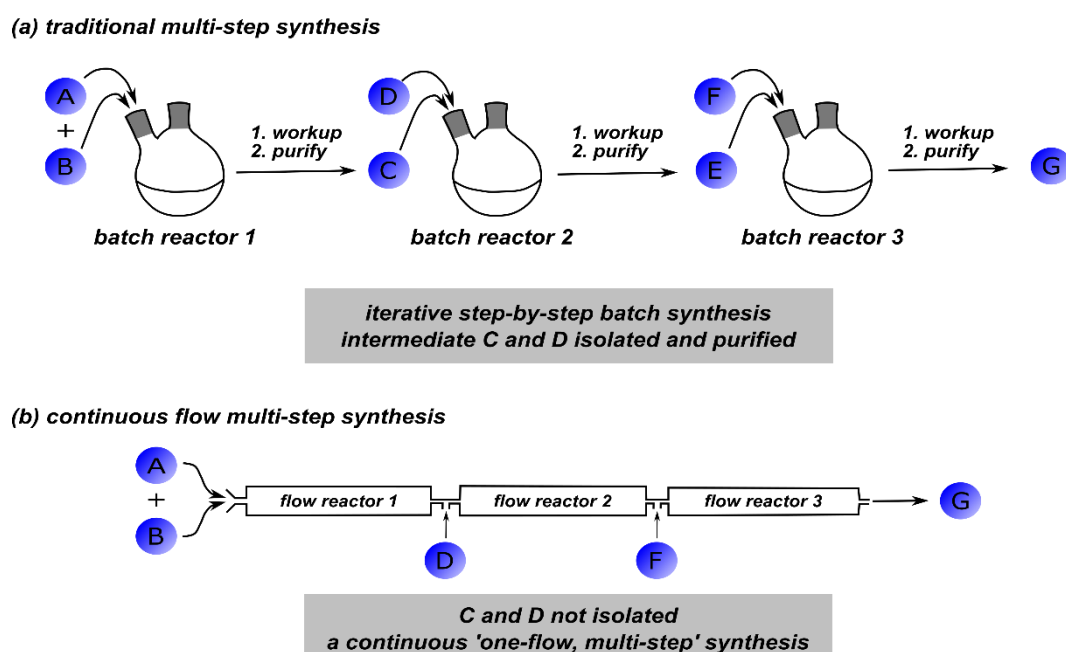

Figure 2. (a) The traditional batchwise multi-step synthesis and (b) novel continuous flow approach for the synthesis of complex molecules [49].

Continuous flow chemistry offers several novel options for the implementation of organic syntheses [50]. In flow systems the materials are flowing in tubes with small diameter (usually

between 50 and 1000 μm), and the reactions take place in these so-called microreactors (Figure 3) [51]. The starting materials are fed in by pumps, and mixer elements provide the sufficient mixing of the liquid streams. Back-pressure regulators (BPRs) can be applied at the end of the tubes to pressurize the system, and directly connectable devices are available for the purification of the reaction mixtures, *i.e.* liquid-liquid extractors. Besides homogenous systems, solid-liquid or gas-liquid reactions are also accessible with packed bed reactors or tube-in-tube reactors [52–55]. The in-line monitoring of the flow reactions is possible by applying *e.g.* flow-through spectroscopic analytical techniques.
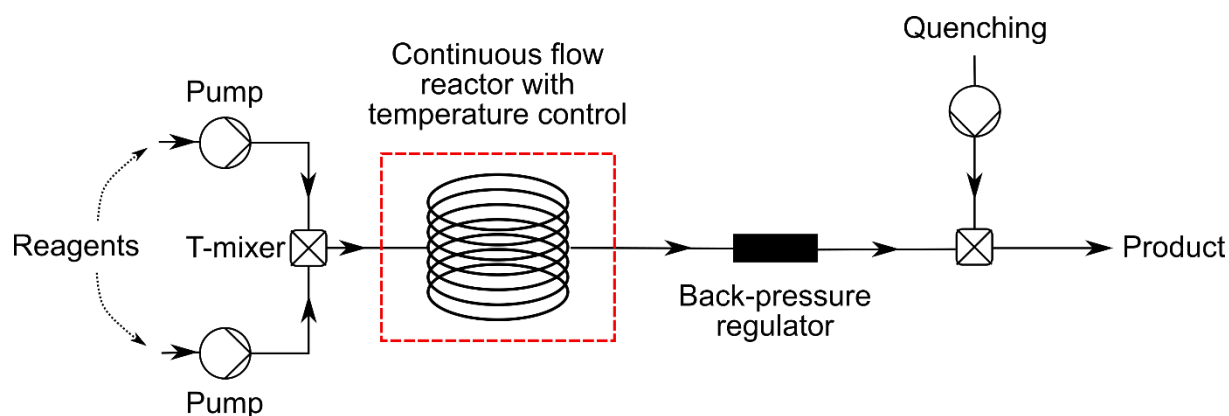
Figure 3. The general structure of continuous flow systems.

These systems have a number of advantages over traditional batchwise reactors. The small cross-section of the tubes means that the ratio of the heat transfer area to the reactor volume is about 50-60 times bigger (calculating with the same kg per a day throughout) [20]. The small channel dimensions of the reactors allow precise control over process parameters: quick heat transfer, or efficient and accurate illumination during photochemical reactions [56,57]. In the pressurized system significantly elevated temperatures can be applied, thus accelerating the reactions and making new pathways possible that are otherwise not accessible [58]. Reduced reaction time, excellent yield and selectivity, enhanced safety and good reproducibility were reported in the literature numerous times [59–61]. Naturally, new challenges have arisen with the new technology, for example dealing with solid materials and the danger of clogging, the integration with in-line purification techniques, or the cost of flow equipment, which all must be handled during the development of a flow chemistry process.

Owing to the advantages of flow chemistry, the number of publications dealing with synthetic organic flow systems has raised significantly in the recent years. The International Union of Pure and Applied Chemistry (IUPAC) organization named flow chemistry among the

top ten emerging technologies in chemistry [62]. The majority of publications deals with different chemical transformations implemented in flow reactors and comparing them to the original batch result. Many excellent review papers have been published summarizing the progress in this area, also highlighting the barriers of this new technique, and providing a guide for the researchers whether is it worth to develop a flow system for a certain process or not [50–52,58,59,63–67].

2.4.1.2 Flow synthesis of pharmaceuticals

By connecting several flow reactors into one continuous line, multi-step syntheses can be carried out in an uninterrupted system [49,68]. The great benefit of this approach is that the isolation of intermediates can be eliminated simplifying and accelerating the process (Figure 2b). Without transportation and off-line quality testing after each step the footprint of production facility can be reduced, improving flexibility at the same time. This is especially true for the synthesis of APIs, as these complex compounds often require 6-10 synthetic steps from the starting materials [63]. Usually some compromises are inevitable and the synthetic route is split up to shorter sequences for the purification of the reaction mixtures or for solvent exchange [69]. Incorporating every operational step into one system, including in-line purification, work-up and real-time analysis requires holistic optimization and deep process understanding. Nevertheless, the total synthesis of APIs under flow conditions has a growing body of literature [56,58,65,68,70,71] and due to the challenge of integration of in-line purification into a flow system, this topic is also gaining more and more attention [52,72,73]. In Table 1 APIs with reported continuous flow total synthesis are summarized. Regarding the industrial application of flow chemistry, in 2018 Hughes collected seven examples from the patent literature for API synthesis, during which at least one reaction step is carried out under flow conditions [74]. However, in these cases it was not public whether these routes are used for commercial manufacturing or not.

Table 1. Examples for published multi-step flow syntheses of APIs.

API	Year of publication	Reference	API	Year of publication	Reference
Ibuprofen	2009	[75]	Imatinib	2013	[79]
Nabumetone	2011	[76]	Tamoxifen	2013	[80]
Fluoxetine	2011	[77]	Diphenhydramine HCl	2013	[81]
Artemisinin	2012	[78]	Amitriptyline	2013	[82]

API	Year of publication	Reference	API	Year of publication	Reference
Olanzapine	2013	[83]	Clozapine	2018	[96]
Rufinamide	2014	[84]	Hydroxychloroquine	2018	[97]
LY2886721	2014	[85]	Dolutegravir	2018	[98]
Aliskiren hemifumarate	2014	[86]	16-DPA	2018	[99]
Efavirenz	2015	[87]	Nicardipine HCl	2018	[100]
Rolipram + phenibut	2015	[88]	Ciprofloxacin HCl	2018	[100]
Telmisartan	2015	[89]	Neostigmine HCl	2018	[100]
Ibuprofen	2015	[90]	Rufinamide	2018	[100]
Ribociclib	2016	[91]	Hymexazol	2019	[101]
Diphenhydramine HCl	2016	[1]	Vortioxetine	2019	[102]
Lidocaine HCl	2016	[1]	Flibanserin	2019	[103]
Diazepam	2016	[1]	Imatinib	2019	[104]
Fluoxetine HCl	2016	[1]	Treprostinil	2019	[105]
Pregabalin	2017	[92]	Ibuprofen	2019	[106]
Flucytosine	2017	[93]	Lomustine	2019	[107]
Captopril	2017	[94]	Linezolid	2019	[108]
Prexasertib	2017	[95]	Lesinurad	2020	[109]

2.4.1.3 API flow syntheses integrated with downstream processes

In order to build end-to-end systems, the developed multi-step flow synthesis of the APIs must be connectable to the following technological steps. The final reaction is usually followed by the purification of the synthesized API, which can be carried out first by liquid-liquid extraction, but eventually the compound must be brought to solid form with a continuous crystallization step. This is usually carried out in either mixed suspension mixed product removal (MSMPR) crystallizers of plug flow reactors (PFRs) (for more detail see Section 2.4.2.1).

Not many studies can be found in the literature in which the described synthetic route is developed bearing in mind the connectability to the subsequent continuous work-up processes. The two-step synthesis of ribociclib – published by Pellegatti *et al.* in 2016 – was followed by an in-house built in-line liquid-liquid extraction and a semi-batch crystallization [91]. Similarly,

in a publication by Snead *et al.* in-line purification was integrated with the flow synthesis of diphenhydramine hydrochloride, followed by semi-batch crystallization [81]. Although not synthesizing an API, Lichtenegger *et al.* developed a system in which flow chemical transformations were truly connected to continuous crystallization in PFRs [110]. Ingham *et al.* presented a system in 2014 for the integration of three connected chemical steps coupled with liquid-liquid extraction, solvent exchange and continuous filtration as well [111]. With the incorporated in-line analysis and process control strategies 6-hour long operations were carried out without human intervention. On the crystallization side, only one example was found when the authors emphasized that the continuous crystallization of an API was developed in a way to be able to integrate into a flow system [112].

In the research area of flow syntheses coupled to continuous work-up procedures, probably the greatest work was accomplished by Ely Lilly and Company, which is one of the leading companies committed to CM [113]. They conducted extensive research in the area of flow chemistry and the integration of the synthetic steps. Johnson *et al.* published a scaled-up system with flow synthesis, continuous crystallization and filtration [114]. They carried out a high-pressure continuous asymmetric hydrogenation reaction in a PFR, then continuous liquid-liquid extraction for purification. Following this step, a semi-batch solvent exchange distillation process, a two-stage MSMPR crystallization, and batch filtration was executed. The entire system was integrated, and stable operation was achieved on a kg per a week production scale. In a next paper they developed the synthesis of a drug candidate, LY2886721 [85]. The system consisted of a flow chemical step and continuous reactive crystallization. In this study they presented the optimization of the processes, the scale-up and development of the equipment and longer operational tests as well. As a continuation of this work Cole *et al.* developed the fully integrated continuous synthesis of prexasertib under cGMP conditions, at a throughput of roughly 3 kg/day [95]. Eight reaction steps were incorporated in one system, and the previously described continuous liquid-liquid extractor, semi-batch solvent exchange device, MSMPR crystallization and batch filtration were all utilized during operation. The developed equipment and the knowledge of this study was transferred to the CM center of Ely Lilly and Company in Kinsale, Ireland.

After reviewing the current literature about the continuous flow synthesis, it is clear that although the total synthesis of a few dozen APIs has already been published, **more research is necessary to build continuous end-to-end systems. The multi-step synthesis of**

pharmaceuticals must be developed in a way to be connectable with the following technological steps for the work-up of the reaction mixture.

2.4.2 *Continuous crystallization and filtration*

Crystallization is a key purification and separation technique in the pharmaceutical industry and it is a critical step in connecting synthesis and formulation [115]. More than 90% of the currently marketed APIs are going through crystallization during their production [116]. The crystal size and shape have a huge impact not only on the following technological steps through bulk density or flowability, but also on the dissolution rate and bioavailability of the final drug product. The importance of the process drew attention on continuous crystallization in the recent years [117–120]. In the technological line crystallization is followed by filtration for the isolation of the solid product [121]. This technique is usually assessed by the filterability of the crystals, the moisture content of the filter cake and the recovered mass. Also, the process might affect the crystal size through agglomeration [122]. Continuous filtration is a relatively new area of study in the pharmaceutical industry, and only a small number of publications can be found in the literature. In the following sections continuous crystallization and filtration will be discussed focusing on connected and integrated continuous crystallization-filtration systems.

2.4.2.1 *Continuous crystallization*

Currently the vast majority of crystallizations in the pharmaceutical industry is carried out in stirred batch reactors [120]. These systems have been used for decades, and the processes are thoroughly optimized and reasonably well-understood [118]. However, there is still significant issues with batch-to-batch variability, which can lead to substantial difficulties in the following downstream processing of the crystal product [115].

The implementation of novel continuous processes can provide a number of advantages in the area of crystallization. Continuous technologies naturally require smaller, and thus cheaper equipment, reducing production footprint [117]. As an example, for a given crystallization process to reach the same annual productivity a 250 L continuous reactor would be sufficient, while in batch mode a 5000 L reactor could provide the appropriate amount of crystalline product [115]. The continuous operation offers improved control and reproducibility over the physical characteristics of the product. After the steady state is reached the product properties become constant in time, and the key parameters such as particle size and shape can be accurately controlled [117]. Additionally, certain downstream processes might be eliminated which are usually applied only for the correction of crystallization, *e.g.* particle size adjustment

22

by granulation. However, taking into consideration the yield of the process, in the steady state of continuous crystallizations – unlike with batch systems – the equilibrium cannot be reached, decreasing the maximum attainable yield. This can be overcome by the application of optimized recycle loops. Fouling of transfer lines and blockages are new challenges arisen with the new technology, which have to be addressed during process development [117].

In the case of continuous crystallization, the API solution (and the antisolvent, if necessary) is continuously fed into the equipment, while the product slurry is continuously withdrawn. Many different systems have been published in the literature for the implementation of such a process [118]. The two most widespread technologies are the MSMPR crystallizers and the PFRs (Figure 4) [120].
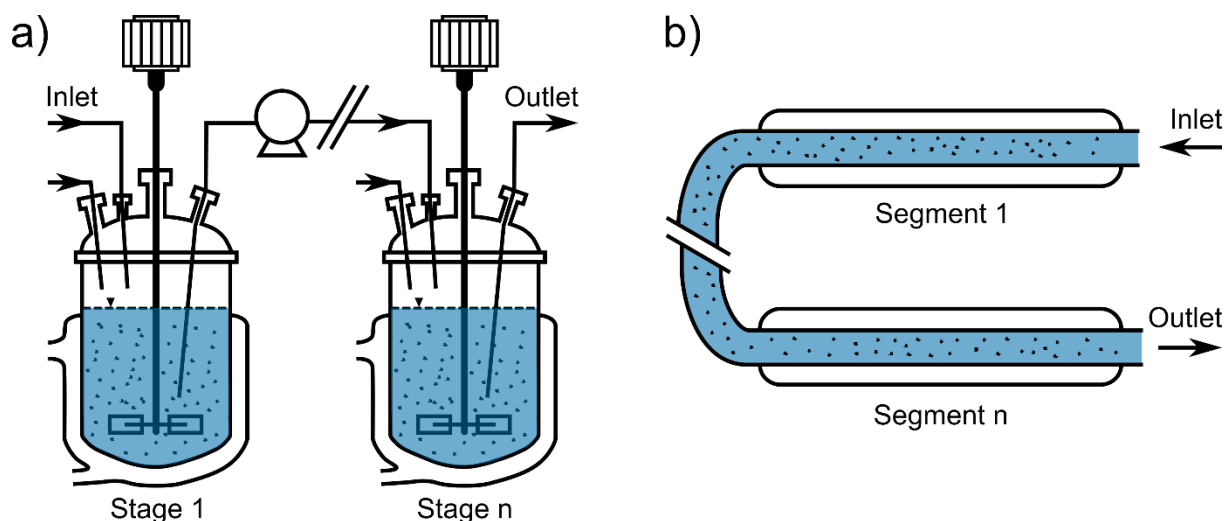
Figure 4. The schematic drawing of (a) a mixed suspension mixed product removal crystallizer and (b) a plug flow reactor.

The MSMPR reactors are conventional jacketed stirred tank reactors, with continuous input of starting material and continuous product removal. The huge advantage of these systems is that the existing stirred tank equipment can be further utilized, which can be easily operated and controlled, and the existing batch crystallization processes can be converted into continuous operation [117]. By connecting several MSMPR reactors into a multi-stage cascade system, flexible temperature profiles can be used for precise supersaturation control, and the yield can be increased close to equilibrium [116,123]. On the challenges side, usually broad residence time distributions can be obtained with MSMPR crystallizations, and the scale-up difficulties of the original batch processes cannot be overcome easily. MSMPR crystallization of APIs is a frequently studied topic in the literature [117,119]. The effect of process parameters [124],

different setups [123,125], strategies [126,127] and novel slurry transfer systems [128–130] are all examined in detail.

Plug flow reactors are tubular crystallizers, in which the API solution is continuously flowing with constant flow rate [117]. The great benefit of these systems is the excellent process control due to the small tube diameter, easy scale-up (similarly as described at flow reactors, in Section 2.4.1), and the narrow residence time distribution, which provides good product uniformity. Nevertheless, the danger of fouling in PFRs is significantly greater than that in MSMPR crystallizers. The literature of PFRs includes substantial number of papers about the continuous crystallization of APIs as well [112,131–135]. An important variant of PFRs is the continuous oscillatory baffled crystallizer, which is also applied for the processing of pharmaceuticals more and more frequently [136–140].

2.4.2.2 Continuous filtration

The produced crystals can be removed from the mother liquor in the following filtration step [121]. This is a technique often developed by practical and empirical understanding due to the complex nature of cake growth and the interacting process parameters [141]. Therefore, it is necessary to carry out experiments with the actual slurry on the required scale since predicting filtration performance is cumbersome [142]. In the pharmaceutical industry filtration is generally carried out in batch mode, but there are already a few examples for continuous filtration devices [141,143]. The low number of publications dealing with pharmaceutical-related continuous filtration is probably due to the fact that it is a complex technical challenge and involves the use of less established technologies [23].

A few examples can be found in the field of pharmaceutical-related continuous filtration. Cross flow filtration is a well-known continuous filtration technique, mainly utilized during the processing of biological products to concentrate slurries [144,145]. Gursch *et al.* and Kossik *et al.* reported studies applying this technique for API suspensions with a membrane-based device [146,147] and a rotary drum filter [148,149]. Researchers at MIT designed, built and tested the prototype of a small-scale continuous pharmaceutical filtration instrument using linear motion [150]. Pfizer developed a semi-continuous filter-drier with a 3-way valve, which filtered small amounts of slurry (15-30 mL) every cycle, yielding a kg per a day productivity [151]. In 2015, BHS Sonthofen marketed a manufacturing scale (up to 85 kg/h) continuous indexing belt filter with pressing and steam-drying capabilities [152]. This apparatus was tested in a study by Hohmann *et al.*, in which they investigated the performance of a modular miniplant during the

continuous downstream processing of an amino acid, L-alanine. The system comprised of a wiped-film evaporator, a tubular crystallizer and a vacuum belt continuous filter [153]. A continuous filter dryer prototype unit, CFD20 (Alconbury Weston Ltd.) was tested by Ottoboni *et al.* (Figure 5a) [122]. Compared to standard batch filtration, similar results were obtained with the CFD20, but significantly less manual intervention was required due to the automated system.
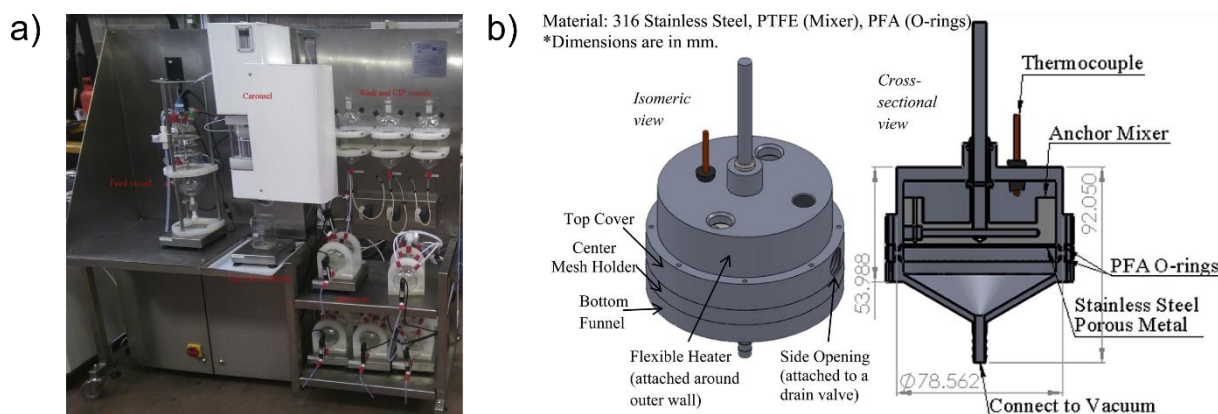

Figure 5. (a) Picture of the CFD20 device applied by Ottoboni *et al.* [122] and (b) the design of the hybrid filtration-drying-dissolution unit developed by Wong *et al.* [154].

2.4.2.3 Integrated continuous crystallization and filtration

A few publications were found from the research area of continuous crystallization, in which the filtration step was addressed in any way. In 2012, Wong *et al.* presented a study about a single-stage MSMPR crystallizer with a recycle system [155]. In this system standard batch filtration was directly connected after crystallization using a coarse glass filter disk with a filter paper having 1 µm thickness. In 2014, Ferguson *et al.* built a similar single-stage MSMPR system with a filtration step connected directly to the outlet [156]. After the filtration of crystals, the mother liquor was subjected to an organic solvent nanofiltration method in order to eliminate the impurities and increase the concentration of the remaining dissolved API, deferasirox. Acevedo *et al.* connected a single-stage MSMPR reactor to a continuous filtration carousel (CFC) device (similar to the one used by Ottoboni *et al.* [122]) [157]. A buffer tank was applied between the two steps, and after the optimization of filtration parameters stable operation was achieved with this two-step system. Paracetamol and benzoic acid were crystallized, and the filtration performance showed significant dependence on crystal properties such as size and shape. Wong *et al.* designed and built a compact system of a continuous MSMPR crystallizer (with novel scraped surface impeller design) coupled with a hybrid filtration-drying-dissolution unit (Figure 5b) [154]. Three APIs with different shape attributes

were used as model compounds: fluoxetine hydrochloride, ibuprofen and diphenhydramine hydrochloride. By applying scraped wall crystallization, improvements were accomplished in terms of better kinetics and reduced aggregation, and the semi-batch application of the hybrid device saved much time and material, while appropriate performance was achieved with each step. Capellades *et al.* designed and investigated a similar device, in which filtration, drying and mechanical processing was integrated [158]. A unique impeller was applied to enhance the processability of needle-like crystals of ciprofloxacin hydrochloride, and this way they successfully reduced the amount of lumps in the material following filtration and drying.

The presented publications are excellent examples of how filtration could be carried out in a (semi-) continuous manner for pharmaceutical purposes, and how it could be built in a certain multi-step process. **Nevertheless, no example could be found for a directly connected continuous MSMPR crystallization - continuous filtration system processing an API, in which the focus is on the challenges emerging from the direct connection of the two steps, and how the interaction of process parameters affects the product quality.**

2.4.3 *Continuous powder blending and tableting*

Blending of powders is an essential step in many industrial sectors such as the manufacture of chemicals, construction materials, foods and drugs [159]. Ensuring the homogeneity of the produced powder blend is pivotal, and it is especially true for drug products [160]. The appropriate distribution of the API in the excipients is the key to produce final dosage forms, *i.e.* tablets with acceptable drug content uniformity. Continuous blending has long been known in the mentioned industries [161], however, during the drug production batch mixers are applied in vast majority to date [162]. The rising of continuous pharmaceutical manufacturing in the recent years gave a new push to continuous blending as well.

Implementing blending in a continuous manner has a number of advantages over the traditional batchwise method, similarly as in the case of the earlier described technologies in previous sections [160]. Steady state operation can be reached within a few minutes, in which process control is much more accurate, improving quality [162]. The equipment used for process development can be used for production, eliminating the difficulty of scale-up and reducing footprint. The continuous operation makes the integration possible with the following, intrinsically continuous tableting step. Thus, the overall efficiency and final product quality can be increased. These advantages can significantly reduce costs during development and manufacturing of pharmaceuticals [163].

The main body of most continuous blenders is a cylindrical chamber with an average diameter of 3.5-20 cm and an average length of 25-75 cm (Figure 6a). At one end of the cylindrical chamber there is a vertical inlet (hopper) for feeding the materials into the blender [8]. At the other end the chamber is open allowing the produced powder mixture to leave the device. Motor-driven rotating impellers can be found in the chamber, which mix the components. Bladed, ribbon, or ribbon-bladed impellers can be applied, which directs the flow in axial direction (Figure 6) [162].
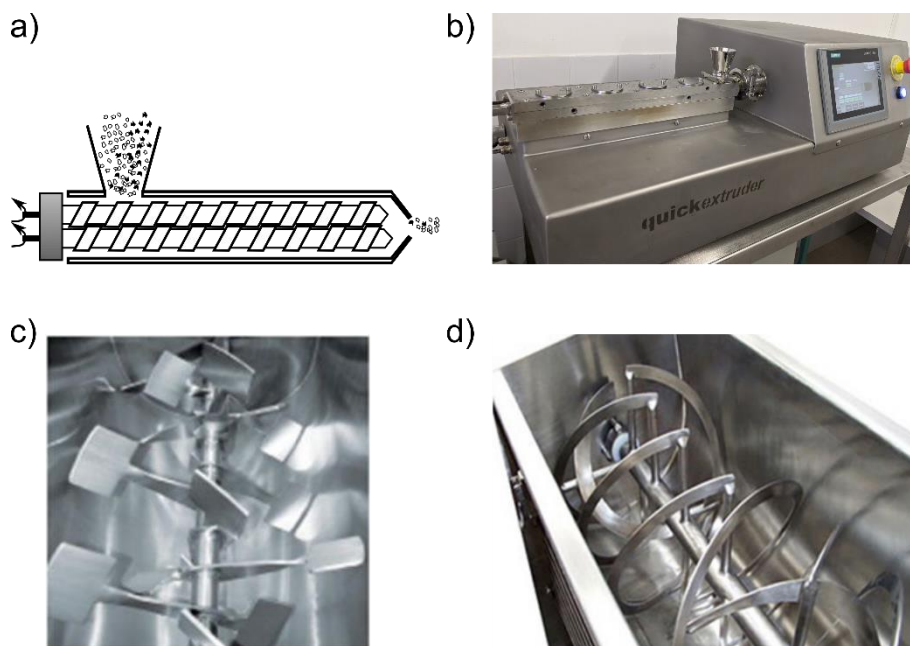
Figure 6. (a) The schematic drawing and (b) the photo of a twin-screw continuous blender; and the photo of a (c) paddle and (d) a ribbon blender.

Vanarase *et al.* published a study about an experimental investigation of the mixing performance and flow behavior in a continuous blender using a pharmaceutical mixture [164]. Impeller rotation rate was found to be the most significant process parameter affecting mixing performance, and the blade configuration also had an effect on powder homogeneity. A similar study was conducted by Osorio *et al.* in 2016 using a novel continuous blender [165].

Different strategies can be applied to reach a final dosage form after the blending step [166]. The tablet is the most common and widespread formulation, which is produced in a tableting machine [167]. The simplest way is direct compression, during which the blend of the API and the excipients is directly sent to tableting (Figure 7a). Granulation can be applied to improve powder characteristics and to reduce the risk of segregation after blending (Figure 7b). In this field, either wet or dry granulation can be applied, followed by drying, milling and

another blending step before tableting. Roller compaction is another way to modify the particle size (Figure 7c). Moreover, the powder mixture can directly be filled into capsules [168]. Both tableting and encapsulation are inherently continuous operations, historically bracketed by batch processes: powder blending in large batch blenders and tablet coating in large batch coating systems.
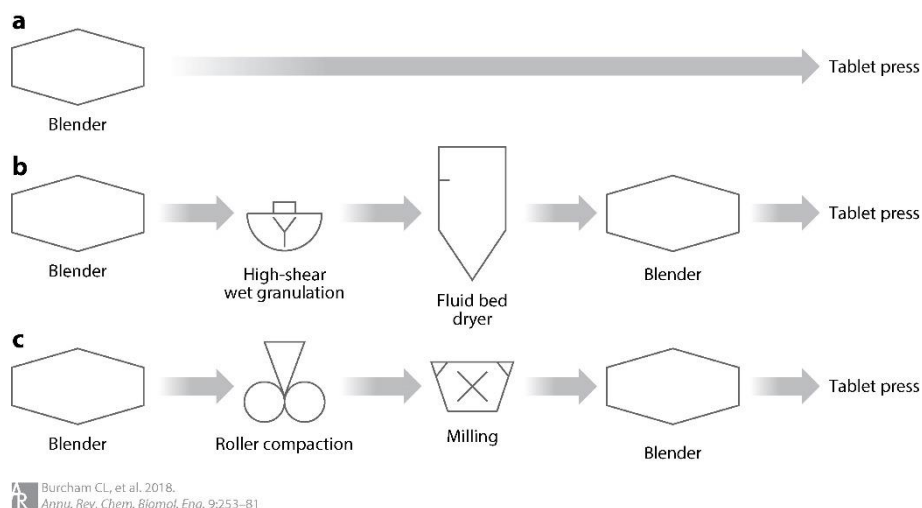
Figure 7. Different strategies for the production of final dosage forms after blending: (a) direct compression, (b) granulation, drying and another blending step and (c) roller compaction followed by milling and blending again [166].

As interest on CM is growing in the pharmaceutical industry, more and more research is performed on integrated powder-to-tablet manufacturing lines [24]. This approach is much beneficial than using single unit operations, since interactions between the individual steps might affect the quality of the final product. Direct compression is the easiest way for the development of such an integrated system [169]. In this case controlling the flowability and compressibility of the components is fundamental to obtain tablets of good quality. Järvinen *et al.* studied the effects of the rotation rate of the mixing impeller, the total feed rate and the drug content on tablet properties and drug release in an integrated continuous blending-direct compression line [167]. All results showed good drug release, while process parameters affected tablet uniformity. Ervasti *et al.* produced HPMC-ibuprofen extended release tablets on a similar continuous blending-direct compression manufacturing line [170]. Their results also showed the importance of good flowability, as the best results were obtained with the good-flowing samples with large particle size. Researchers at the University of Eastern Finland constructed a modular CM line [171]. This system was tested in a study by Simonaho *et al.* during the continuous production of tablets with three different system configurations. Van

Snick *et al.* conducted a study for the production of sustained release tablets with a continuous direct compression system [172]. Azad *et al.* designed and built a compact, portable, re-configurable and automated tableting machine at MIT. On-demand flexible tablet manufacturing was feasible with this device, which was demonstrated in two studies with several compounds [173,174].

In order to ensure the blend uniformity of the powder blend produced during the continuous blending procedure, real-time analytical techniques have to be applied. Several measurement methods are known in the literature, such as spectroscopy (NIR, Raman), image analysis, acoustic techniques and many others, which are carefully collected in reviews [175–178]. These analytical methods were applied numerous times in published studies. Nagy *et al.* used Raman spectroscopy for the monitoring and feedback control of a continuous blending and tableting process [179]. Successful experiments were carried out with the model system of caffeine, glucose and magnesium stearate, introducing the Process Analytical Controlled Technology (PACT) method. In a recent paper by Palmer *et al.*, the performance of a direct compression system was tested for a wide range of process parameters and material attributes [180]. The API content in the powder blend was monitored by an NIR probe. A DoE approach optimization was carried out in the system to find the relationship between process parameters, material properties and the quality of the produced tablets. Many further great examples can be found in the literature for the development of continuous blending processes, for the investigation of the connectability with continuous tableting, and for the implementation of in-line analysis in a complex continuous blending-tableting system [181–188].

After the literature review, it can be stated that despite many examples can be found for integrated continuous blending-tableting systems, **no connection was made with the preceding filtration step. It would be important to evaluate the processability of continuously filtered pharmaceutical materials in such continuous direct compression manufacturing lines.**

2.4.4   *Novel continuous formulation techniques*

On the way moving from batch production towards CM, besides evaluating the applicability of the traditional production steps for continuous operation novel methods utilized not yet broadly should be tested as well. Many technologies exist which are naturally continuous, and the spread of CM in the pharmaceutical industry can bring the breakthrough for these processes. Such techniques are for example electrospinning (ES) and hot-melt

extrusion, with which amorphous solid dispersions (ASDs) can be prepared [189]. ASDs are innovative drug delivery systems designed to enhance the bioavailability of poorly soluble drugs. Since a substantial part of recently discovered APIs have very low water solubility, the significance of similar drug delivery systems is increasing [190].

ES is a well-known technique to create fibrous ASDs with large specific surface area [191–193]. During ES a polymeric solution is pumped through a spinneret and exposed to an electrostatic field inducing the formation of a thin jet from the spinning tip (Figure 8). The jet elongates due to the Coulombic repulsion of the surface charges and the solvent evaporates instantaneously, leaving the drug evenly distributed in the matrix of the formed micro- or nanofibrous non-woven web on the grounded collector. The utilization of the technique for pharmaceutical purposes has a vast literature, since the versatility of the available polymers allows the formation of ASDs with sustained, controlled or even ultrafast drug release [194–198]. Thus, ES is also a promising method for the production of orally dissolving immediate-release dosage forms [199–201].
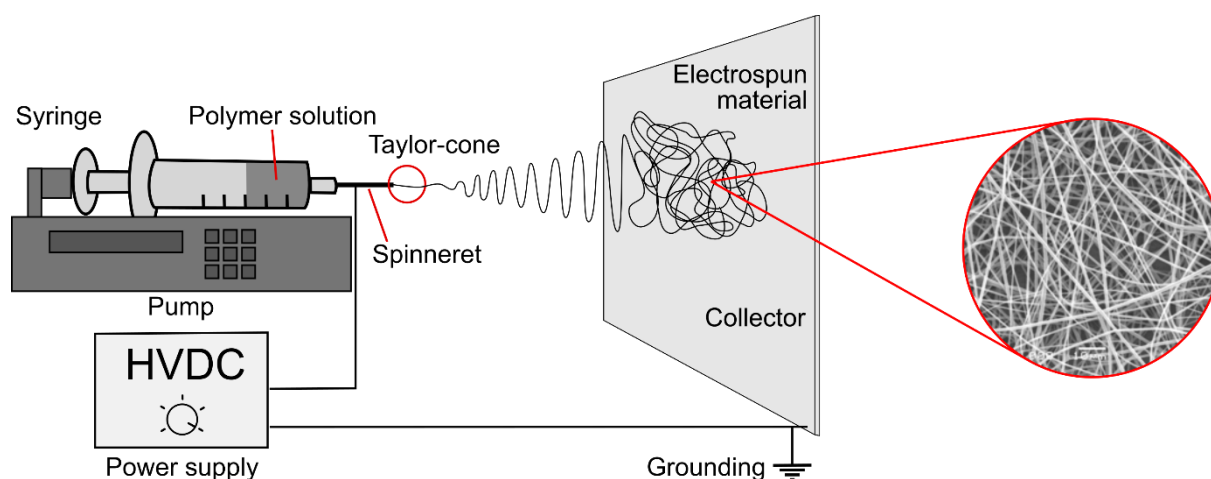
Figure 8. The schematic drawing of a single-needle electrospinning process, with the scanning electron microscopic picture of the electrospun material on the right.

As regards the industrial applicability of ES, scaling up the low productivity laboratory scale ES method to industrially applicable volume has recently been presented [202,203]. The downstream processing of the electrospun material, and thus making possible the integration into a CM line has also been published [204,205]. **However, no example can be found for the coupling of ES to the upstream stage of API manufacturing. It would be of great interest to investigate the applicability of ES coupled to continuous API synthesis as a work-up technique. Furthermore, the integration of the process to the continuous production of final dosage form has not been accomplished yet.**

2.4.5 End-to-end continuous production of final dosage forms

As it has been presented, significant progress has been made in the field of continuous pharmaceutical manufacturing. The published research studies cover the entire production line from drug substance to drug product manufacturing. Nevertheless, the majority of them deal with one individual continuous process, and not many examples refer to processes that were developed in a way to be connectable to other technological steps, and even less publications were found in which two or more continuous processes have been integrated. However, in order to thoroughly utilize the advantages of continuous technologies, the connection of more and more technological steps must be pursued to exploit all the advantages of CM. The final aim would be the development of end-to-end systems, in which the materials are flowing through from raw materials to the final dosage forms in one complete, continuous system. In the following part the published examples for such systems will be presented.

The Novartis-MIT Center for Continuous Manufacturing was one of the first locations where intensive and thorough continuous process research was conducted. The model API in their earlier publications was aliskiren hemifumarate, which was synthesized starting from an advanced intermediate. They designed and built the first example of a system for the end-to-end production of heat-mold tablets of the API, in which all synthetic steps, continuous crystallizations, filtrations and extractions were integrated and automated (Figure 9a) [9,86,206]. In a following work the previous, container-sized continuous production unit was reduced to the size of a refrigerator (Figure 9b) [1,207]. This was designed in a re-configurable manner, and four different APIs (diphenhydramine hydrochloride, lidocaine hydrochloride, diazepam, fluoxetine hydrochloride) could be synthesized. The flow synthesis was followed by batch downstream steps of crystallization, filtration and re-dissolution to obtain liquid dosage forms. This platform was further improved by incorporating continuous crystallization, semi-continuous filtration, washing, dispensing and drying [100]. In this second-generation system nicardipine hydrochloride, ciprofloxacin hydrochloride, neostigmine hydrochloride and rufinamide was synthesized, purified and formulated into the previously mentioned liquid oral dosage form. The first fully automated end-to-end commercial ready CM pilot plant was developed by Continuus Pharmaceuticals, a spin off company of the Novartis-MIT collaboration, and presented by Hu *et al.* in 2019 [208]. This system consisted of a dissolution unit for the raw materials, a five-stage reactive MSMPR crystallization cascade, a continuous filter followed by resuspension, a novel continuous drum dryer and hot melt extrusion for the

preparation of the final heat-mold tablets. PAT probes were applied for real-time analysis, *e.g.* at the end of the reactive crystallization and for the monitoring of particle size after filtration.
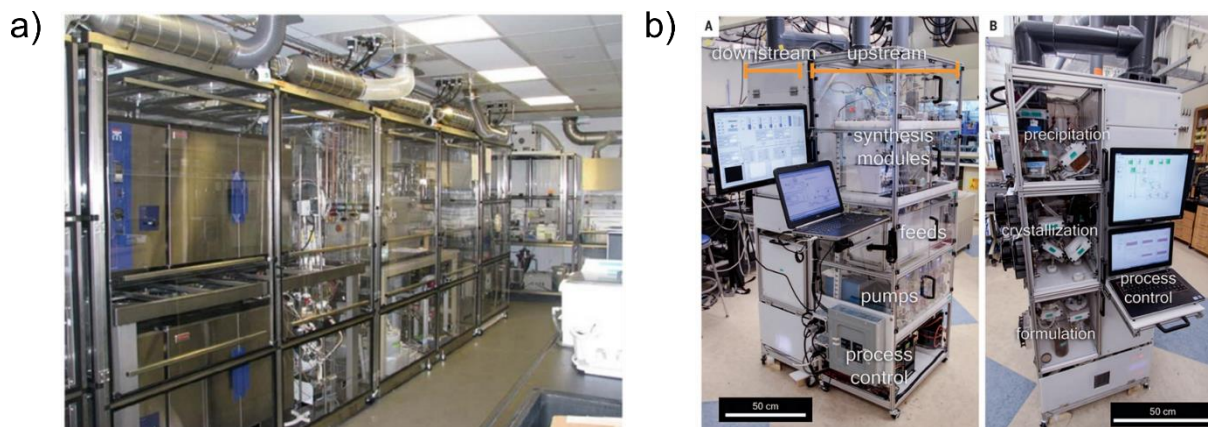

Figure 9. Examples for published continuous end-to-end manufacturing systems for the production of (a) heat-mold tablets of aliskiren hemifumarate [9] and (b) liquid dosage form of diphenhydramine hydrochloride, lidocaine hydrochloride, diazepam and fluoxetine hydrochloride [1].

Although not technically end-to-end solution, the study of Hadiwinoto *et al.* is worth mentioning here, since they accomplished the production of a final dosage form in an integrated continuous system as well [209]. They applied a spray drying technique directly connected to the plug flow crystallization of two APIs (rifapentine and beclomethasone dipropionate). Process performance was evaluated, and the continuous operation was optimized to produce a dosage form applicable for pulmonary delivery.

The literature review revealed that the development of end-to-end CM systems for the production of any type of final dosage form is an important scientific topic, while only a very small number of publications can be found in the literature. **Among these, the end-to-end continuous production of the most common and widespread compressed tablet cannot be found. Therefore, it would be of great interest to develop further end-to-end systems to produce either novel drug delivery systems or conventional tablets.**

2.5   Objectives

After surveying the current 'state of the art' related to integrated continuous pharmaceutical technologies, the main objectives of the experimental work could be set up:

- the development of the multi-step synthesis of an API, which has not been published yet, with special focus on the connectability of the process to the following work-up procedures;
- the direct connection of ES to a flow synthesis as a work-up tool of the reaction mixture, and the development of a system for the continuous formulation of electrospun fibers into orally applicable final dosage forms;
- the development of an orally dissolving formulation containing a poorly water-soluble API, carvedilol, and the investigation of the continuous production of the product;
- the integration of MSMPR crystallization with continuous filtration, and the investigation of the effect of process parameters on the quality of the filtered API product;
- the implementation of the continuous blending of the continuously filtered API with excipients, and the production of conventional compressed tablets from the powder blend.

3 Materials and methods

3.1 APIs

Acetylsalicylic acid (ASA)

Acetylsalicylic acid, or aspirin is one of the oldest pharmaceuticals on the market, first commercialized in the late 1890s (Figure 10a) [210]. Traditionally the salicylates were used for the treatment of pain, fever and inflammatory diseases. The antiplatelet activity has been discovered almost 70 years later [211,212]. Despite this drug is more than 100 years old, it is the subject of extensive research, seeking novel possible applications and possible treatment activities, and it can be considered as a blockbuster to date [213]. For the experiments in Hungary, ASA (>99%) was purchased from Sigma Aldrich (Budapest, Hungary) and Molar Chemicals (Budapest, Hungary). For the experiments in the United States, ASA was purchased from Acros Organics (New Jersey, US).

Carvedilol (CAR)

Carvedilol is a non-selective beta blocker, indicated in the treatment of mild to moderate congestive heart failure and high blood pressure (Figure 10b) [214]. It has a poor water solubility (20 mg/L at pH = 6.8) and undergoes significant first pass metabolism after administration. This results in an absolute bioavailability of about 25%. Carvedilol was obtained from Sigma Aldrich (Budapest, Hungary).
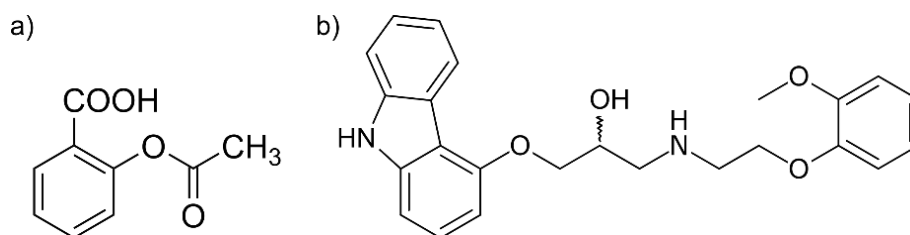

Figure 10. Molecular structure of (a) acetylsalicylic acid and (b) carvedilol.

3.2 Excipients

Table 2. List of reagents used in synthesis.
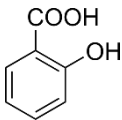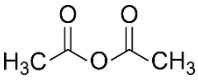
Chemical name	Structure	Supplier	Characteristics
Salicylic acid (SA)	COOH OH	Sigma Aldrich (Budapest, Hungary); Fischer Scientific (US)	Biologically active metabolite of ASA, white powder (>99%)
Acetic anhydride (Ac$_2$O)	H_3C–O–CH_3 (O, O)	Sigma Aldrich (Budapest, Hungary)	Colorless liquid, smells strongly as acetic acid (99%)

Table 3. List of excipients used for formulation.

Chemical name	Brand name	Structure	Supplier	Characteristics
Polyvinylpyrrolidone K30 (PVPK30)	Kollidon® 30	Figure 11a	BASF (Ludwigshafen, Germany)	M_w: 40000 Da
Polyoxyethylen sorbitan mono-oleat	Tween® 80	Figure 11b	Sigma Aldrich (Budapest, Hungary)	Viscous liquid M_w: 1310 Da
α-1,4-; α-1,6-glucan	Pullulan®	Figure 11c	Hayashibara Co., Ltd. (Okayama, Japan)	Commonly applied excipient in food industry, white powder
(2-Hydroxypropyl)-β-cyclodextrin (HPβCD)	HPβCD	Figure 11d	Cyclolab Cyclodextrin Research and Development Laboratory Ltd.	Molar substitution nominal value: DS = 4.3

			(Budapest, Hungary)	
Citric acid	-	Figure 11e	Sigma Aldrich (Budapest, Hungary)	White powder used for buffering agent and pH modifier
Microcrystalline cellulose (MCC)	Vivapur® 200	Figure 11f	JRS Pharma GmbH (Rosenberg, Germany)	Applied as a filler and binder in tablets, mean particle size = ~200 μm, bulk density 0.31-0.37 g/cm^3

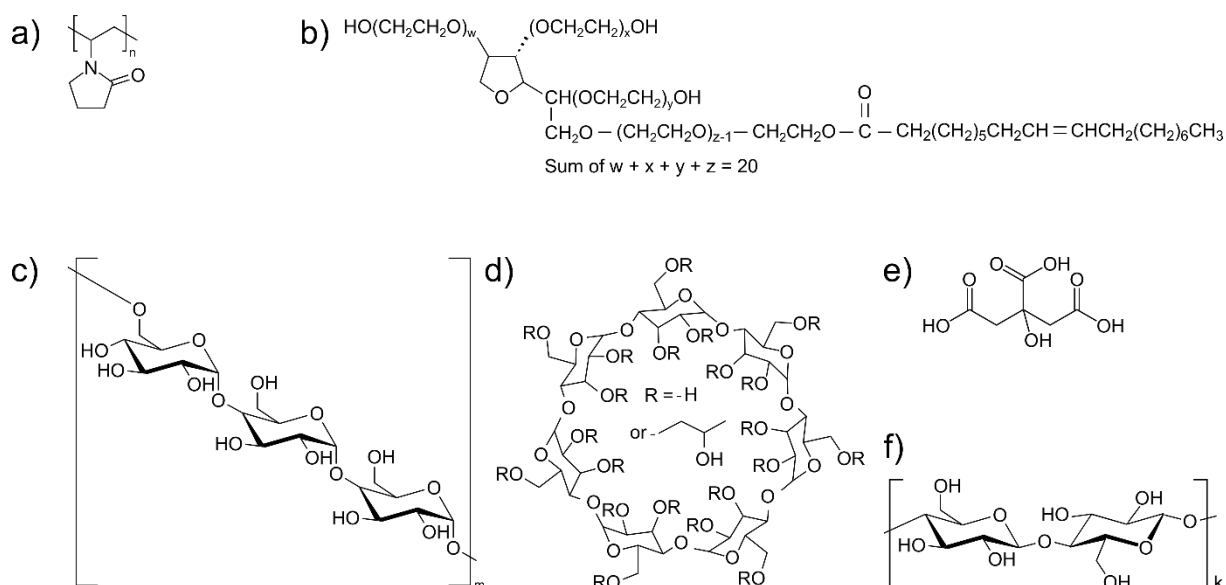Figure 11. Chemical structure of (a) PVPK30, (b) Tween® 80, (c) pullulan, (d) HPβCD, (e) citric acid and (f) MCC.

3.3   Other materials

Acidic ion-exchange resin (Amberlite IR-120), **formic acid (HCOOH)** (95-97%), **phosphoric acid (H$_3$PO$_4$)** (85 wt%), **sulfuric acid (H$_2$SO$_4$)** (96%), **hydrochloric acid (HCl)** (37%) were purchased from Sigma Aldrich (Budapest, Hungary).

Ethyl acetate (EtOAc), **methanol (MeOH)**, **acetonitrile (ACN)**, **ethanol (EtOH)**, **acetic acid (AcOH)**, *N,N*-**dimethylformamide (DMF)**, **dimethyl sulfoxide** and **deuterated methanol (CD₃OD)** were obtained from Merck (Budapest, Hungary).

For the experiments in the United States, lab grade **EtOAc**, **EtOH**, **AcOH**, **H₃PO₄ (85 wt%)** and **heptane** was purchased from Fisher Scientific (US).

3.4 Methods

3.4.1 Flow chemistry experiments

The continuous synthesis of ASA was carried out in flow reactors constructed of PTFE tubing (1.59 mm OD, 0.79 mm ID). T-mixers (Supelco, 57661) and fittings compatible with the tubing were purchased from Sigma Aldrich. The reagents and solutions were fed by Syrris Asia® syringe pumps and a Jasco PU-980 pump. An SSITM flow-through back-pressure regulator (BPR) (Supelco, 59284) adjusted to 4 bars was used to maintain constant fluid flow conditions.

3.4.2 Electrospinning (ES)

3.4.2.1 Optimization of the ES processes

Preliminary ES tests were conducted using an NT-35 high voltage direct current supply (MA2000; Unitronik Ltd, Nagykanizsa, Hungary). The electrical potential applied on the spinneret electrode was varied between 15-30 kV. During optimization of ES, a grounded aluminum plate covered with aluminum foil was used as collector. The distance of the spinneret and the collector was 20 cm. Solutions of the polymeric excipient and the drug were prepared for electrospinning using a magnetic stirrer (600 rpm). The solutions were transferred by a SEP-10S Plus type syringe pump (Aitecs, Vilnius, Lithuania) through a needle spinneret (1 mm ID, 2 mm OD) at predetermined flow rate.

The ES experiments including those with the continuous system were conducted at 25 ± 1°C and a relative humidity of 50 ± 10%.

3.4.2.2 Continuous production of ASA/CAR-loaded orally dissolving webs (ODWs)

The continuous system contained an ES unit, which was equipped with the same NT-35 high voltage direct current generator. The solution was transferred either from drug synthesis (ASA) or by the same SEP-10S Plus type syringe pump (CAR). A rotating drum collector was applied with a metal surface made of 1 mm thick aluminum sheet connected to earth. For further details see Section 4.1.4 and 4.2.5.

3.4.3 Film casting of the pullulan carrier

250 mg pullulan, 10 mg Tween® 80 and in the case of CAR-loaded ODWs, 120 mg citric acid was added to 1490 mg purified water and stirred until a clear solution was obtained. Commercial red food coloring (Dr. Oetker, Germany) was added to the solution to improve the observability of the deposition of the white fibers on the film. The solution was spread on a glass surface and casted by a film applicator in predetermined thickness of 30 μm. The smooth pullulan films were dried for 24 hours under ambient conditions. The final red pullulan film could be readily removed from the glass surface by manually pulling it off. It should be noted that for longer experiments with the continuous system not pullulan, but a similar strip made of polypropylene (available in larger quantity) was used.

3.4.4 Continuous crystallization

A 500 mL round-bottom jacketed vessel was used as an MSMPR crystallization reactor. Masterflex L/S peristaltic pumps were applied to feed the antisolvent and the reaction mixture of ASA into the crystallizer. A Huber Ministat 230 thermostat was used for temperature control through a PT100 thermocouple. An overhead stirrer with a PTFE three-blade retreat curve impeller provided the proper agitation of the system, which was set to 550 rpm in the case of each experiment. The volume of the suspension in the crystallizer was set to 360 mL every time.

3.4.5 Continuous filtration

A continuous filtration carousel (CFC) device was used for the filtration and drying of the ASA crystals (Alconbury Weston Ltd., UK) [157]. The schematic drawing and the picture of the CFC are shown in Figure 12. During operation, small-scale Nutsche filtrations were repeated in an automated manner. The main filtration unit was a rotating carousel with five cylindrical chambers (1.52 cm diameter, 8.89 cm height), of which ports 1-4 were used to filter, wash and dry the filter cake, respectively, and the product was discharged at port 5 by a moving piston. The bottom of chambers in positions 1-4 was covered by a kidney-shaped Poremet metal filter (20 μm pore size), while the 5th position was open to the air. The device used vacuum to transfer slurry from a feeding vessel and to filter the crystals in the filtration carousel. For this purpose, an external vacuum pump was connected to the apparatus (200 mmHg). The filtrate was collected in the receiving vessel. The CFC was equipped with user-controlled washing and automated clean-in-place (CIP) capabilities to prevent the fouling of the filter medium. In continuous mode, the throughput of the device could be changed by varying the volume of the transferred slurry and by adjusting the cycle time (t_c). This was the time interval during which

a slurry portion was being filtered and dried before moved to the next position by the rotating carousel. A more detailed description of the CFC operation mechanism can be found in previous publications [157,215].
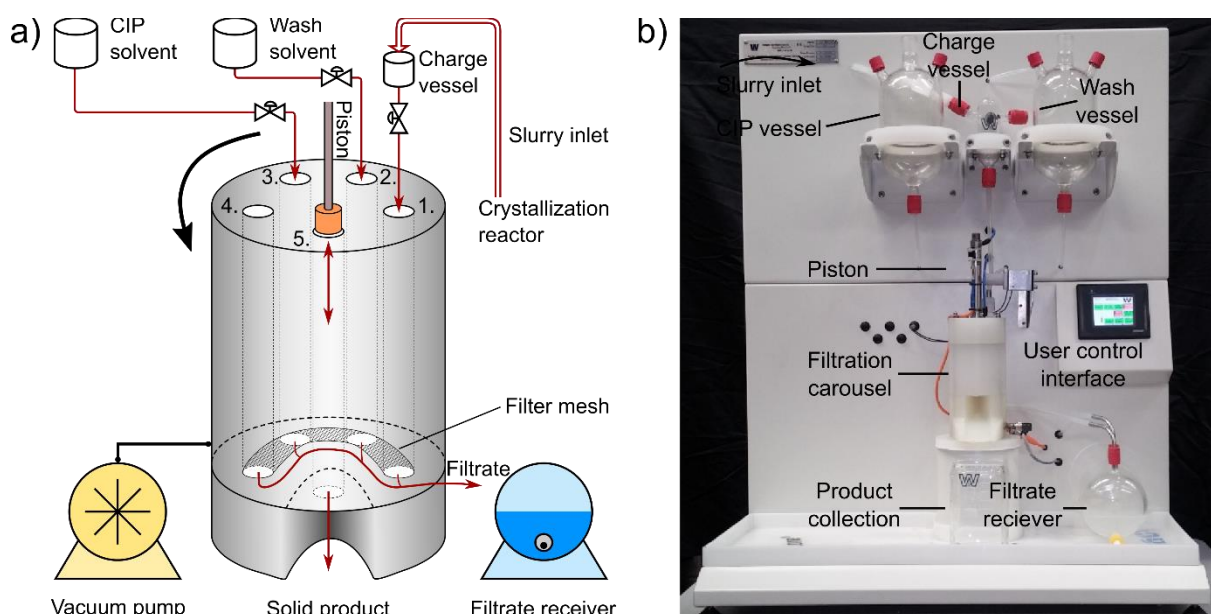

Figure 12. (a) The schematic drawing and (b) the picture of the continuous filtration carousel (CFC).

3.4.6   Continuous crystallization-filtration experimental procedure

At the beginning of the experiments, the thermostat (Huber Ministat 230) was turned on to adjust the temperature of the cooling liquid. Then 30 mL of reaction mixture was mixed with 60 mL of heptane in a beaker and poured into the crystallizer after the nucleation started (~15 s). Stirring was set to 550 rpm and the feeding of the two liquid streams was started corresponding to the actual residence time. The reactor was filled up to 360 mL working volume during each experiment. The continuous operation of the crystallizer began when the volume of the stirred suspension reached the setpoint, and the product removal adjusted to the liquid input was started by turning on the CFC. The time required for filling up the reactor was enough to reach the target temperature of the crystallization.

In the case of the integrated continuous crystallization-filtration experiments, instead of using an additional pump, the inlet tubing of the CFC served as the outlet of the MSMPR reactor. Thus, in order to keep the system in equilibrium, it was necessary to reach the total inlet flow rate of the crystallizer provided by the peristaltic pumps using the semi-continuous slurry transfer mechanism of the CFC. This was accomplished by calibrating the transferred volume (V, mL) to 10 mL in each cycle, and the frequency of the transfers, *i.e.* cycle time (t_c, min) was set to reach the required flow rate (F, mL/min) (Eq. 1).

$$t_c = \frac{V}{F} \tag{1}$$

3.4.7   Continuous homogenization and tableting

The blending and tableting of the crystallized, filtered and dried ASA were carried out using a similar technological line as in a previous work by Nagy *et al.* (Figure 13) [179]. A continuous twin-screw multipurpose equipment, TS16 QuickExtruder® (Quick 2000 Ltd., Hungary) was used in continuous blending mode. A screw diameter of 16 mm (25 L/D ratio) was used to mix ASA and MCC as an excipient. ASA was fed by a single-screw feeder in volumetric mode (FPS Pharma, Fiorenzuola d'Arda, Italy), while MCC was dosed by a Brabender twin-screw loss-in-weight gravimetric feeder (Brabender® GmbH & Co., Germany). The powder leaving the continuous blender was carried further by a belt conveyor towards tableting. A NIR probe was mounted above the conveyor to collect real-time spectra of the moving powder mixture using the reflection NIR mode. Tableting of the blend was carried out in a Dott Bonapace CPR-6 eccentric tablet press equipped with a gravity feeder with a moving shoe and a single concave punch. Biconvex tablets were produced in automatic mode with a diameter of 14 mm. This is a practical laboratory setup for process and analytical method development. In an industrial environment the blender and the tableting machine could be directly connected further reducing footprint [216].
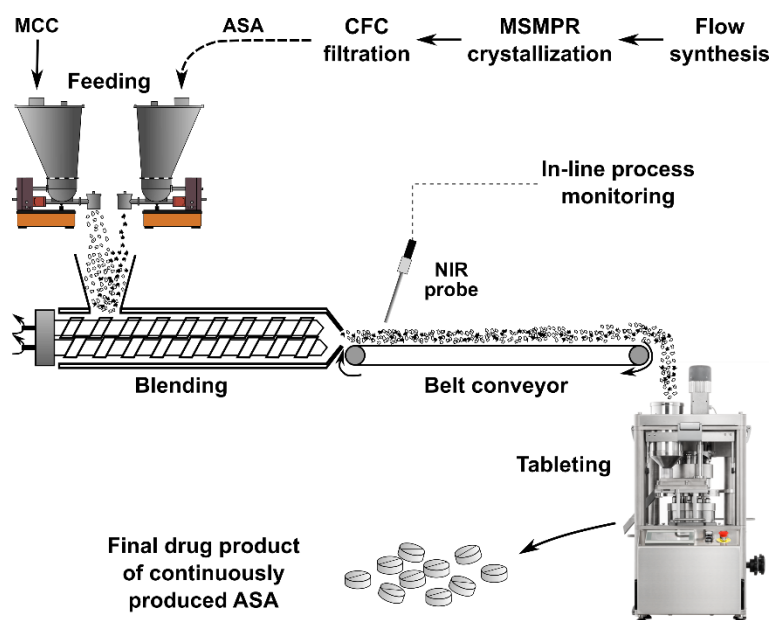

Figure 13. Experimental setup for the continuous blending and tableting of the CFC-filtered ASA.

The blending experiment was initiated by setting 50 rpm in the twin-screw blender, and by starting to feed ASA and MCC together into the hopper. A total mass flow of 300 g/h was set

during the process with an API content of 20%. This was reached by 60 g/h ASA and 240 g/h MCC feeding rate. Although this relatively low throughput is presumably less challenging for *e.g.* NIR monitoring, the mass flow was chosen to emphasize the integration of the individual steps, and to examine the technological line as a whole. However, NIR spectroscopy can be applied for even industrial-scale throughputs, as it was demonstrated by Pauli *et al.* (up to 70000 tablets per an hour) [217]. Tableting was started after a small amount of material was accumulated in the feed pipe of the tablet press, in order to prevent running out of powder and producing deficient tablets. Direct compression of tablets was performed with a compression force of approximately 10 kN. The tablet weight was set to 500 mg. The ASA-MCC powder blend was an excellent self-lubricating material mixture, thus no additional lubrication was applied.

3.5 Analytical methods

3.5.1 HPLC analysis

3.5.1.1 Analysis of ASA samples

The purity of ASA in the reaction mixture, in the electrospun solid dosage forms and in the filtered product was determined using RP-HPLC (Agilent 1200 series LC System). An isocratic elution of water containing 0.5% phosphoric acid and ACN (40:60 V/V ratio) was performed at a flow rate of 1.5 mL/min and 25°C for 7 min. The UV detection wavelength was set to 237 nm. Samples of ASA were prepared at 50 µg/mL concentration using a mixture of ACN, MeOH and phosphoric acid (85%) (92:8:0.5 V/V ratio) as solvent due to the limited chemical stability of ASA [218]. Samples containing PVPK30 were diluted or dissolved in MeOH due to the precipitation of the polymer with ACN. A 3 µL of sample volume was injected onto a Supelco Inertsil ODS-2 C18 column (5 µm; 250 × 4.6 mm). The amount of the impurities was determined based on the peak areas.

3.5.1.2 Analysis of CAR samples

Quantitative analysis of CAR in the cut solid dosage forms and during dissolution was determined using RP-HPLC (Agilent 1200 series LC System). An isocratic elution of water containing 0.5% phosphoric acid and ACN (60:40 V/V ratio) was performed at a flow rate of 1.0 mL/min and 25°C for 5 min. The UV detection wavelength was set to 285 nm. A 5 µL of sample volume was injected onto a Phenomenex Luna 3 µm C18 column (3 µm; 100 × 4.6 mm).

3.5.2 HPLC-MS measurements

The identification of major impurities in the synthesized reaction mixture was carried out using HPLC-MS. The measurements were performed using an Agilent 1200 liquid chromatography system coupled with an Agilent 6130 single quadrupole mass spectrometer equipped with an ESI ion source (Agilent Technologies, Palo Alto, CA, USA). Analysis was performed at 40°C on a Supelco Inertsil ODS-2 C18 column (5 µm; 250 × 4.6 mm) with a mobile phase flow rate of 0.6 mL/min. Composition of eluent A was pure ACN, while eluent B was 0.1 V/V% HCOOH in water. The ratio of eluent A and B was 60:40 V/V%. The injection volume was 3 µL. The chromatographic profile was registered at 237 nm. The operating parameters of the mass selective detector were set as follows: positive ionization mode (70 eV), scan spectra from m/z 120 to 1200, drying gas temperature 300°C, nitrogen flow rate 12 L/min. Spray chamber was pre-flushed with 0.1% solution of NH_4CO_3 in ACN/water (92:8 V/V ratio).

3.5.3 Gel permeation chromatography

Gel permeation chromatography tests were conducted to investigate the chemical changes of PVPK30 during quenching. A HPLC system comprising a Waters 515 HPLC pump, Jetstream 2 Plus column heater and a Jasco RI-4035 Refractive Index Detector was used for the measurements. Prior to analyses the PVPK30 samples were prepared by suspending ca. 0.5 g of solid material in 3 mL of EtOAc, then dissolving the polymer by adding 0.5 mL of MeOH. The obtained clear solution was stirred on elevated temperature (80°C) in order to evaporate the solvents. Thus, the PVPK30 precipitated from the remaining solution rich in EtOAc. Following cooling in ice bath the suspension was vacuum filtered and dried. The PVPK30 samples were dissolved again in *N,N*-dimethylformamide obtaining an 1 mg/mL solution; 200 µL of this stock solution was injected onto Waters Styragel HT 2 and HT 4 columns connected consecutively. The mobile phase consisted of *N,N*-dimethylformamide containing 0.05 M LiBr. The measurements were performed at 85°C column temperature and 1 mL/min flow rate after 24 h of equilibration. For data analysis PSS WinGPC software was used.

3.5.4 NMR measurements

^{1}H NMR spectra were obtained on a Bruker DRX-500 instrument on 500 MHz at 25°C, while ^{13}C NMR spectra were recorded on a Bruker-300 instrument on 75 MHZ at 25°C. Samples were dissolved in CD_3OD setting concentrations to 18.75 mg/mL. Tetramethylsilan was used as internal standard and chemical shifts were given in ppm.

3.5.5 Scanning electron microscopy (SEM) and fiber diameter analysis

Morphology of the electrospun samples was investigated by a JEOL 6380LVa (JEOL, Tokyo, Japan) type scanning electron microscope. Each specimen was fixed by conductive double-sided carbon adhesive tape and sputter-coated with gold prior to the examination. Applied accelerating voltage and working distance were 15-30 kV and 10 mm, respectively. A randomized fiber diameter determination method was used based on SEM imaging as described in our previous work [219], n = 100 measurements were made on each sample.

3.5.6 Differential scanning calorimetry (DSC)

Differential scanning calorimetry measurements were carried out using a Setaram (Calure, France) DSC 92 apparatus (sample weight: $\sim$10-15 mg, open aluminum pan, nitrogen purge gas). The temperature program consisted of an isothermal period, which lasted for 1 min at 25°C, with subsequent linear heating from 25°C to 200°C at the rate of 10°C/min. Purified indium standard was used to calibrate the instrument.

3.5.7 X-ray powder diffraction (XRPD)

Powder X-ray diffraction patterns were recorded by a PANanalytical X'pert Pro MDP X-ray diffractometer (Almelo, The Netherlands) using Cu-Kα radiation (1.542 Å) and Ni filter. The applied voltage was 40 kV while the current was 30 mA. The untreated materials, a physical mixture composition, the casted pullulan film and the fibrous samples as spun were analyzed for angles 2θ between 4° and 42°.

3.5.8 Phase solubility studies of CAR

The solubility studies were carried out by adding excess quantity of CAR to the dissolution media, which was either 25 mM KH_2PO_4 (pH = 6.8) buffer or purified water containing HPβCD in different concentrations (0, 5, 10, 15 mM). The suspensions were stirred by magnetic stirrer for 4 hours at 25°C, and then filtered through 0.45 µm PTFE membrane filters (La-Pha-Pack, Germany). The filtrated solutions were diluted with purified water according to the CD concentrations (from 10 to 100-fold) and the dissolved CAR content was determined by HPLC (see Section 3.5.1.2).

3.5.9 In vitro dissolution tests

3.5.9.1 ASA-loaded ODW formulations

The *in vitro* dissolution tests of 30 × 30 mm cut pullulan films covered with different amounts of ASA-loaded fibers were carried out by dissolving them in purified water. Layered ODWs corresponding to 1, 5, 12.5, 25 and 50 mg ASA doses were placed in Petri dishes

containing 10 mL dissolution media. The dissolution of the ODWs was recorded using a Lenovo P70 camera device. After 10 min the dissolved ASA quantity was confirmed by HPLC measurements using the same method as during purity testing (Section 3.5.1.1).

3.5.9.2   CAR-loaded ODW formulations

The *in vitro* dissolution tests of 30 × 30 mm cut pullulan films covered with fibers containing 6.25 mg doses of CAR were carried out by dissolving them in 25 mM KH_2PO_4 buffer (pH = 6.8). The dissolution rate of the layered ODWs was compared to pure crystalline CAR and the physical mixture of CAR and the pullulan combined with citric acid. The samples were placed in glass vessels containing 20 mL of dissolution media stirred by magnetic stirrer (100 rpm) at 25°C. 50 µL of samples were taken at 1, 2, 3, 4, 5, 10, and 30 min, and diluted 20 times with purified water and the dissolved CAR quantity was analyzed by HPLC (Section 3.5.1.2).

3.5.10 Disintegration tests

The disintegration of the double-layered CAR-loaded formulation was carried out using a procedure similar to the slide frame method [220,221]. The 30 × 30 mm cut films covered with fibers were fixed at the corners of a plastic plate with a center hole and a 25 µL droplet of purified water was placed on the film by pipette. The disintegration of the ODWs was filmed using a Lenovo P70 camera device. The endpoint was reached when the droplet bore a hole through the formulation.

3.5.11 Content uniformity tests (CU)

3.5.11.1 ASA- and CAR-loaded electrospun ODW formulations

In order to investigate the consistency of the dosage units content uniformity measurements were carried out. The system was operated in steady state either for 8 hours (ASA) or for 4 hours (CAR), and in each hour 10 cut film samples were dissolved either in purified water (ASA) or in a mixture of ACN and water containing 0.5% H_3PO_4 (20:80 V/V ratio) in 50 mL volumetric flasks. The deposited ASA/CAR dosage on the carrier was measured with HPLC either without further (ASA) or after appropriate (CAR) dilution using the HPLC method described in Section 3.5.1.1 (ASA)/ in Section 3.5.1.2 (CAR).

3.5.11.2 ASA-loaded compressed tablets

Content uniformity measurements were carried out to investigate the consistency of drug content in the continuously produced tablets. 10 tablets from the steady state were dissolved in

volumetric flasks in HCl buffer (pH = 1.2). The ASA quantity in each tablet was measured using the previously described HPLC method after appropriate dilution (Section 3.5.1.1).

3.5.12 Residual solvent content determination

3.5.12.1 Measurement of ASA-loaded fibers

The residual solvent content of the electrospun fibers was determined by gas chromatography (GC) in the case of EtOH and EtOAc and by HPLC in the case of AcOH.

The determination of EtOH and EtOAc was performed on an Agilent 6890 N GC system combined with a CTC Combi PAL HS autosampler. A 10 m long HP-INNOWax capillary column with 0.25 mm inner diameter and 0.25 µm film thickness with polyethylene glycol stationary phase was used for separation. Helium (purity: 99.999%) was used as carrier gas with a constant flow rate of 1.7 mL/min. Split injections of 250 µL were made at a split ratio of 50:1. The temperature of the injector was maintained at 250°C and samples were thermostated at 140°C for 3 min. For detection an Agilent 5973 inert mass selective detector was used with electron collisional ionization (70 eV). Samples for GC measurements were prepared by dissolving ca. 50 mg fibers in 6 mL of dimethyl sulfoxide in 20 mL GC vials.

For the determination of AcOH content, a RP-HPLC (Agilent 1200 series LC System) method was developed based on isocratic elution of water containing 0.5 V/V% phosphoric acid and ACN (95:5 V/V ratio). The chromatography tests were performed at a flow rate of 1.5 mL/min and 25°C for 5 min. The UV detection wavelength was set to 210 nm. Samples containing the PVPK30-based fibrous samples were dissolved in purified water due to the precipitation of the polymer in ACN. 20 µL of this solution was injected onto a Supelco Inertsil ODS-2 C18 column (5 µm; 250 × 4.6 mm). The non-eluting compounds such as ASA and SA were periodically washed off after 15 injections with a mobile phase of 0.5 V/V% phosphoric acid and ACN (30:70 V/V ratio) and then the column was re-equilibrated for 60 min prior to further analyses. The amount of the AcOH was determined based on the peak area.

3.5.12.2 Measurement of CAR-loaded fibers

The residual solvent content of the electrospun fibers was determined by gas chromatography (GC) in the case of EtOH and by HPLC in the case of DMF.

The determination of EtOH content was performed on a Perkin Elmer Autosystem XL Gas Chromatograph system combined with a Perkin Elmer Headspace Sampler HS 40 autosampler. A 30 m long Elite-624 capillary column with 0.53 mm inner diameter and 3.0 µm film thickness

with (6%-cyanopropyl-phenyl)-94%-dimethylpolisiloxane stationary phase was used for separation. Nitrogen (purity: 99.996%) was used as carrier gas with a constant inlet pressure of 1.2 bar. Samples were thermostated at 120°C for 20 min. The needle was thermostated at 130°C and the transfer line at 140°C. Samples were pressurized for 1 min, the injection time was 0.15 min and the withdrawal time was 0.5 min. The GC injector was held at 150°C. The column was set at 35°C for 2 min, then heated to 100°C with a 30°C/min rate and the final temperature was held for 3 min. The flame ionization detector was thermostated at 220°C, the flow rates for hydrogen and air were 45 and 450 mL/min, respectively. Samples for GC measurements were prepared by dissolving ca. 20 mg fibers in 1 mL dimethyl sulfoxide in 20 mL GC vials.

For the determination of DMF content a RP-HPLC (Agilent 1200 series LC System) method was developed based on isocratic elution of water containing 0.5% phosphoric acid and ACN (95:5 V/V ratio). The chromatography tests were performed at a flow rate of 1.0 mL/min and 25°C for 8 min. The UV detection wavelength was set to 210 nm. The fibrous samples were dissolved in a solvent mixture identical to the eluent. 5 µL of this solution was injected onto a Phenomenex Luna 3 µm C18 column (3 µm; 100 x 4.6 mm). The non-eluting compounds such as CAR was periodically washed off after 15 injections with a mobile phase of 0.5% phosphoric acid and ACN (30:70 V/V ratio) and then the column was re-equilibrated for 60 min prior to further analyses. The amount of the DMF was determined based on the peak area.

3.5.13 FTIR spectroscopy during the flow chemistry experiments

IR spectra were recorded using a Bruker Alpha FTIR spectrometer (Bruker Optik GmbH, Ettlingen, Germany) equipped with an on-line diamond ATR flow cell and an RT-DLaTGS detector. All spectra were collected in the spectral range of 4000-400 cm^{-1} with 32 co-added scans at a resolution of 4 cm^{-1}. The spectrometer recorded a full spectrum in every 30 s. The background was acquired using a solvent mixture identical with that used in the acetylation reactor (see Table S8).

3.5.14 Raman spectroscopy

A Kaiser RamanRxn2® Hybrid analyzer (Kaiser Optical Systems, Ann Arbor, USA) coupled with PhAT (Pharmaceutical Area Testing) probe was utilized in reflection mode to acquire the spectra of the pullulan film covered with ASA-loaded fibers. Prior to analysis, controlled doses of fibers were electrospun on cut films. Each sample was illuminated by a 400 mW, 785 nm Invictus diode laser on 3 different positions, and the reflected Raman photons were collected by the PhAT probe. The diameter of laser spot size was optically expanded to

6 mm and the nominal focus length was 250 mm. Spectra were acquired in the spectral range of 200-1890 cm^{-1} with a resolution of 4 cm^{-1}. Acquisition time of 30 s was required to achieve spectra with the desired quality.

3.5.15 Particle size measurements

The particle size distribution (PSD) of the ASA crystal samples was measured using a Malvern Mastersizer 3000 Aero S. A standard venturi dispenser and a general-purpose tray with hopper was used. During the measurements 1 bar air pressure, 100% feeding rate, 10 s background measurement, 22.15 s sample measurement and 1-20% obscuration was applied. The set particle type was non-spherical. The refractive index of ASA was 1.5623, the absorption index 0.01, and the density $\rho = 1.39$ kg/m^3. The mean crystal size was characterized in terms of the equivalent volume-weighted moment mean diameter also known as the De Brouckere mean moment diameter (D43) [222].

3.5.16 Crystal flowability tests

The flowability of ASA was measured by filling 100 g material into a metal funnel with a circular orifice at the bottom (15 mm diameter). The time required for the crystals to flow out of the funnel was measured in triplicate.

3.5.17 NIR spectroscopy and spectral evaluation of the continuous blending and tableting experiment

A Bruker MPA FT-NIR (Bruker Optik GmbH, Ettlingen, Germany) spectrometer equipped by a Solvias fiberoptic probe was used for spectra collection in reflection mode. Each NIR spectrum was collected by accumulating 16 scans in the case of the at-line measurement of the tablets and 4 scans for the in-line measurement of blending with 8 cm^{-1} resolution at the range of 4000-12500 cm^{-1}. During the continuous blending experiment, the ASA concentration was calculated from approximately the same mass as of the tablets, since 4 scans were completed in ~3.5 s, and ASA concentration was calculated from the average of 2 spectra. Spectrum accumulation was completed using OPUS® 7.5 software (Bruker), while the real-time evaluation of the spectra was carried out using MATLAB 9.7. (MathWorks, USA) and PLS Toolbox 8.7.1. (Eigenvector Research, USA). A Matlab script and an interface have been developed in-house to import the acquired spectra to Matlab in real-time. After that, another script was used to carry out the chemometric analysis using the PLS model developed in PLS Toolbox. Partial Least Squares (PLS) calibration model was applied for the determination of the ASA content in the powder blend and in the tablets.

4 Results and discussion

4.1 Coupling flow synthesis and formulation by electrospinning

In this work phase we developed an end-to-end continuous model system (CMS) using ES as the key technology to turn the synthesized API solution into a fibrous solid product with the incorporation of a polymer. Both synthesis and formulation were monitored by PAT tools with chemometric analyses. Acetylsalicylic acid (ASA) was selected as the model drug being one of the oldest APIs still marketed. Accordingly, continuous production of a beneficial electrospun orally dissolvable ASA formulation was envisioned to target the treatment of cardiovascular diseases. The design consideration details of our benchtop-scale CMS (described as a whole in Figure 23) are presented along with the results of detailed product analyses and system performance testing.

4.1.1 Optimization of the acetylation step of ASA synthesis

To begin with, the optimal parameters and composition of the reaction mixture had to be found for continuous-flow synthesis of ASA. Further processing of the produced API by ES or continuous crystallization was also taken into consideration during the development of the synthesis. The first step of ASA synthesis was the acetylation of SA with excess Ac_2O. EtOAc was selected as solvent readily dissolving SA (concentration: 0.138 g/mL) and being also excellent for ES. Acid catalyst was also required for the fast and complete conversion of SA [223]. Besides many acids tested, such as H_2SO_4, HCl, acidic ion-exchange resin, H_3PO_4 was found to be suitable owing to its high activity and low toxicity.

The aim of the optimization of the acetylation step was to maximize the conversion of SA, minimize process time and impurity content. The effects of the applied amounts of Ac_2O and H_3PO_4, process temperature as well as residence time were explored with Design of Experiment (DoE) studies in batch reactors (Figure S1, Table S1). Higher temperatures (*e.g.* reflux) and more catalyst (*e.g.* 0.5 eq.) led to less favorable impurity profiles, while higher excess of Ac_2O (*e.g.* 10 eq.) did not result in practically better conversion rates. Accordingly, moderately large excess of Ac_2O (5 eq.), lower acid catalyst concentration (0.1 eq.) and 50°C process temperature was selected for starting parameters of flow experiments.

The impurity profile of the reaction mixture after the acetylation step was investigated using HPLC-MS in order to better understand the chemical background of ASA synthesis (Figure S2) The two main impurities of acetylation were identified as acetylsalicylic ethanoic

anhydride (*Impurity A*) and acetylsalicylic anhydride (*Impurity B*). While decomposition of *Impurity A* to pure ASA seemed to be possible with quenching, *Impurity B* turned out to be chemically resistant against nucleophiles. These findings were essential during further optimization of acetylation and the following quenching step.

After the batch experiments the optimization was carried out in continuous-flow reactors to achieve high ASA conversion rate and purity. Compared to the use of batch vessels, the continuous implementation of ASA synthesis resulted in more homogenous temperature distribution, allowed easier process monitoring and control. Wider temperature range was also available in pressurized tube reactors. The reactants were mixed and fed into a capillary tube reactor denoted as R1 (0.79 mm ID, PTFE) immersed into a heated oil bath and combined with a 4 bar BPR at the end. Optimal conditions of 55°C and 180 min residence time were determined with another two DoE studies (Figure S3-4. Table S3-4) reaching high conversion (>99%) and a favorable impurity profile (see next section).

4.1.2 *Optimization of the quenching step without or with a polymer*

A quenching step was required after acetylation not only to remove the excess Ac_2O, but also to convert *Impurity A* to ASA due to its high relative concentration of ∼60% in the reaction mixture (Figure 14a). Different nucleophilic substances were tested as quenching agent. Water appeared at first as a suitable choice, however, aqueous solutions can be processed poorly with ES due to the high specific heat of vaporization. Thus, EtOH was applied instead, generating EtOAc and AcOH from Ac_2O while turning *Impurity A* to pure ASA during quenching. It should be mentioned that the amount of the other major by-product of acetylation, the symmetric ASA anhydride, *Impurity B* remained unchanged under any condition of quenching. Nevertheless, the amount of *Impurity B* was minimized to <1% for this reason in the acetylation reaction. The simultaneous deacetylation of ASA back to SA was another hurdle to deal with in the development of quenching.
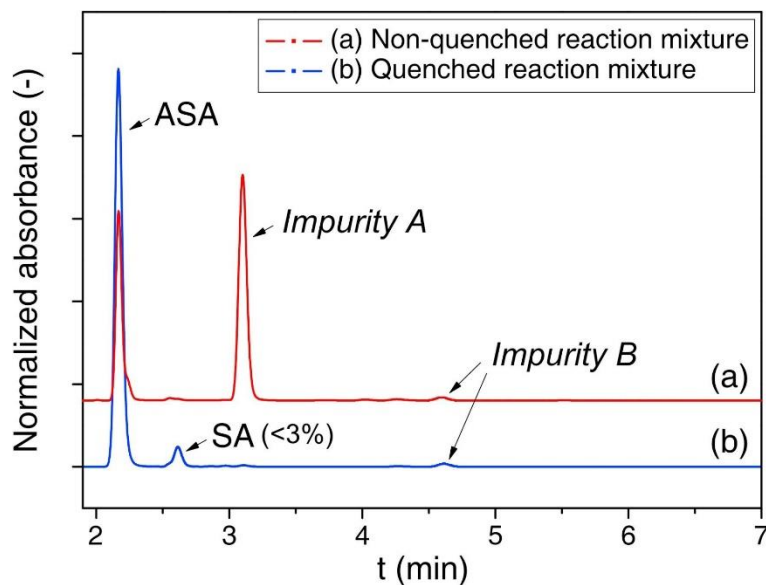
Figure 14. HPLC chromatograms of the optimized (a) non-quenched and (b) subsequently quenched (with PVPK30) reaction mixtures of the two-step continuous-flow ASA synthesis.

Our primary approach was feeding EtOH (1.3 eq. relative to excess Ac₂O) to the stream of the reaction mixture in flow reactors. Quenching was optimized utilizing further DoE studies to find the highest purity through varying temperature and residence time. At last, the optimal conditions were found to be 90°C and 26 min using pure EtOH. This method resulted in ≥95% ASA purity.

The introduction of a selected polymer (PVPK30) into the liquid flow required for final dosage formulation by ES can be carried out after quenching, but it is also possible to dissolve it in the quenching reagent if it is chemically inert under the conditions of quenching. PVPK30 is soluble in EtOH, however, EtOAc – the solvent of acetylation – can precipitate it. Small amounts of AcOH were added to the polymeric EtOH solution as co-solvent to prevent the undesired clogging. At last, 3.2 eq. of EtOH relative to the remained Ac₂O was found to be appropriate for quenching in combination with AcOH (3:1 (V/V) EtOH-AcOH ratio) and PVPK30. Yet another optimization of quenching was conducted for improving ASA purity with two DoE studies (Figure S6, Table S6-7). For the polymeric quenching in the second capillary reactor (denoted as R2) an optimum of 95°C and 20 min was found with ASA purity of >95% and SA content below 3% (Figure 14b).

Gel permeation chromatography measurements verified that no chemical reaction occurs with PVPK30 in the quenching reactor in the presence of Ac₂O at high temperature (Figure S7). The reaction scheme with the optimized conditions of the two-step flow synthesis of ASA is concluded in Figure 15. By applying these process parameters, high ASA purity (~95%) was

attained along with <3% SA as the main impurity according to the HPLC (Figure 14b) and NMR (Figure S8-9) measurements. These results were satisfactory enough to apply ES for formulation without an additional purification step in the continuous system.
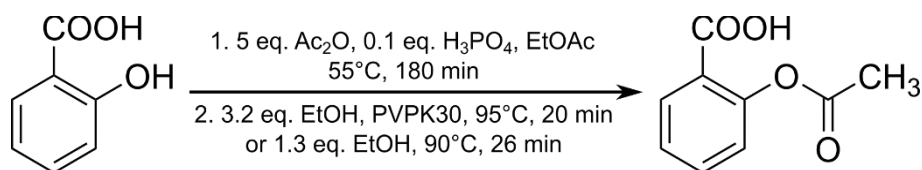

Figure 15. Optimized two-step flow synthesis of ASA providing high purity (>95%) with or without the presence of PVPK30 during quenching.

4.1.3   *Connecting flow synthesis and electrospinning*

There are two ways to connect ES with synthesis. The universal method involves mixing the API with a polymer directly after synthesis (or usually a continuous-flow final-product purification) to form a co-solution. Nevertheless, the polymer can also be added earlier into the API stream when assuming no chemical interactions with the reactants. PVPK30 was selected as polymer applicable in a fast dissolving formulation due to its excellent fiber forming property and good water solubility [224,225]. PVPK30 could be fed after synthesis or together with the quenching reagent (EtOH) without chemical alteration in the second capillary reactor (R2) as mentioned earlier thereby avoiding the use of an additional pump (see Section 4.1.2).

However, care must be taken with both the above explained approaches, since adjusting the critical parameters for ES (*e.g.* polymer concentration, flow rate) substantially affects the overall process design often in an iterative way. For instance, although the formerly explained addition of AcOH as co-solvent during quenching prevented the precipitation of PVPK30 in R2, but the optimal solution composition for the ES is shifted – in our case towards higher polymer concentrations – which might cause precipitation again in the capillary tubes.

Good quality PVPK30-ASA micro- and nanofibers could be obtained using ES with one needle type spinneret after adjusting the polymer concentration in the reaction mixture (Figure 16). The optimal PVPK30 concentration was determined to be 3.25 g in 10 mL pure solvent based on preliminary experiments (Figure S10). The feeding rate was fixed at 4 mL/h (or 67 µL/min), the continuously produced polymeric fibers contained approximately 18% (w/w) ASA and possessed an average diameter of 0.97 ± 0.25 µm. The morphology of the fibers did not deteriorate in a wide range of dosing rates (20-120 µL/min) indicating the robustness of ES for coupling with flow operations (Figure S11). Above a certain throughput – in our case ~7 mL/h – the excess polymeric solution dripped down from the spinneret instead of fiber formation.

Higher throughputs are achievable with the modified versions of ES such as alternating current ES [226] or high-speed ES [202]. However, latter cases would require different types of formulation unit design.
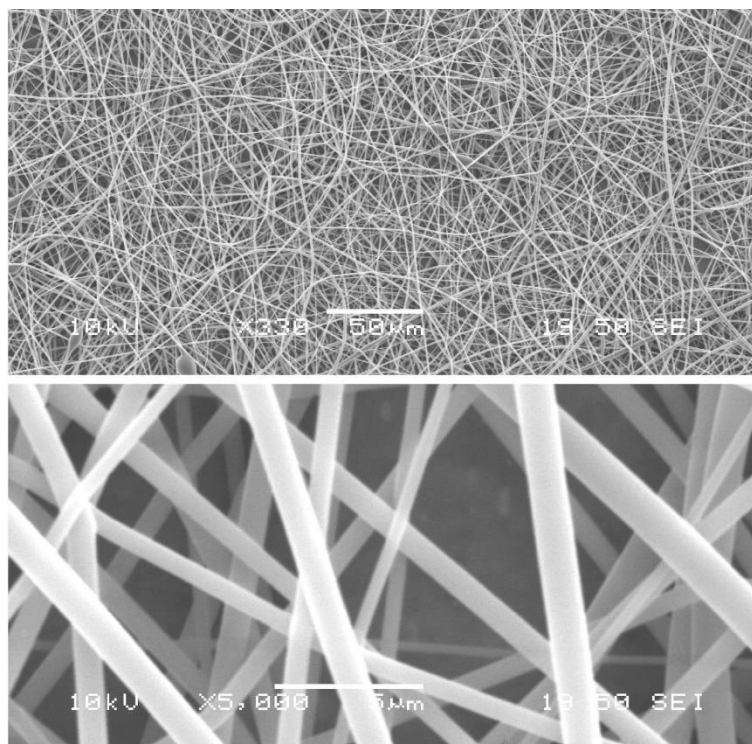

Figure 16. Scanning electron microscopic images of the optimized PVPK30-ASA fibrous product at different magnifications (4 mL/h, 20 kV).

The instantaneous conversion of the synthesized API stream into a solid electrospun product was carried out in the ES unit developed and built in-house (Figure 17a). The drying of the fibers was facilitated by applying active air ventilation in the otherwise closed box. Thus, ES can be considered as a special method to remove solvents. The solvents can be recovered from the purging air, for instance, with the use of a condenser [227].
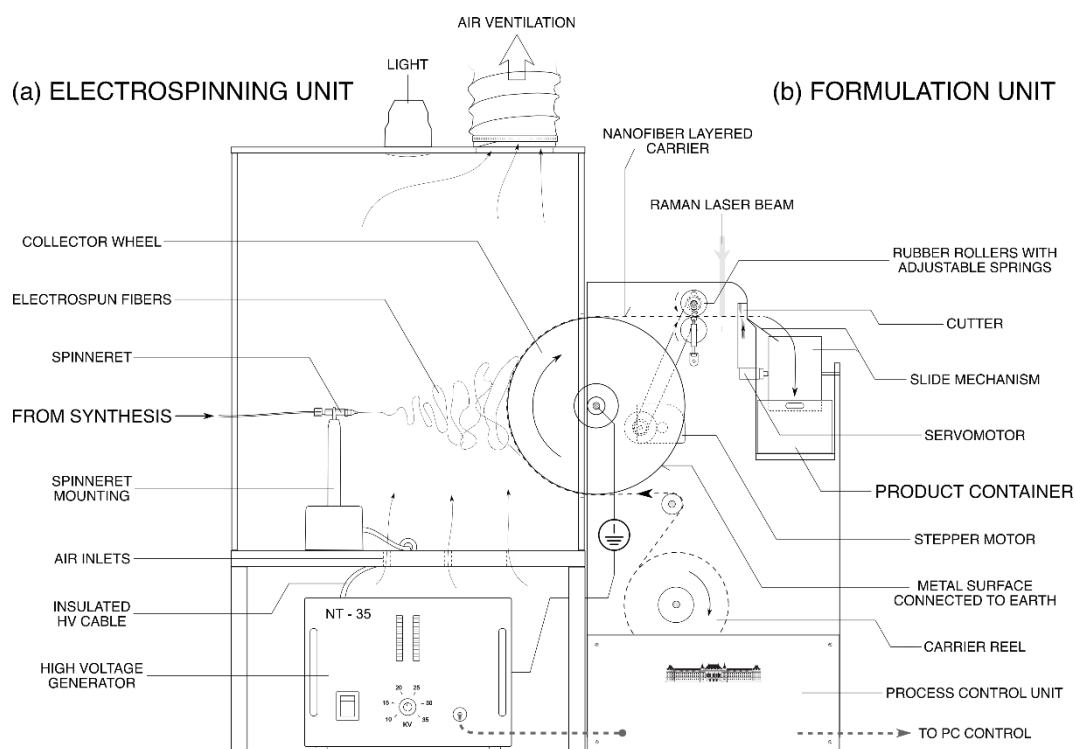
Figure 17. Schematic drawing of the (a) electrospinning and (b) formulation units developed to process synthesized API streams for the continuous production of layered orally dissolving webs.

4.1.4   Continuous formulation of layered fibrous ODWs

The collection of the fibers was a key challenge as it determines further formulation. For this purpose, another special feature of ES was exploited. Controlled deposition could be achieved through the attraction of the fibers towards a collector possessing a suitable wheel geometry as part of the ES unit (Figure 18a). The electrically grounded metallic surface of the wheel was covered with a long wide carrier sheet during ES; the deposited ASA-loaded nanofibers and the carrier film formed a double-layered composite structure. Pullulan, a water-soluble polysaccharide (Figure 11c), was applied to develop a carrier quickly dissolving in the oral cavity. Higher productivity can be achieved using melt-extruded water-soluble films. For modelling this case, the longer experiments were performed with a similar strip made of polypropylene (available in larger quantity). The PVPK30-ASA nanofibers were layered onto the 30 mm wide and ca. 30 μm thick film. The wheel was rotated slowly, thus ES combined with the electrostatic deposition on the carrier could be continuously operated to form consistent flat sheets without clogging (Figure 18b). Besides the good spinnability of PVPK30 and the use of a less volatile solvent mixture preventing undesired drying at the tip of the spinneret, careful optimization of solution concentration and adjustment of the electrostatic field strength were also essential for a stable operation of ES.
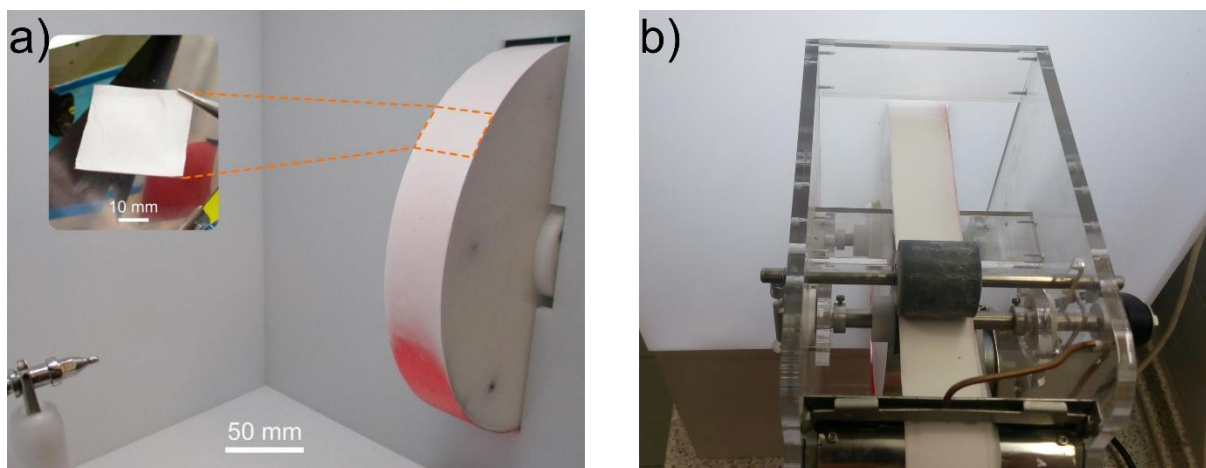
Figure 18. (a) Collection of the PVPK30-ASA electrospun product on the carrier film. The inset shows the final layered fibrous ODW. (b) The continuously conveyed double-layered strip with the deposited white ASA fibers and the cutter mechanism at the bottom of the picture.

The continuously conveyed ASA-loaded nanofibrous filmstrip was cut into single pieces (see the inset of Figure 18a) by a cutter device integrated into the developed formulation unit (Figure 17b, Figure 18b). Thus, the obtained dosage units can be considered as layered ODWs. ASA doses of 1, 5, 12.5, 25 and 50 mg were prepared with dimensions of 30 × 30 mm after cutting. In addition to factors inherited from the synthesis (*i.e.* mass flow rate and composition of the fibers), the drug dose can be quickly adjusted for each cut film through varying the parameters of film convection and cutting. Altering convection speed affects the thickness of the fibrous mat, while the size of the layered ODWs can be set by changing the time delay between two cuttings. Both mat thickness and the area of the covered surface contribute to the final dosage strength. This feature of the CMS also enables the approach of personalized medicine by being capable to produce tailored dosage units accommodating patient needs.

4.1.5   Product characterization and CMS testing

The physical state of ASA was investigated in the nanofibrous product by DSC and XRPD measurements (Figure 19). Both analytical techniques showed that ASA turned into an amorphous form during ES. The physical mixture of 5% crystalline ASA and PVPK30 served as reference to demonstrate the sensitivity of the methods. The DSC thermogram of the physical mixture clearly indicate the sign of ASA crystallinity as an endothermic melting peak at around 140°C beside the wide peak of water loss of amorphous PVPK30 below 120°C. In contrast, the melting peak of ASA is absent on the thermogram of the PVPK30-ASA nanofibers proving the amorphous state of the drug. The most intense characteristic X-ray diffraction peaks of crystalline ASA also appear on the diffractogram of the physical mixture at 2θ = 16.3°, 23.8°

and 27.7°. These signs of crystallinity could not be detected in the case of the PVPK30-ASA nanofibers in good accordance with the DSC results, only the amorphous humps of the polymer matrix emerge from the scattering background. The ultrafast drying effect of ES presumably froze the fibers into a solid solution where ASA is present molecularly dispersed in the polymer.
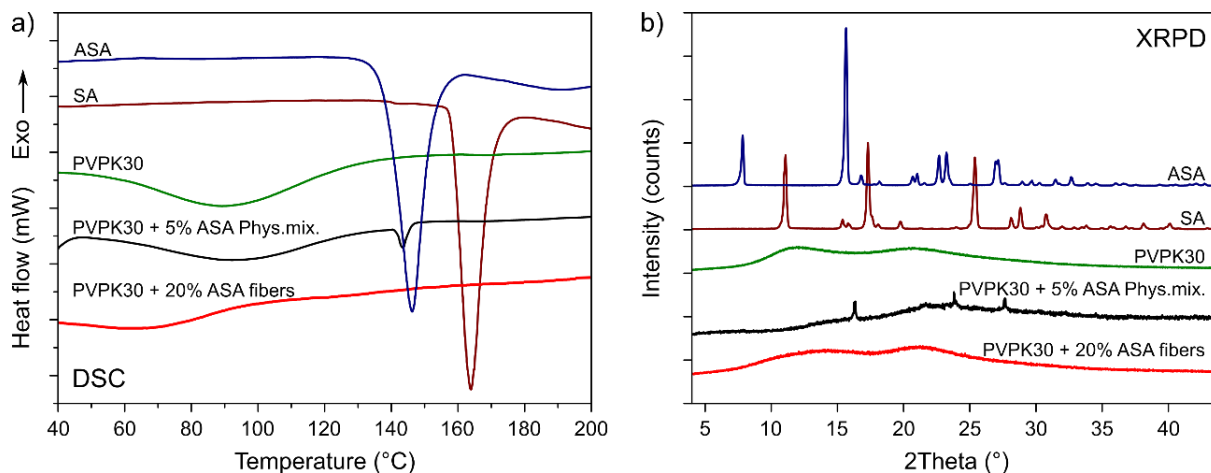

Figure 19. (a) Differential scanning calorimetry thermograms and (b) X-ray powder diffraction patterns of crystalline acetylsalicylic acid (ASA), salicylic acid (SA), PVPK30, physical mixture of PVPK30 and 5% ASA, and PVPK30 + 18%ASA electrospun fibers.

Dissolution tests were carried out with different doses of layered PVPK30-ASA nanofibers on pullulan carrier (Figure 20 and S12). The ODWs were dissolved in 10 mL purified water without additional stirring at 25°C. Between the range of 1 and 25 mg ASA doses the dissolution of the fibers was instantaneous, the nanofibers disappeared in less than 2-3 s. The dissolution of the red pullulan carrier was not so spectacular, but it also disintegrated within 10 s. The dissolution results were in good agreement with the information provided by the solid phase analyses. The ultrafast drug release can be attributed not only to the large surface area of the nanofibers, but also to the increased solubility of the amorphous form of ASA.

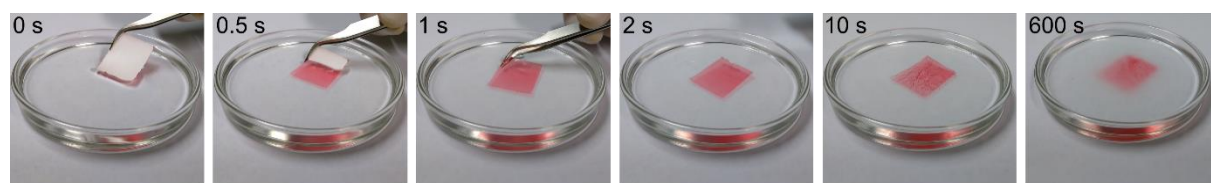**Figure 20. Dissolution test of layered PVPK30-ASA nanofibers on pullulan carrier of 5 mg ASA dose (10 mL purified water, 25 °C, without stirring).**

Residual solvent content measurements were conducted during a 4-hour long continuous operation in steady state. The results revealed satisfactorily low amount of solvents in the fibrous product (Figure 21a). The quantities of EtOH, EtOAc and AcOH were below the

regulatory limit (5000 ppm) in all cases [228]. The more volatile EtOH and EtOAc solvents with similar boiling points of 77-78°C were barely present in the fibers, concentrations below 1000 ppm could be determined. Even AcOH with a boiling point of 118°C could be eliminated using ES from the fibers obtaining around 4000 ppm concentration in the final product.
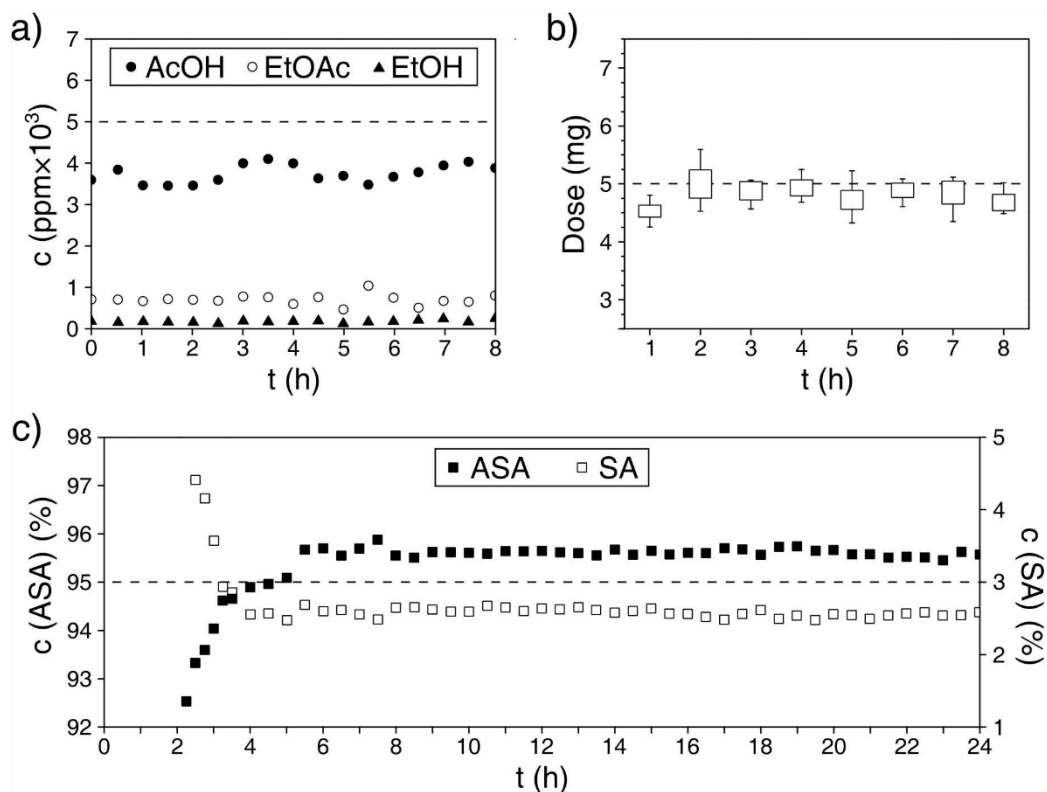

Figure 21. Quality attributes of ODWs over time produced by the CMS: (a) residual solvent content, (b) content uniformity, (c) and purity (HPLC). The dashed lines indicate either regulatory (residual solvent) or specified process (minimal accepted ASA purity and target dose) limits.

Repeated content uniformity measurements were conducted for 8 h after the synthesis unit had reached steady state conditions. The settings of the formulation unit (*i.e.* film speed and cutting frequency) were determined earlier for 5 mg ASA dose. As it can be seen in Figure 21b the collected layered ODWs showed mean contents close to the original target dose of 5 mg with satisfactorily low fluctuations. In the 1st hour dosage units only with ~4,5 mg ASA were produced due to some deposition of the fibers on other surfaces in the ES box. However, after 2 hours fibers deposited mainly on the carrier.

Overall, the CMS was successfully operated for 24 h, *i.e.* approximately 7 times of the residence time of the whole system including formulation. As it can be seen in Figure 21c, the purity of ASA in the nanofibers produced from the reaction mixture reached the > 95% level

not long after passing the nominal residence time of R1 and R2 combined. The purity of the ODWs produced by the CMS was comparable to a marketed ASA tablet formulation (Fig. S16).

4.1.6 Integration of PAT-based control strategies

Real-time quality monitoring was integrated into the CMS with spectroscopic PAT tools. A Bruker Alpha FTIR spectrometer was used with an ATR flow cell to analyze the purity of ASA in the synthesized reaction stream. The flow cell was placed after the BPR and directly before the ES unit. Purity was calculated from the spectra by a quantitative model based on partial least squares (PLS) regression built with different ASA-SA ratios (Figure 22a) [229]. Following the pretreatment of the IR spectra the relevant spectral regions in terms of the regression were selected by a genetic algorithm (GA). Applying 4 latent variables (LV) on the selected ranges led to an effective PLS model for the commonly experienced high purity reaction mixtures corresponding to the region between 91 and 100% ASA content with low root mean squared error of calibration (RMSEC) and root mean squared error of cross-validation (RMSECV) values (0.64 and 0.90, respectively). In the case of insufficient purity, the high voltage generator turned off automatically to prevent the production of low-grade fibers. The concept of using switching valves to redirect the stream of lower purity into a waste container had to be reconsidered since the drying of the polymeric solution in the stagnant tubing would lead to clogging when switching back.
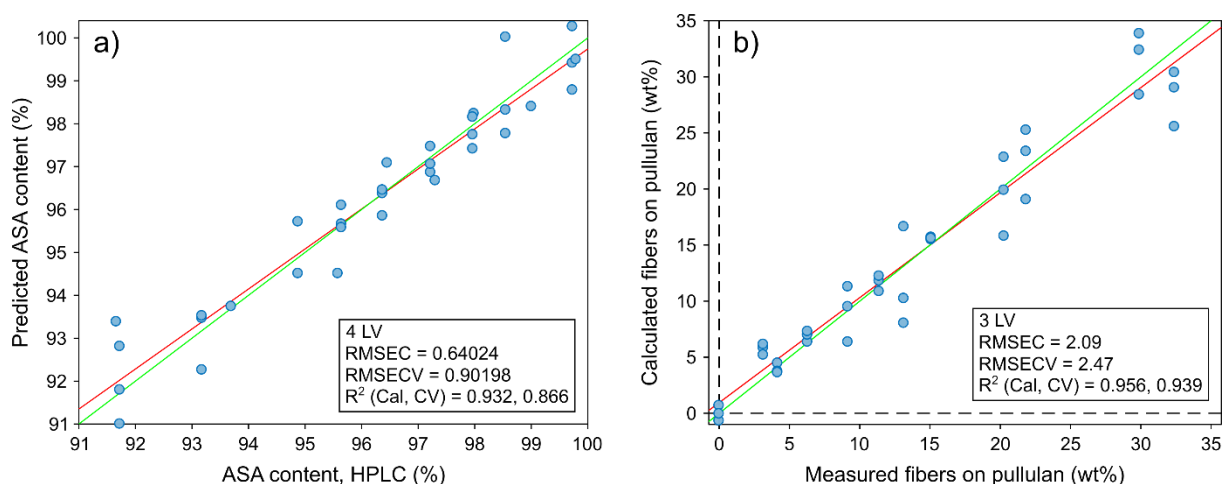
Figure 22. (a) Comparison between actual and calculated ASA content in the reaction mixtures in the range of 91-100% (ATR-FTIR, PLS-GA regression). (b) Comparison between actual and calculated weight ratios of PVPK30 + 18%ASA nanofibers on pullulan film-based layered ODWs (Raman, PLS-GA regression).

A Raman probe was applied for the inspection of the fibers on the pullulan strip placed before the cutting mechanism (Figure 17b). The probe was motorized providing transversal

movement of the laser beam (6 mm spot size) patrolling on the surface of the nanofibrous film (Figure S19a). The Raman spectra were preprocessed before model building for the fiber quantities. GA was used again for variable selection, the final PLS-GA model used 3 LVs. The indicators of model goodness (RMSEC = 2.09, R^2_{Cal} = 0.956) showed that the built model can be suitable for estimating the fiber quantity on the pullulan film (Figure 22b). If the deposition of the fibers was uneven on the film, meaning the cases where certain pullulan areas remained partly or completely uncovered, a bistable slide mechanism redirected the product to the waste bin instead of the approved product container (Figure S19b).

The details of the chemometric analyses on the FTIR and Raman spectra are given in the Supporting Information.

4.1.7   Conclusions

In this work phase we presented a novel approach based on ES for the continuous production of a solid dosage form from the synthesis of the API to the final formulation of layered ODWs with integrated PAT quality assurance. The main characteristics of the developed CMS (Figure 23) are concluded in Table 4. As for productivity, at 5 mg dosage strength ∼1016 doses per day can be reached. Hence, a continuous benchtop device such as the one presented is able to produce considerable amounts of dosage units with ES especially when formulating high-potency APIs.
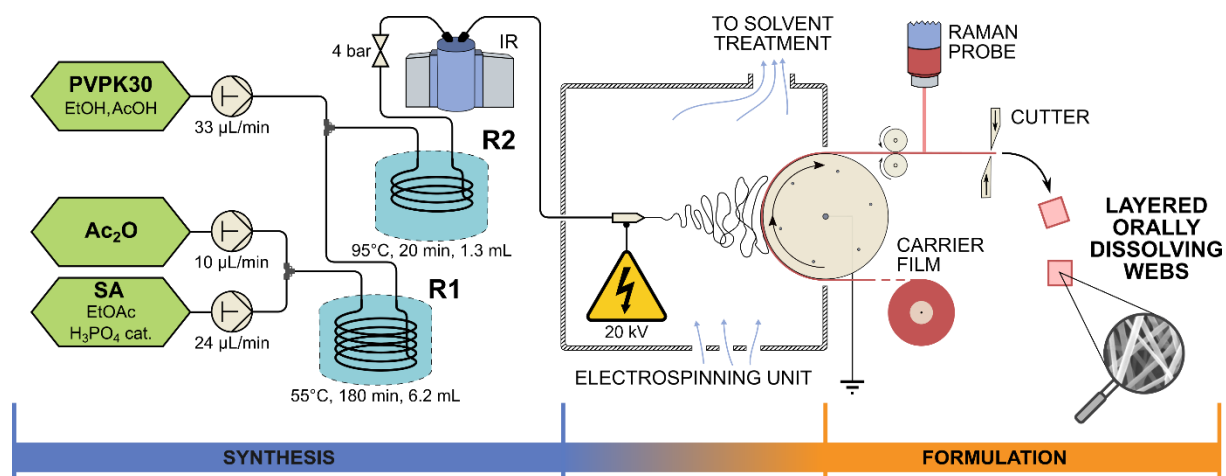

Figure 23. Schematic diagram of the developed CMS for the production of ASA-loaded fibrous ODWs based on ES. R1 and R2 microreactors, IR Bruker FTIR cell, Kaiser Raman PhAT probe.

Table 4. Main characteristics of the CMS.

CMS parameter	Value
Synthesis residence time	212 min[a]
Formulation residence time	14 min[b]
API throughput	5.08 g/day
Formulation throughput	5084/1016/406 units/day (at 1/5/12.5 mg dose)
Benchtop size (width × length × height)	1.5 × 0.6 × 1.1 m[c]

[a] R1 + R2 + IR flowcell + tubing.

[b] At 5 mg ASA dose.

[c] Excluding air pipes and Raman optical box.

Besides the optimization of ASA synthesis together with ES for purity and fiber morphology, DSC and XRPD analyses were conducted on the nanofibers verifying the amorphous form of the drug. Ultrafast dissolution could be observed with the pullulan-based nanofibrous composites at 1-25 mg ASA dose levels. The CMS was operated for 24 h covering several cycles of the mean residence time (∼3.5 h); detailed measurements showed excellent stability of drug purity over time in addition to content uniformity and residual solvent content. Real-time monitoring of both synthesis and formulation was developed using ATR-FTIR and Raman tools combined with chemometric analyses.

Our CMS also demonstrates how personalized medicine can be implemented through prompt control of the scaled-down continuous process providing tailored dosage units. In the field of continuous pharmaceutical manufacturing ES can be a feasible technique in processing the reaction mixture also after purification as an advanced solvent removal step. The fibrous product can be formulated into a layered solid product or further processed to tableting, even at higher throughputs [202,230].

4.2 Continuous manufacturing of ODWs containing a poorly soluble drug via electrospinning

In the previous chapter it was demonstrated how ES can be applied for the continuous processing of a flow reaction mixture to produce ODW final dosage forms. A desktop-size apparatus was built for this purpose, in which the electrospun fibers were deposited on the surface of a carrier film. The carrier was strained on the circumference of a rotating wheel, and the produced double-layered strip was conveyed further to be cut into small units ready for patient administration. As next step, in this work phase our aim was to extend the applicability of the developed apparatus for the formulation of ODWs containing a poorly water-soluble API. Carvedilol (CAR), a non-selective beta blocker was selected as model drug with low water solubility (0.02 mg/mL at pH = 6.8) at a dosage strength of 6.25 mg [214]. Herein the selection of the excipients, the formulation development and the analytical characterization of the ODW product are presented along with detailed investigation of system performance.

4.2.1 Preformulation tests with HPβCD

The dissolution of the API can be enhanced in the oral cavity by solubilizing agents, *e.g.* cyclodextrins (CDs) or pH-modifying additives. Thus, at the beginning we attempted to create an electrospun formulation containing CDs and obtaining a thermodynamically stable solution during dissolution with ultrafast release kinetics of CAR due to the CD content and the large surface area of the fibers. HPβCD was selected as solubilizer among the few FDA-approved CD derivatives well soluble in both aqueous and organic solvents. The propensity of β-CDs to enhance the solubility of CAR has also been shown earlier [214]. In order to investigate the solubilizing effect of HPβCD and other excipients, phase solubility studies were conducted in purified water and in buffer modelling the human saliva (25 mM KH_2PO_4 (pH=6.8) [231] (Figure 24).
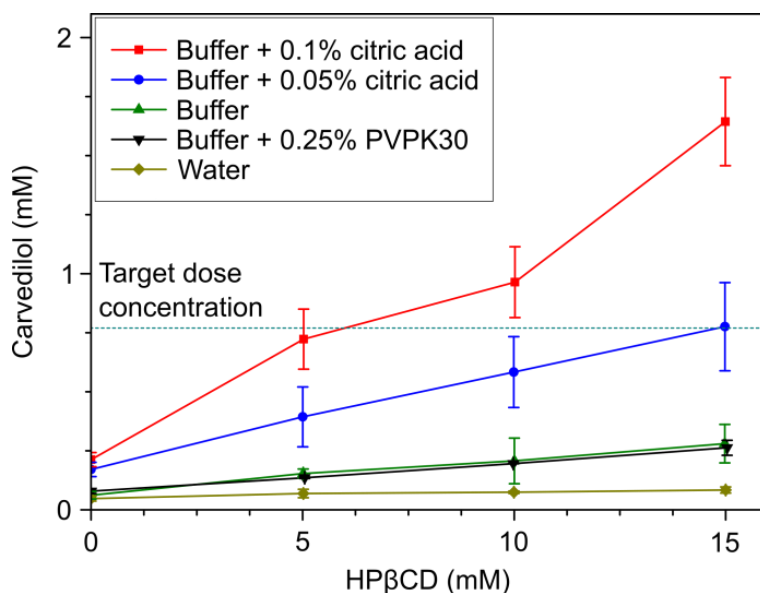
Figure 24. Phase solubility diagram of CAR as a function of HPβCD concentration in pH = 6.8 phosphate buffer with or without citric acid or PVPK30.

HPβCD had practically no solubilizing effect on CAR in purified water and only a slight increase could be observed at the pH of the saliva. However, the target dose concentration, *i.e.* 6.25 mg CAR dose dissolved in 20 mL media (0.8 mM), could not be reached. Since CAR is a weak base, citric acid was added to the dissolution media at two different levels (0.05 and 0.1% solutions) in order to enhance the complexation efficiency of HPβCD. Through the modification of the pH significant solubility enhancement was achieved and the target dose concentration could be reached even though the 0.05% and 0.1% levels of citric acid modified the pH from 6.8 only to 6.3 and 5.5, respectively.

Preliminary ES tests were conducted using PVPK30 as a good fiber forming hydrophilic polymer. The molar ratio of the API and HPβCD in the polymeric fibers was decided to be at least 1:5 based on the phase solubility results. Applying such excess amounts of HPβCD led to low CAR mass percentage values in the fibrous products (<5%), *i.e.* the total dose weight would be undesirably high also taking into account the PVPK30 content. It should be noted that HPβCD can also be electrospun into nanofibers without a polymer, but earlier studies have shown that the process can hardly be operated in a continuous manner due to the perpetual re-drying of the spinning tip [232]. Similar difficulties were encountered with the HPβCD-PVPK30-based composition due to the high solution concentrations despite the thorough optimization of the ES process. Consequently, the drawbacks of HPβCD electrospinning, *i.e.* the attainable low mass ratio of the API and the incapability for stable continuous operation hindered the development of a CAR- and HPβCD-loaded fibrous formulation.

Besides poor spinnability, the dissolution of these CAR-loaded fibrous mats was unexpectedly slow: several minutes were required for the formulation to dissolve with 0.1% citric acid present in the buffer (results not shown). Therefore, we decided to omit the application of HPβCD and rather focused on an alternative approach with special attention on the stable and continuous operation of the ES process.

4.2.2 Preparation of amorphous nanofibers with ES

Processing CAR into an amorphous solid dispersion was expected to ensure fast dissolution rates and low dose weights without the use of a solubilizer in the formulation. PVPK30 remained as polymeric matrix with excellent spinnability. Extensive optimization of ES was conducted based on PVPK30-CAR compositions by varying the applied solvent, the polymer concentration of the ES solution, and the mass ratio of CAR and PVPK30. During the optimization exclusively 15, 20 and 25% of CAR contents were tested due to the following reasons: lower percentages of CAR were not preferred in order to limit the total weight of the formulation while 30% or higher drug contents could not be reached due to the solubility limitations of CAR in the ES solutions. Higher drug loadings are not favorable either for the dissolution behavior owing to the hydrophobizing effect of the poorly soluble API [233].

In the case of an unstable ES process, the clogging of the needle tip as well as the spattering of liquid droplets are likely to deteriorate the quality of the collected fibers. These phenomena could be avoided by adjusting the volatility of the solution through changing the applied solvent. Several solvents (AcOH, DMF, EtOH, EtOAc, MeOH and tetrahydrofuran) and their mixtures were tested; at last the 1:1 (V/V) EtOH-DMF mixture was chosen and applied in further experiments.

The optimal concentration of PVPK30 in the EtOH-DMF 1:1 (V/V) mixture was explored by gradually increasing the amount of the dissolved polymer at fixed CAR ratios (Figure 25). Besides morphological analysis based on the SEM pictures, the ES process was also thoroughly evaluated in terms of the occurrence of undesired drying or spattering of the spinning liquid. The concentration of 5.125 g PVPK30 in 10 mL pure solvent mixture with the appropriate amount of CAR provided fibers with the best quality possessing an average diameter of 0.56 ± 0.11 µm and a process with satisfactory stability at a flow rate of 2 mL/h.
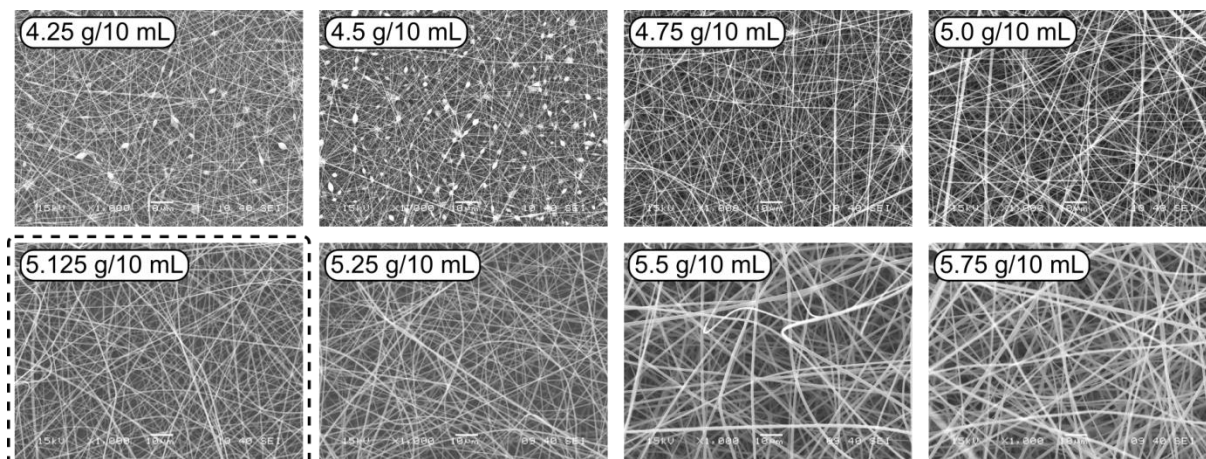
Figure 25. Scanning electron microscopic images of electrospun fibers of different concentrations of PVPK30 dissolved in EtOH-DMF (1:1) mixture containing 20% CAR (20 kV, 2 mL/h).

As the phase solubility studies have revealed citric acid highly promoted the solvation of CAR. Thus, the incorporation of citric acid into the nanofibers was also attempted. However, the presence of even small amounts of citric acid altered the spinning solution into a highly viscous gel preventing ES presumably due to the intermolecular H-bondings. Hence, citric acid had to be introduced into the formulation in another way as it is detailed in the following subsection.

4.2.3 Construction of double-layered ODWs

Although the electrospun fibers possess a macroscopic nonwoven structure, these PVPK30-based fibrous mats are sensitive to physical impacts, therefore they are not applicable alone as a final dosage formulation. Poor handling can be resolved if the fibers are deposited on the surface of a water-soluble sheet providing strength and thus a double-layered structure is formed [234].

Pullulan was selected as film forming excipient, which can be applied as mucoadhesive excipient as well [235–237]. The flexibility of the pullulan film was enhanced with Tween® 80 (ca. 2.5 w/w%) acting as a plasticizer. Red food coloring was also added to alter the colorless appearance of the film (Figure 26a). Citric acid could be incorporated into the casted films instead of the electrospun fibers. In order to reach the 0.1% citric acid concentration during dissolution, 20 mg had to be embedded in each piece of cut films. The dissolved citric acid apparently did not influence either the casting process or the disintegration of the modified pullulan film.

The drug-loaded nanofibers were electrospun onto the surface of the pullulan films fixed to the grounded collector. After a certain time, the double-layered structure was removed and manually cut into smaller pieces. The initial electrostatic force and the surface energy of the nanofibers ensured good adhesion between the pullulan film and the fibrous layer. The rationale behind the selection of the final drug-polymer ratio in the fibers was as follows. Although lower drug loading (*e.g.* <10%) of the solid dispersion may significantly improve drug dissolution rate, it inversely increases total dose weight. Thus, PVPK30 nanofibers with 20% CAR content were prepared during further experiments. The proposed ODW formulation of 30 × 30 mm (Figure 26b) consisted of approximately 80 mg pullulan film (20 mg citric acid incorporated) combined with a nanofibrous layer containing 6.25 mg CAR nominally.
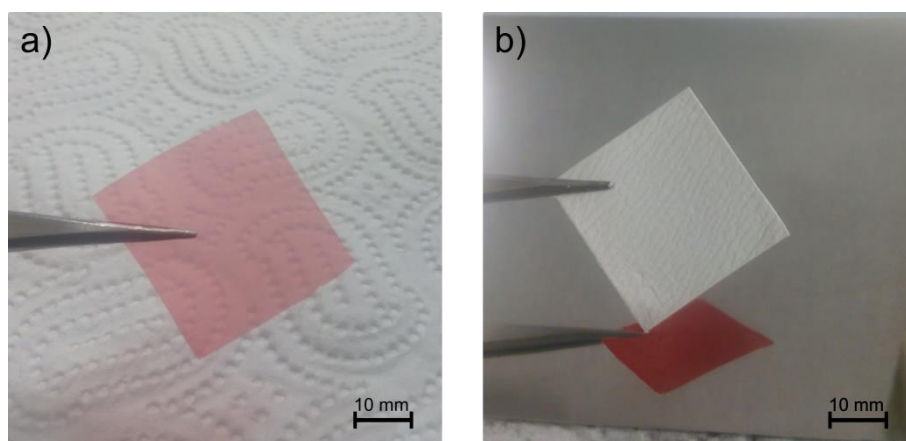
Figure 26. (a) Casted and cut (30 × 30 mm) pullulan film with incorporated citric acid and (b) the final ODW with the nanofibrous layer containing 6.25 mg CAR.

4.2.4   Characterization of the layered ODW product

4.2.4.1   Physical state of CAR in the nanofibers

The physical state of the components in the fibrous product was investigated using DSC and XRPD (Figure 27). The physical mixture of 5% crystalline CAR and PVPK30 served as reference to demonstrate the sensitivity of the methods. The thermogram of the physical mixture clearly indicate the melting of crystalline CAR as an endothermic peak at around 117°C while the X-ray diffractogram of the same physical mixture contains the main characteristic CAR diffraction peaks. Both analytical techniques verified the expected amorphous state of CAR in the fibers owing to the fast drying during ES, the aforementioned signs were completely absent in the case of the PVPK30 + 20% CAR nanofibrous product. Regarding the casted pullulan film, no signs of crystallinity could be detected showing the similarly amorphous form of

pullulan and citric acid which could be also deduced from the transparent appearance and the fast dissolution of the film.
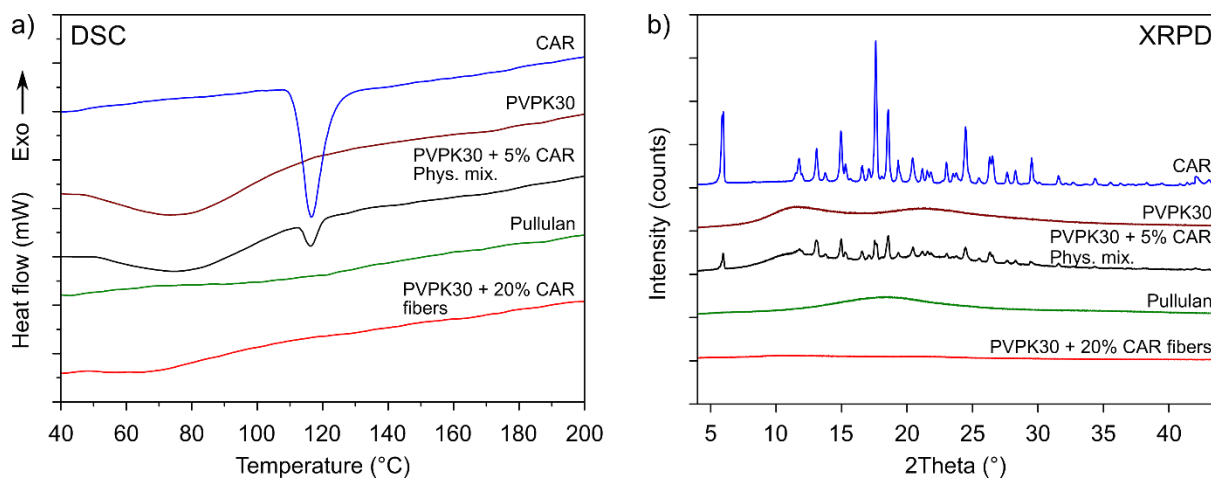
Figure 27. (a) Differential scanning calorimetry thermograms and (b) X-ray powder diffraction patterns of crystalline CAR, PVPK30, physical mixture of PVPK30 and 5% CAR, the casted pullulan film and the PVPK30 + 20% CAR electrospun fibers.

4.2.4.2   Disintegration and dissolution tests

The extent and rate of dissolution was investigated by dissolving the double-layered ODWs equivalent to 6.25 mg CAR in 20 mL of buffer modeling the oral cavity. The dissolution characteristics of the product were compared to pure crystalline CAR and the corresponding physical mixture of CAR, PVPK30 and the pullulan film with citric acid (Figure 28).
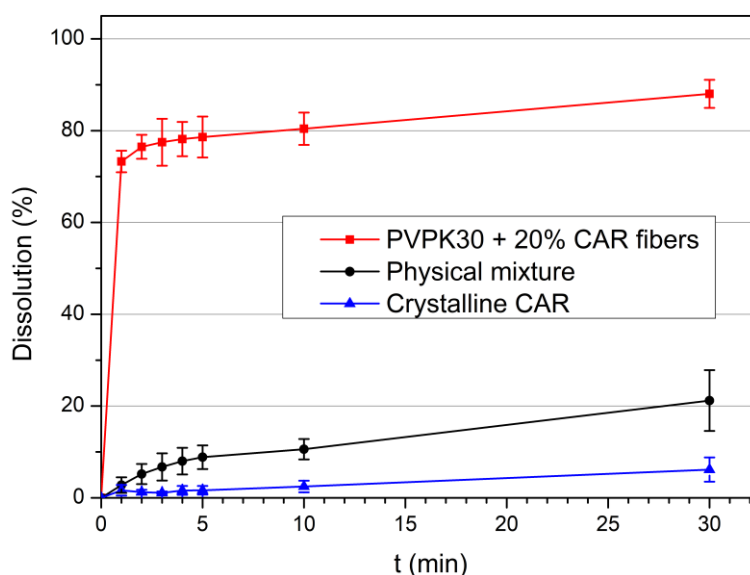
Figure 28. Dissolution profiles of CAR from electrospun PVPK30 fibers collected on pullulan films containing citric acid. The error bars indicate the standard deviations (n=3). [6.25 mg dose, 20 mL pH = 6.8 25 mM KH_2PO_4 buffer, 100 rpm magnetic stirrer, 25°C]

According to the dissolution results, in the case of the layered ODW formulation ultrafast dissolution of CAR could be reached, and the apparent solubility of the amorphous formulation was approximately 4-5 times higher than that of the corresponding physical mixture (the thermodynamical solubility of CAR was measured to be 85 ± 12 µg/mL (0.21 mM) at 25°C, see Figure 24). The supersaturated state persisted for at least 30 min which might provide sufficient absorption through the oral mucosa. Although the dissolved quantity of CAR did not reach total drug release under these conditions, with the simultaneous absorption of the drug the complete dissolution may also be attainable. Compared to crystalline CAR and the physical mixture composition, the several times higher dissolution rate and dissolved quantity of CAR from the electrospun layered formulation can be attributed to the amorphous form of the API, the ionizing effect of citric acid and the large surface area of the nanofibers. It should be noted that even if citric acid was also present in the physical mixture, the dissolution of crystalline CAR did not improve significantly, signifying the importance of the amorphous form.

The time required for disintegration is yet another important quality attribute of OD formulations. Various methods can be found in the literature to test the disintegration of such products [238]. From these the "slide frame" method applies the lowest volume of media (one droplet) for the test, helping the imitation of the conditions in the oral cavity, and it has a clear endpoint as well (see Section 3.5.10 disintegration tests method) [220,221]. Thus, this method was selected to measure the disintegration of our fibrous layered ODW. With this technique the sheet-like formulation is fixed into a horizontal frame and one droplet of distilled water is placed onto the surface of the product. The time required for complete perforation of the droplet through the sheet was taken as disintegration time.

Based on pre-experiments the rate limiting step of disintegration was determined to be the wetting of the pullulan film, since the drug-loaded nanofibers instantaneously dissolved when brought in contact with the droplet. Therefore, the formulation was clamped in the position facing upwards with the pullulan film (Figure 29). This way the disintegration time of the nanofibrous layered ODW was measured to be 10 ± 2 s, meeting the requirements of regulatory guidelines (<30 s) [239].
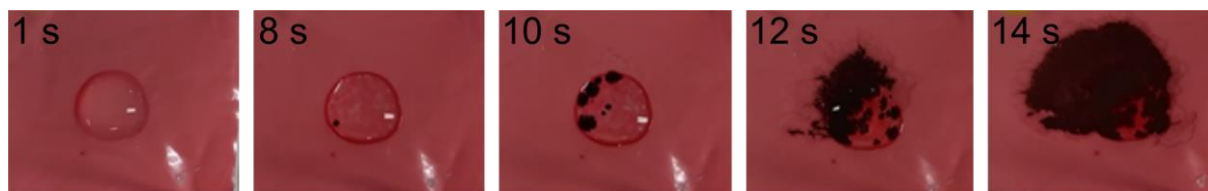
Figure 29. Disintegration of the double-layered ODW formulation. The darkening spots indicate the appearance of the black background.

4.2.5 Continuous production of the ODWs

After formulation development, the feasibility of the continuous production of the double-layered ODW was also investigated. In our preceding work we have built a continuous system applicable for the controlled deposition of the electrospun fibers on the surface of a carrier film, and also for continuously cutting it into final solid dosage forms (Figure 17).

Briefly, instead of a collector plate, a plastic wheel combined with a metal sheet on its circumference was used. The electrically grounded metal sheet part of the slowly turning wheel was covered with the carrier film (*e.g.* pullulan, Figure 18a) used for the collection of the nanofibers, which was automatically conveyed towards cutting into fibrous double-layered ODWs (Figure 18b). The design of this benchtop-scale continuous system also enables real-time analytical inspection and feedback on product quality, for instance when a Raman probe is applied before cutting (see Section 4.1.6). Drug dose could be altered by changing the convection speed of the carrier and/or the frequency of the cutting. During the experiments we adjusted these parameters to obtain nominally 31.25 mg fibers (6.25 mg CAR) per dosage unit with 30×30 mm cut size. This system setup resulted in an average residence time of approximately 20 minutes and a throughput of ~6.15 g CAR/day and ~984 dosage units/day.

4.2.6 Investigation of system performance

The stability of ODW production using our continuous system was investigated by conducting test runs of longer time intervals. Content uniformity and residual solvent content of the fibers were periodically measured in steady state for 4 hours of operations.

For content uniformity measurement 10 samples were taken in each hour and CAR content was determined by HPLC. The mean content showed satisfactory low fluctuation within the hours and during the total 4-hour period as well with relative standard deviations of 3-4% (Figure 30). The calculated Acceptance Values (AV) were also satisfactorily low (<15) for each hour (average AV = 9.45).
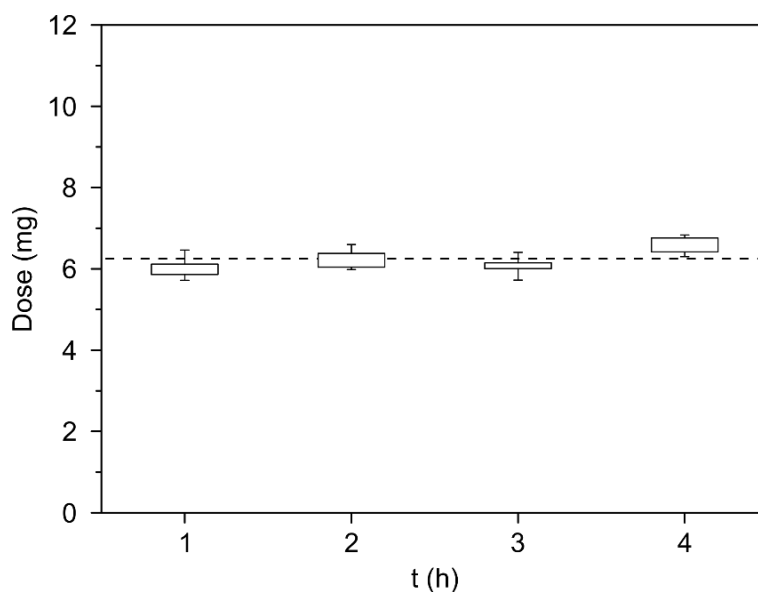
Figure 30. The results of content uniformity measurements of the ODW products prepared using the continuous system in steady state. The drug content of 10 samples was measured in each hour. The height of the box indicates the interquartile range while whiskers represent the maximum and minimum values.

The residual solvent content of the electrospun fibers was measured during another 4-hour long period. The 1:1 solvent mixture of EtOH and DMF was applied during ES; the more volatile EtOH with low toxicity has a limit of 5000 ppm in the product, while the quantity of DMF with higher surface tension has to be reduced below 880 ppm for acceptance [228]. To our experience the removal of DMF from the fibers was significantly more challenging, the ODW product contained ca. 2000 ppm DMF without further drying after ES (Figure 31). In contrast, EtOH concentration was below the detection limit (~250 ppm) of the GC method even directly after fiber formation.
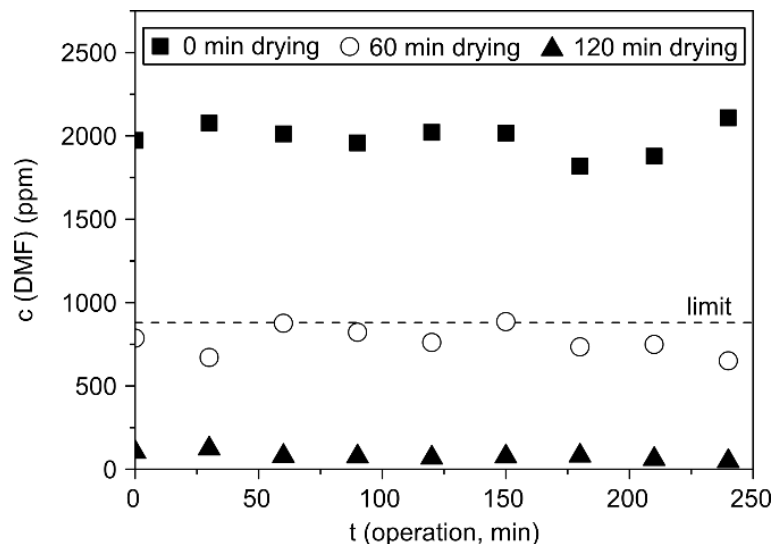
Figure 31. Residual DMF content of the final product during 4-hour long operations of the continuous system at different drying times.

Thus, further ventilation was applied using a 120 mm 2.4 W fan at room temperature to remove DMF from the cut dosage units. After 60 minutes of secondary drying, the DMF concentration has reached the regulatory limit in the double-layered formulation (Figure 32), but due to the variation of the results longer ventilation was found to be necessary.
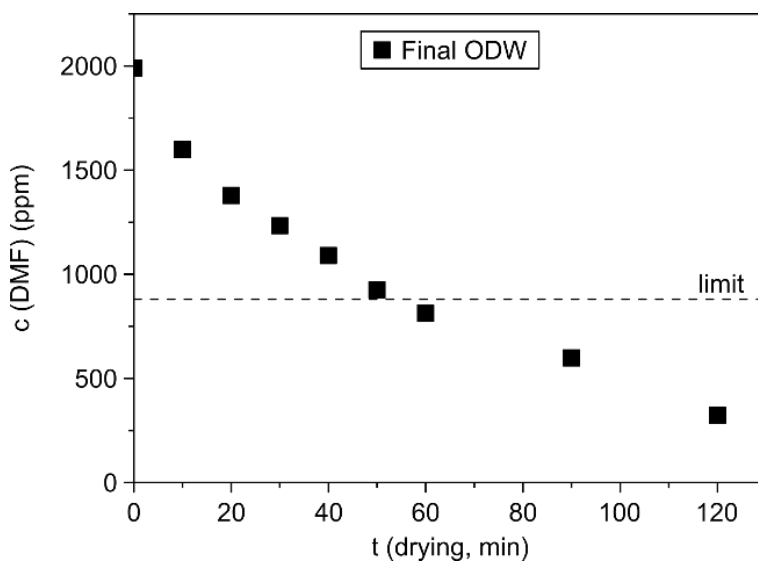
Figure 32. DMF concentration in the ODW product over secondary drying time.

4.2.7 Conclusions

In this work phase, the applicability of the earlier developed continuous formulation apparatus was widened to produce a double-layered ODW formulation containing the poorly water-soluble CAR. Phase solubility measurements showed that the target dose concentration of CAR could be reached with HPβCD if complexation efficiency was improved with citric

acid, though the total weight of the formulation containing one dose CAR (6.25 mg) increased significantly, making the application more difficult. Instead of using CDs, the API was embedded in PVPK30 nanofibers produced by electrospinning in an amorphous form, confirmed by DSC and XRPD measurements. During the ES process the fibers were collected on the surface of a carrier film made of pullulan and citric acid forming a double-layered structure. The created formulation showed ultrafast dissolution and disintegration in small volumes of dissolution media modeling the oral cavity, while precipitation of the API from the supersaturated solution could not be observed. The continuous production of the product was carried out using the continuous system built in our laboratory: the electrospun fibers were collected on the carrier strip strained on a grounded wheel. The covered carrier was slowly conveyed further and automatically cut into smaller pieces ready for patient administration. The amount of the collected fibers and the size of the cut units were adjustable by changing the convection speed of the carrier and the frequency of the cutter. The performance of the continuous system was investigated during 4-hour long test runs regarding content uniformity and residual solvent content of the produced ODWs. The results showed low fluctuations in drug content over time, negligible EtOH concentration and by applying ventilation at room temperature the residual DMF content could also be decreased below the regulatory limit. In conclusion, the CM device was suitable to process electrospun nanofibers into layered orally disintegrating formulations, which was demonstrated for more, pharmacologically different APIs.

4.3 End-to-end continuous manufacturing of conventional compressed tablets: from flow synthesis to tableting through integrated crystallization and filtration

In the previous chapters the flow synthesis of acetylsalicylic acid (ASA) directly connected to electrospinning to obtain good quality ODW dosage forms was presented. As a step forward, in this work phase we aimed the end-to-end production of the industrially most common, conventionally compressed tablets, which has not been described in the literature yet. Moreover, we intended to incorporate continuous purification into the system, which is unavoidable after most syntheses, and was not applied in our previous studies. Thus, the main goal of this work phase was the proof-of-concept demonstration of such a CM system. For this purpose, we needed to resolve the crystallization of the described reaction mixture from the flow synthesis, the filtration and drying of the formed crystals as well as the blending and tableting steps all in continuous and connectable way.

4.3.1 Continuous crystallization of the flow reaction mixture

The continuous crystallization of ASA was carried out from the reaction mixture of the flow synthesis of the API in an MSMPR crystallizer (see Section 3.4.4). During the development of the synthesis the second, quenching reaction step was optimized in two different ways: with and without a dissolved polymer (see Section 4.1.2). Thus, it was possible to work-up the final reaction mixture by ES when it contained PVPK30 (see Section 4.1.3), and by continuous crystallization when it did not. The composition of the final reaction mixture in the latter case is presented in Table 5. Along with the synthesized ASA it contained SA as the main impurity, which had a regulatory limit of 0.15% after production.

Table 5. Composition of 1000 mL of the flow reaction mixture containing ASA.

Material	Quantity
Acetylsalicylic acid	97.61 g
Salicylic acid	5.14 g
Ethyl acetate	794.61 mL
Acetic acid	163.26 mL
Ethanol	38.25 mL
Phosphoric acid (85%)	3.90 mL

During crystallization the API solution modelling the flow reaction mixture was prepared according to this recipe prior to the experiments, typically in a quantity of 1000 mL. Heptane was used as the antisolvent during the process in a volumetric ratio of 2:1. The MSMPR crystallizer was directly connected to the CFC. During the integrated continuous crystallization-filtration experiments, the residence time (τ) and the temperature (T) of the crystallization were varied by changing the settings of the peristaltic pumps (keeping the 2:1 heptane-reaction mixture volumetric ratio) and the thermostat.

4.3.2 Investigation of the integrated MSMPR-CFC system

The aim of the experiments was to precisely investigate the effect of the MSMPR process parameters on the quality of the filtered product. A series of experiments was carried out with the integrated crystallization-filtration system by changing the residence time and temperature of the crystallization reactor. The settings of the crystallizer and the corresponding CFC parameters are listed in Table 6. Washing of the filter cake in the CFC was turned off since appropriate purity could be achieved without it.

Table 6. The setup of the continuous filtration-crystallization experiment series. By changing the residence time (τ) and the temperature (T) of the crystallizer, different input flow rates (F_{ASA}, $F_{heptane}$), filtration cycle times (t_C) and solid concentrations were obtained.

Experiment	τ (min)	F_{total} (mL/min)	F_{ASA} (mL/min)	$F_{heptane}$ (mL/min)	T (°C)	t_c (s)	Max. solid concentration (kg/m^3)*
1	20	18	6	12	0	29	25.4
2	20	18	6	12	25	29	14.9
3	40	9	3	6	0	63	25.4
4	40	9	3	6	25	63	14.9
5	30	12	4	8	12.5	46	20.4

*Calculated from the solubility data of ASA in steady state operation [240].

During the experiments, the operation of the connected continuous crystallization-filtration system was carried on for 10 residence times (200, 300 and 400 min according to τ = 20, 30 and 40 min). After each residence time, 3 consecutive filter cakes discharged from the CFC were collected in weight boats, weighed on an analytical scale and placed in an oven to dry at 40°C. The mass of the filtered samples was measured again after 24 hours of drying for the

moisture content determination. Finally, the particle size distribution (PSD) was measured using a Malvern Mastersizer 3000 instrument (see Section 3.5.15).

The first experiences with the directly connected crystallization-filtration system showed that it was advantageous to apply the vacuum-driven slurry transfer system of the CFC as the outlet of the MSMPR reactor. During continuous MSMPR crystallizations, usually a peristaltic pump is applied for this purpose, which can break the crystals and the risk of fouling in the tubing is considerably higher. Nevertheless, precise calibration of the transferred volume was fundamental to prevent variations in the filtered product quality. The connected system during the experiments is shown in Figure 33.
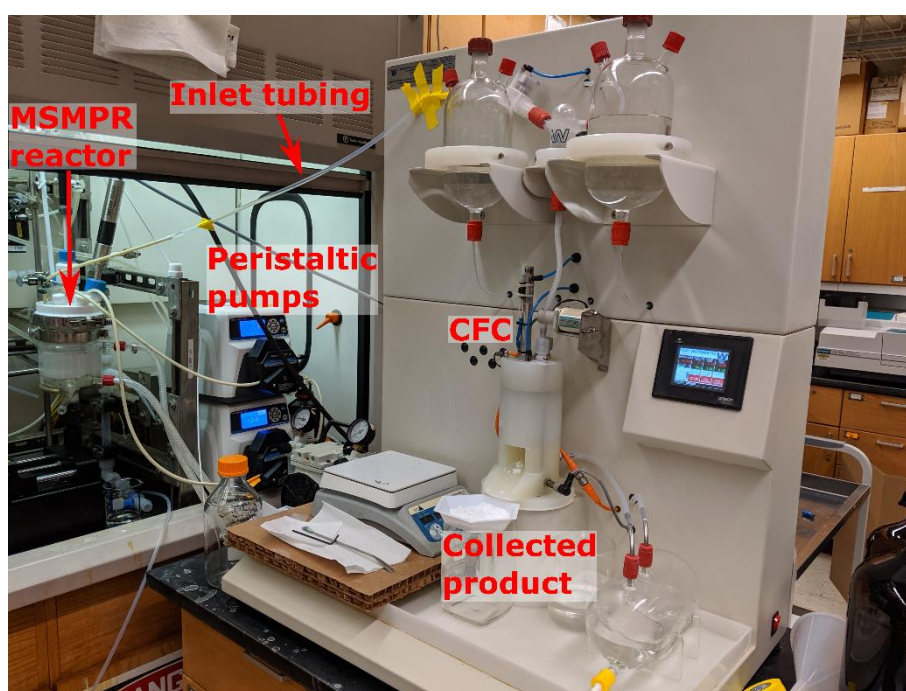
Figure 33. Experimental setup of the integrated continuous crystallization and filtration.

As it was shown in Section 3.4.6, the cycle time, *i.e.* the time available to filter and dry the filter cakes was fixed by the flow rate of the continuous crystallizer. This was affected only by the residence time of the crystallization since the volume of the suspension was set to 360 mL. Besides the residence time, the inner temperature of the MSMPR reactor was the other main controlled parameter of the crystallization. Changing the temperature affected the solid concentration of the suspension, which resulted in a different amount of crystals in the 10 mL portions transferred into the CFC. Obviously, a smaller quantity of crystals could be dried to a greater extent during the same time. The system performance was evaluated by analyzing the yield, the moisture content and the PSD of the filtered product.

The yield of the 2-step process is shown in Figure 34. Depending on the temperature of the reactor, ~40-60% of the total ASA mass was recovered as solid product after filtration: $59.74 \pm 0.74\%$ at 0°C, $53.83 \pm 1.24\%$ at 12.5°C and $41.88 \pm 2.97\%$ at 25°C, while the residence time settings of the crystallizer showed minimal effect on these results. The measured yields corresponded to approximately 19.4 kg/m^3 solid concentration at 0°C, 17.2 kg/m^3 at 12.5°C and 12.5 kg/m^3 at 25°C (Figure 34). These were in good correlation with the calculated theoretical maximum achievable solid concentrations listed in Table 6. Regarding the throughput, with short residence times (*i.e.* high flow rates) (20 min) circa 24 g/h maximum mass flow was reached at the end of the 2-step process.

Figure 34. Yield of the connected continuous crystallization-filtration experiments with different MSMPR process parameters. The continuous lines are only to guide the eye.

According to the PSD measurements, the crystallization reached steady state after 5-6 residence times, after which the mean size of the crystals did not change significantly (Figure 35a). As it can be seen on the diagram, the temperature of the process had the greatest impact on crystal size, while the results showed that the residence time had no significant effect. A mean crystal size of 453 ± 7 μm was achieved by crystallizing at 12.5°C, which was larger than the crystals obtained at 0°C (~400 ± 12 μm) and smaller than that of at 25°C (~601 ± 8 μm). However, these results showed that the temperature dependence of the crystal size is not linear.
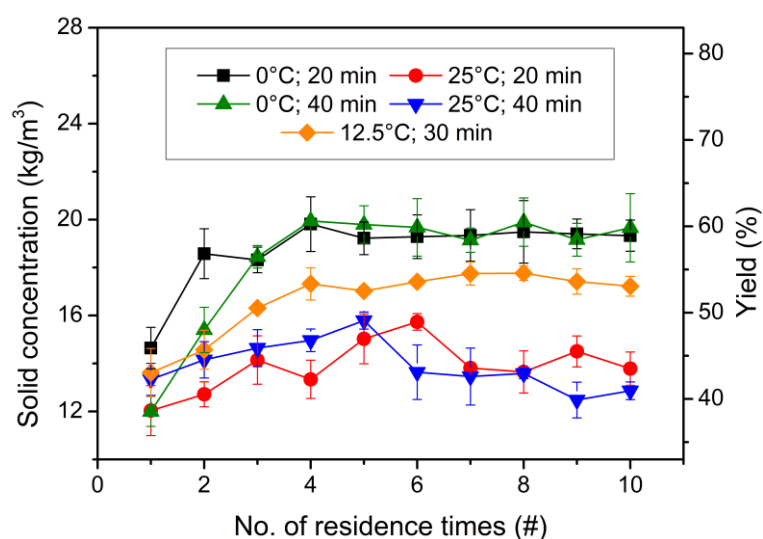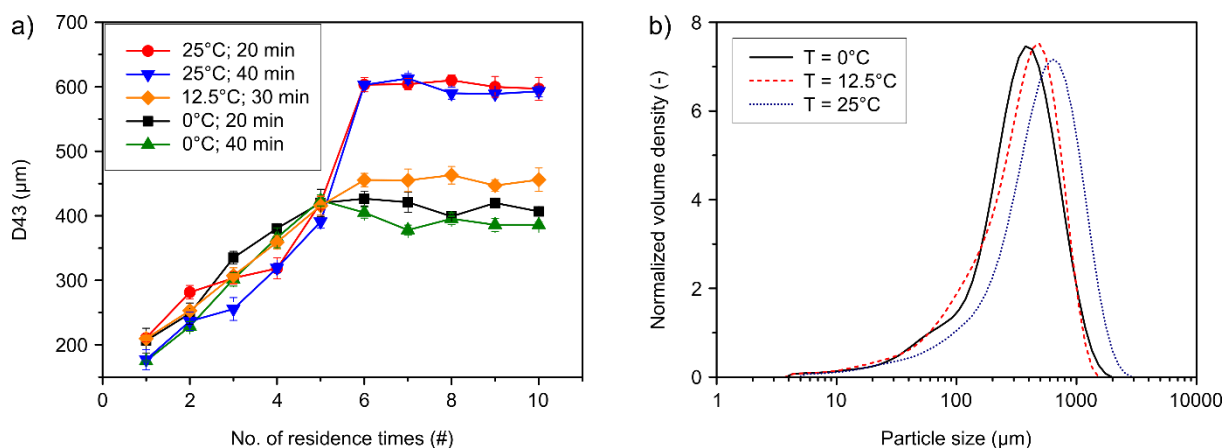
Figure 35. (a) D43 value of the crystal PSD of the connected continuous crystallization-filtration experiments with different MSMPR process parameters (the continuous lines are only to guide the eye) and (b) crystal size distributions of filtered product from the steady state of experiments with different crystallization temperatures.

The flowability of the filtered product was an important parameter in the following continuous feeding and blending steps (see Section 4.3.3), which is usually affected by the crystal size and the moisture content. According to our tests with sieved ASA, crystals smaller than D43 = 100 μm had poor flowability (16.07 ± 0.33 s), which gradually improved until D43 = ~200 μm (11.01 ± 0.53 s), and above D43 = 250 μm the flowability did not change and was very good (8.49 ± 0.33 s). The measured D43 value of the continuously crystallized and filtered crystals was between 400 μm and 600 μm and unimodal crystal size distributions were obtained close to each other (Figure 35b). These might be the reasons of the observed similar and very good flowability during each experiment (see later). Additionally, the residual solvent content was between 1% and 6% (see later), which apparently did not deteriorate the feedability of the material in this range.

The measured moisture content of the filtered crystals is depicted in Figure 36. As it can be seen, the residual solvent content was constant from the beginning, there was no need to reach a steady state. This parameter was impacted by both the temperature of the crystallizer and the residence time: increasing the residence time gave a longer CFC cycle time, extending the time available for drying in chambers 2-4 after filtration (see Section 3.4.6), while at higher crystallization temperatures the lower solid concentration resulted in smaller filter cakes, which were easier to dry.
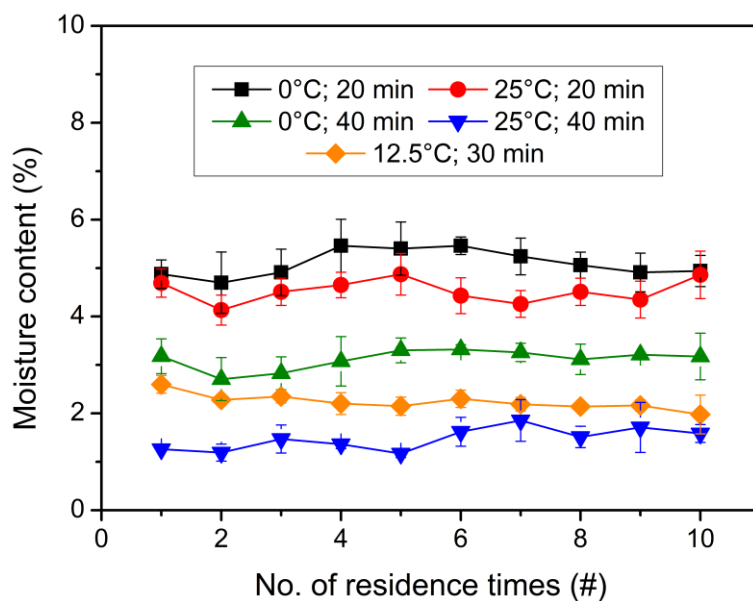
Figure 36. Moisture content of the connected continuous crystallization-filtration experiments with different MSMPR process parameters. The continuous lines are only to guide the eye.

The crystal size is known to have an impact on the filtration performance, which should be visible on the moisture content results [241,242]. Nevertheless, in our experiments, no trend was found when the PSD and residual solvent content data were compared. Also, despite the crystal size was changing until the steady state was reached, the moisture content was constant from the beginning of the experiments. This phenomenon might be the result of the significantly downsized process compared to industrial Nutsche filtration, as both the filtration time and the mass of the filter cake were very small in each cycle.

The average moisture content in the steady state is plotted against the corresponding MSMPR settings in Figure 37. As it can be seen, the low crystallization temperature (*i.e.* high solid concentration) with short residence time (*i.e.* short cycle time) resulted in the highest moisture content (~5%). On the other hand, long residence time with high crystallization temperature lead to almost 1% residual solvent content. The regulatory requirement of moisture content for each component of the crystallized solution (EtOAc, EtOH, AcOH and heptane) is 0.5% or 50 mg per day [228]. Since the tablets produced in the following steps (see Section 4.3.3) contained 100 mg ASA, the residual solvent content of the final product complies to the regulatory requirement. If necessary, the moisture content reducing capability of the CFC could be improved either by increasing the number of chambers in the carousel or by applying heating on the air flowing through the ports during the process.
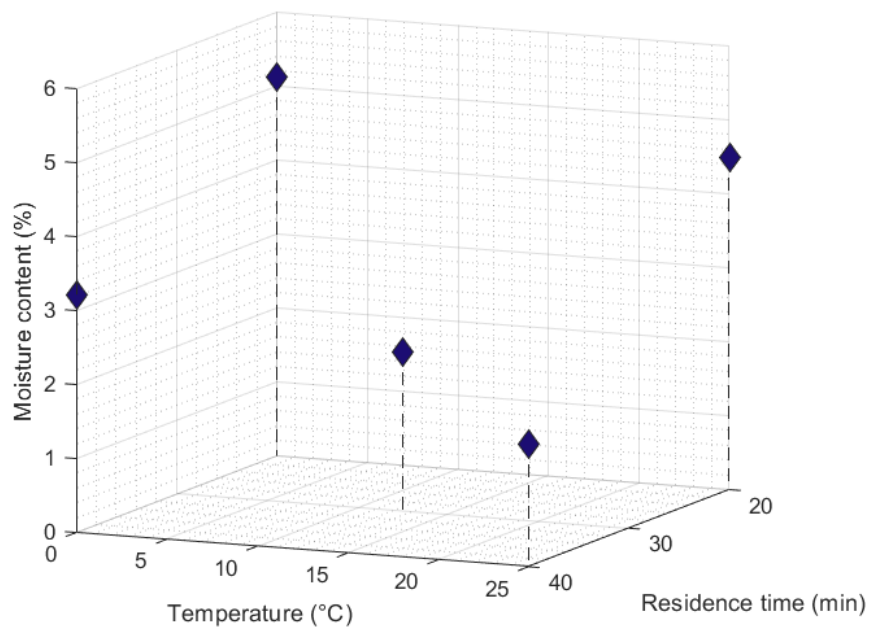
Figure 37. The average residual solvent content in the steady state in the different temperature and residence time settings of the MSMPR reactor.

The crystallized reaction mixture contained 5% salicylic acid (SA) impurity along ASA. Hence, it was necessary to analyze the purity of the filtered product. During Experiment 3 (T = 0°C, τ = 40 min, see Table 6), the CFC-filtered crystals were collected for purity measurements at each residence time. The result of the HPLC purity measurement is presented in Figure 38. As it can be seen, the SA content remained below 0.5% during the entire experiment.
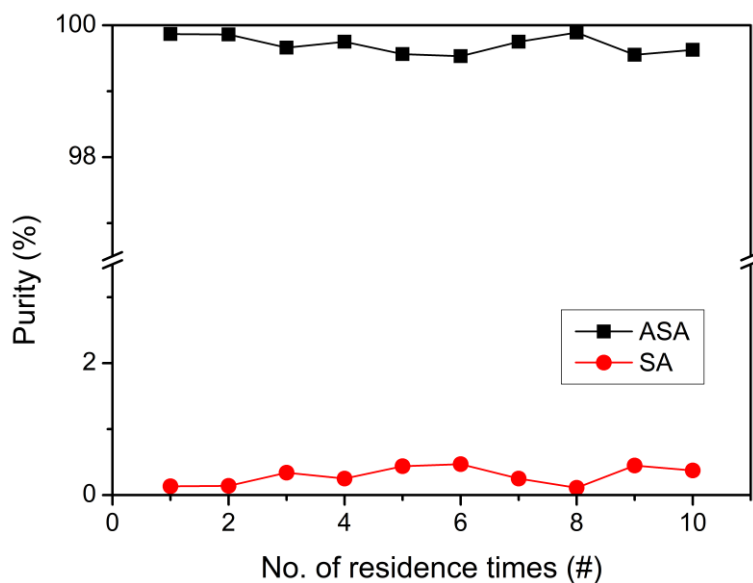
Figure 38. Purity of the CFC-filtered crystals during Experiment 3 (T = 0°C, τ = 40 min, see Table 6). The continuous lines are only to guide the eye.

The results clearly demonstrate how a certain MSMPR crystallization setup had a direct impact on the continuous filtration process as well as on the filtered product. During each experiment, the produced ASA showed good flowability in the obtained particle size (D43 = ~200-600 µm) and moisture content (~1-5%) range (Figure 39). In order to carry on to the following continuous blending and tableting experiment, the ASA collected during the individual experiments was poured together (see Section 4.3.3). The flowability of this united product was measured to be 9.56 ± 0.30 s, similarly to the tests of the good-flowing sieved ASA when D43 was above 250 µm.
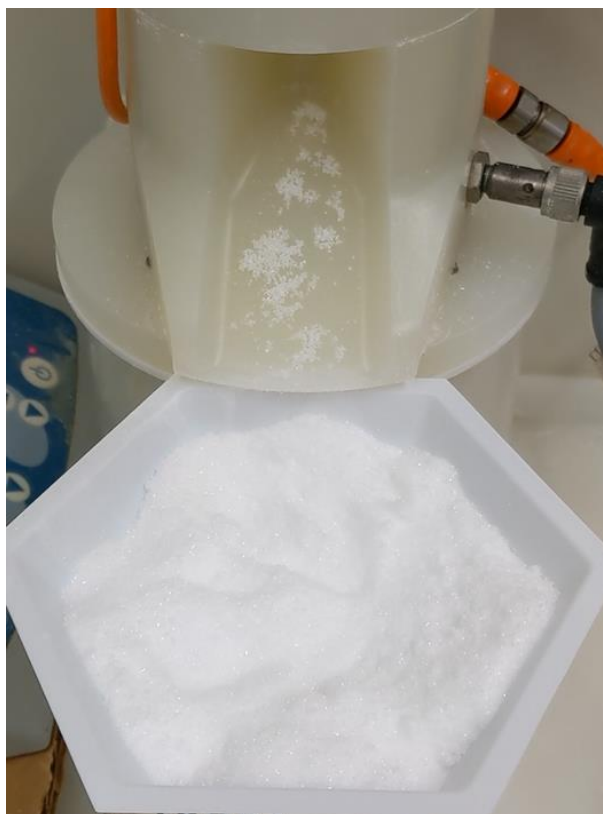
Figure 39. Dry, free-flowing ASA crystals from the integrated continuous crystallization-filtration experiments.

4.3.3 Continuous homogenization and tableting

Following the integrated continuous crystallization and filtration experiments, the produced ASA was moved to continuous blending and tableting. In these steps the API was first mixed with MCC as an excipient and then conventional tablets were compressed from the powder blend (Figure 40). During processing in the CFC, the moisture content of ASA could be decreased enough to obtain an appropriately dried, free-flowing material with good physical properties (see Section 4.3.2 and Figure 39). Since the current scale of the crystallization-filtration process (max. ~24 g/h API mass flow) did not meet the minimal mass flow of our available feeders (min. ~60 g/h API mass flow), the continuous blending and tableting experiment was executed separately starting from a larger quantity of collected CFC-filtered ASA. Nevertheless, with a smaller feeder, no additional material handling would be required, and these two steps can be connected by placing the hopper of the feeder under the 5th, discharge port of the CFC. Moreover, the currently applied feeders could be used with a scaled-up crystallization-filtration process. This would be feasible by using a larger MSMPR reactor [95] and one of the larger, commercially available versions of the CFC.

Figure 40. Feeding of MCC and ASA into the hopper of the continuous blender (left); NIR probe mounted above the belt conveyor after blending (middle); continuous blender, belt conveyor and tableting machine integrated in one CM line (right).

The continuous blending of ASA and MCC was carried out in a ~70 min long experiment. The API concentration of the powder mixture coming out from the blender was monitored in-line by the NIR probe (Figure 41). As it can be seen in the diagram, the measured ASA content reached the 20% setpoint after an approximately 6 minutes long start-up period. From this point, the steady state lasted for approximately 60 minutes (indicated from ~6 to ~66 minutes in the diagram), when the ASA feeding was stopped, and the measured API content decreased. During this period the in-line measured mean value of the drug ratio in the mixture was 20.70% with a relative standard deviation (RSD) of 5.78% (Table 7). As it can be seen, small fluctuations were detected in the steady state. The deviation might be the result of the less accurate volumetric feeding of ASA, which can be improved either by using a more precise, gravimetric twin-screw feeder, or by the application of a spectroscopy-based control system [179].
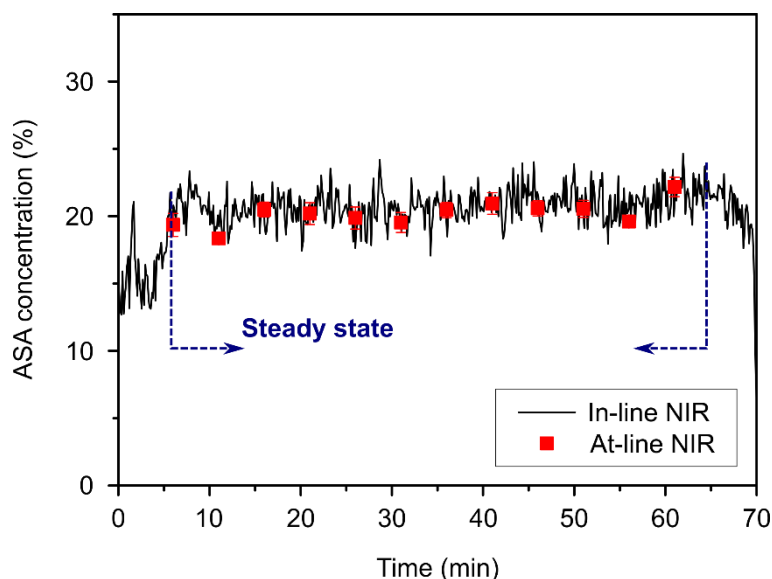
Figure 41. ASA concentration in the powder blend measured by an in-line NIR probe after blending, and the result of at-line NIR analysis of the produced tablets from the steady state.

The tablet press continuously produced compressed tablets of a mean weight of 500.42 ± 2.71 mg from the powder blend. With the 300 g/h total mass flow circa 14400 dose units could be produced per day. The average residence time of the continuous blending-tableting system was ~5 min. The product in the steady state was collected separately in every 5 minutes for further analysis. In order to assess the stability of the continuous blending and tableting process, the NIR probe was applied at-line to examine the ASA-loading of the separately collected tablets. The measured drug content representing every 5 minutes of the steady state is depicted in Figure 41. The average ASA concentration in the tablets was found to be 20.18% with a relative standard deviation of 4.70%. This was in good correspondence with the in-line recorded data during the experiment (Table 7). Nevertheless, the deviation of the drug-loading of the tablets was apparently smaller than that of the powder mixture (comparing the error bars of the at-line data points and the minimum and maximum values of the in-line data). This might be the result of additional mixing in the pipe of the tablet press, which is thus probably able to eliminate smaller API content fluctuations in the powder blend.

Table 7. Average ASA content and relative standard deviation during the steady state of the continuous blending-tableting experiment measured in-line (left) and at-line (right) by a NIR probe.

	In-line NIR	At-line NIR
Mean ASA concentration	20.70%	20.18%
RSD	5.78%	4.70%

4.3.4 Tablet content uniformity

Ten randomly selected tablets collected during the steady state were further analyzed by conventional content uniformity measurement. The ASA dose was measured by both reflection NIR spectroscopy and HPLC. The API concentrations of the tablets derived from the measurements are plotted in Figure 42.
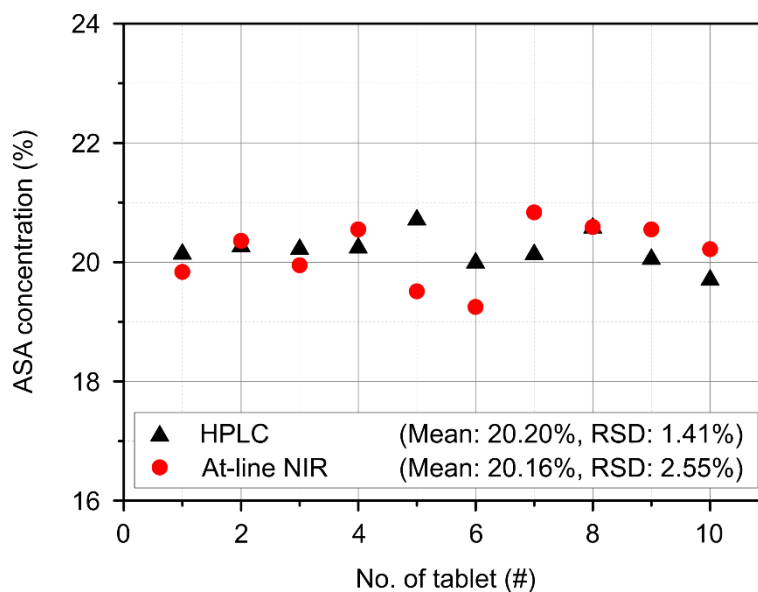
Figure 42. Content uniformity of 10 randomly selected tablets from steady state measured by HPLC and at-line NIR reflective spectroscopy.

The result of the two methods was in good agreement, as the mean concentration and the relative standard deviation were very similar. Based on the 10 samples, the continuously produced tablets passed the USP ⟨905⟩ content uniformity test [243], since the AV was well below the L1 = 15.0 acceptance limit (Table 8). The mean drug content and relative standard deviation calculated from the at-line content uniformity measurements were very similar to the outcome of the in-line NIR process monitoring in the steady state (20.70% mean value, 5.78% RSD, Table 7). These results indicate the applicability and advantages of continuous processes in powder blending and tableting to produce pharmaceutical products with consistent quality. Furthermore, the comparison of the NIR and HPLC results suggests that the faster NIR methods with much more data from the production could replace the destructive and slower off-line HPLC measurements.

Table 8. Content uniformity test result of continuously produced tablets; values are given as % label claim.

	HPLC	At-line NIR
X (sample mean)	100.8	101.0
S (sample standard deviation)	0.28	0.52
M*	100.8	101.0
AV (Acceptance Value)*	0.67	1.25

*AV = |M-X| + kS, k = 2.4 for 10 tablets. M depends on the sample mean. If 98.5<X<101.5 then M = X, if X<98.5 then M = 98.5, if X>101.5 then M = 101.5. The content uniformity is accepted when the AV does not exceed the L1 = 15.0 limit [243].

4.3.5 Conclusions

In this study, we presented the first example for the continuous end-to-end production of conventionally compressed tablets on a proof-of-concept level. The flow synthesis reaction mixture of ASA was continuously crystallized in an MSMPR reactor. The crystallizer was directly connected to a continuous filtration carousel device for the filtration and drying of ASA crystals. The performance of the 2-step system was investigated, and the effects of the MSMPR settings on the filtered product quality were presented. The filtered material was collected and introduced into a continuous blender by a screw feeder along with MCC as a tableting excipient. PAT was integrated into the system as the homogeneity of the powder blend coming out from the mixer was monitored by an in-line NIR probe. A belt conveyor carried the material to a lab-scale eccentric tablet press, in which the continuous production of compressed 500 mg ASA-MCC tablets of 100 mg dose strength was accomplished and acceptable purity and content uniformity of the product was achieved according to the HPLC investigations. In conclusion, the end-to-end continuous production of conventional compressed tablets starting from raw materials is demonstrated in this study for the first time. It might be a significant step forward to close the gap between the current industrial practice and the desired future pharmaceutical manufacturing [14].

5 Summary

In this work the development and integration of different continuous pharmaceutical manufacturing technologies were presented. Two APIs, acetylsalicylic acid (ASA) and carvedilol (CAR) were applied as model compounds. Two types of final dosage forms, orally dissolving webs (ODWs) and conventionally compressed tablets were produced in the developed end-to-end continuous systems. Production performance was evaluated during longer periods of operation and the characterization of the products was carried out using several analytical techniques.

ASA was synthesized in flow reactors from salicylic acid (SA) using acetic anhydride. The two-step synthesis was thoroughly optimized to obtain the API with high yield and purity. Electrospinning was applied to directly work-up the reaction mixture, and to instantaneously formulate ASA into nanofibers. A continuous model system (CMS) was designed and built to integrate the flow microreactors and ES. In this system the produced fibrous product was collected on the surface of a carrier film. The film was strained on a slowly rotating wheel with a grounded metal sheet on its circumference. The formed double-layered strip was conveyed further and cut into small units ready for patient administration (30×30 mm). The performance tests of the CMS showed low amount of residual solvent content in the fibers (<5000 ppm), acceptable content uniformity of the cut dosage units (AV<15) and high purity of the synthesized ASA (>95%). All measurements confirmed the applicability of ES as a tool to turn APIs into fibrous dosage forms coupled to flow synthesis.

The wider applicability of the CMS was tested during the production of ODWs containing CAR, an API with poor water solubility and low dose strength. The ES process of CAR with PVPK30 was optimized to achieve stable operation in the CMS. The fibers were collected on the surface of cast pullulan film carrier, in which citric acid was also incorporated as pH modifier. The dissolution and disintegration tests of the produced ODWs showed ultrafast dissolution rate (80% in 5 minutes) and 10 seconds of disintegration, meeting the regulatory requirements for orally disintegrating formulations. The CAR-loaded ODW was produced in the CMS in a 4-hour long experiment to assess residual moisture content and content uniformity over time. The results showed low deviation of drug loading (average AV = 9.45), and by applying additional drying on room temperature even the strict regulatory limits of the less volatile DMF could be met (<880 ppm).

The integration of the continuous MSMPR crystallization of the reaction mixture with continuous filtration followed by the continuous blending and tableting of the produced ASA was also presented. The effect of critical crystallization process parameters on the filtered product quality was investigated in detail. The moisture content of the filtered crystals was affected by both the residence time and the temperature of the crystallization through the solid concentration and the cycle time of the filtration process. The amount of residual solvents could be decreased below 1%, and the flowability of the product was very similar with all the experimental settings. This was essential in the following continuous blending with microcrystalline cellulose (MCC), which was carried out in a twin-screw blender. Finally, the tableting of the powder blend was accomplished to obtain immediate release tablets of 100 mg dose strength. Real-time analysis was implemented during blending, showing low variation in the API concentration in the powder blend in steady state (RSD = 5.78%). The content uniformity of the tablets was analyzed by off-line HPLC and at-line NIR. The results were in good agreement with the in-line data (RSD = 4.70%) and the obtained AV values were well below the regulatory limit with both techniques ($AV_{HPLC} = 0.67$, $AV_{at\text{-}line\ NIR} = 1.25$).

6 Application of the results

More and more pharmaceutical companies recognize the need to reform the current manufacturing practice and start moving towards continuous technologies. However, the transition is a slow and costly process, as most companies do not have expertise in continuous manufacturing (CM). Typically, one or two steps from the long production line is chosen to develop an alternative of the existing batch process, which takes low risk. However, the real advantage of CM lies in integrated technological steps, with which significant improvements could be accomplished.

In this work several continuous pharmaceutical processes were developed from drug substance to drug product manufacturing. Emphasis was put on the connectability to each other. The interaction of process parameters was evaluated as well. This unprecedented approach towards the development of continuous pharmaceutical processes can facilitate the industrial application of more and more continuous technologies and can contribute to the spread of CM in the pharmaceutical industry.

A significant part of this work was performed in the frame of FIEK project of the National Research, Development and Innovation Office in Hungary. The aim of this project is to conduct research of increased industrial interest, and produce results which can be directly applied by the industrial partners of the collaboration, *i.e.* Richter Gedeon Plc. and Egis Pharmaceuticals Plc.

7 Publications

Publications on which thesis findings are based:

I. A. Balogh, **<u>A. Domokos</u>**, B. Farkas, A. Farkas, Z. Rapi, D. Kiss, Z. Nyiri, Z. Eke, G. Szarka, R. Örkényi, B. Mátravölgyi, F. Faigl, G. Marosi, Zs. K. Nagy, Continuous end-to-end production of solid drug dosage forms: coupling flow synthesis and formulation by electrospinning, *Chemical Engineering Journal*, **350** (2018), 290-299.
https://doi.org/10.1016/j.cej.2018.05.188

IF: 8.355 C: 32

II. **<u>A. Domokos</u>**, A. Balogh, D. Dénes, G. Nyerges, Z. Levente, B. Farkas, G. Marosi, Zs. K. Nagy, Continuous manufacturing of orally dissolving webs containing a poorly soluble drug via electrospinning, *European Journal of Pharmaceutical Sciences*, **130** (2019), 91-99.
https://doi.org/10.1016/j.ejps.2019.01.026

IF: 3.616 C: 8

III. Y. C. Liu, **<u>A. Domokos</u>**, S. Coleman, P. Firth, Z. K. Nagy, Development of continuous filtration in a novel continuous filtration carousel integrated with continuous crystallization, *Organic Process Research & Development*, **23**, 12 (2019), 2655-2665.
https://doi.org/10.1021/acs.oprd.9b00342

IF: 3.023 C: 1

IV. **<u>A. Domokos</u>**, B. Nagy, M. Gyürkés, A. Farkas, K. Tacsi, H. Pataki, Y. C. Liu, A. Balogh, P. Firth, B. Szilágyi, G. Marosi, Z. K. Nagy, Zs. K. Nagy, End-to-end continuous manufacturing of conventional compressed tablets: from flow synthesis to tableting through integrated crystallization and filtration, *International Journal of Pharmaceutics*, **581** (2020), 119297.
https://doi.org/10.1016/j.ijpharm.2020.119297

IF: 4.845 C: 0

Related publications:

V. E. Borbás; B. Sinko, O. Tsinman, K. Tsinman; É. Kiserdei, B. Démuth, A. Balogh, B. Bodák, **<u>A. Domokos</u>**, G. Dargó, G. Balogh, Zs. K. Nagy, Investigation and mathematical description of the real driving force of passive transport of drug molecules from supersaturated solutions, *Molecular Pharmaceutics*, **13**, 11 (2016), 3816-3826.

https://doi.org/10.1021/acs.molpharmaceut.6b00613

IF: 5.037 C: 38

VI. A. Balogh, B. Farkas, Á. Pálvölgyi, **<u>A. Domokos</u>**, B. Démuth, G. Marosi, Zs. K. Nagy, Novel alternating current electrospinning of hydroxypropylmethylcellulose acetate succinate (HPMCAS) nanofibers for dissolution enhancement: the importance of solution conductivity, *Journal of Pharmaceutical Sciences*, **106**, 6 (2017), 1634-1643.

https://doi.org/10.1016/j.xphs.2017.02.021

IF: 3.075 C: 15

VII. A. Balogh, B. Farkas, **<u>A. Domokos</u>**, A. Farkas, B. Démuth, E. Borbás, B. Nagy, G. Marosi, Zs. K. Nagy, Controlled-release solid dispersions of Eudragit® FS and poorly soluble spironolactone prepared by electrospinning and melt extrusion, *European Polymer Journal*, **95** (2017), 406-417.

https://doi.org/10.1016/j.eurpolymj.2017.08.032

IF: 3.741 C: 20

VIII. B. Farkas, A. Balogh, A. Farkas, **<u>A. Domokos</u>**, E. Borbás, G. Marosi, Zs. K. Nagy, Medicated straws based on electrospun solid dispersions, *Periodica Politechnica Chemical Engineering*, **62**, 3 (2018), 310-316.

https://doi.org/10.3311/PPch.11931

IF: 1.382 C: 7

IX. T. Casian, A. Farkas, K. Ilyés, B. Démuth, E. Borbás, L. Madarász, Z. Rapi, B. Farkas, A. Balogh, **<u>A. Domokos</u>**, G. Marosi, I. Tomuta, Zs. K. Nagy, Data fusion strategies for performance improvement of a Process Analytical Technology

platform consisting of four instruments: An electrospinning case study, *International Journal of Pharmaceutics*, **567** (2019), 118473. https://doi.org/10.1016/j.ijpharm.2019.118473

IF: 4.845 C: 3

X. P. Vass, E. Szabó, **A. Domokos**, E. Hirsch, D. Galata, B. Farkas, B. Démuth, S. K. Anderson, T. Vigh, G. Verreck, G. Marosi, Zs: K. Nagy, Scale-up of electrospinning technology: Applications in the pharmaceutical industry, *WIREs Nanomedicine and Nanobiotechnology*, **12**, 4 (2019), e1611. https://doi.org/10.1002/wnan.1611

IF: 7.689 C: 6

XI. L. A. Mészáros, D. L. Galata, L. Madarász, Á. Köte, K. Csorba, Á. Z. Dávid, **A. Domokos**, E. Szabó, B. Nagy, G. Marosi, A. Farkas, Zs. K. Nagy, Digital UV/VIS imaging: A rapid PAT tool for crushing strength, drug content and particle size distribution determination in tablets, *International Journal of Pharmaceutics*, **578** (2020), 119174. https://doi.org/10.1016/j.ijpharm.2020.119174

IF: 4.845 C: 0

XII. K. Tacsi, H. Pataki, **A. Domokos**, I. Csontos, I. Markovits, F. Farkas, Zs. K. Nagy, G. Marosi, Direct processing of a flow reaction mixture using continuous MSMPR crystallizer, *Crystal Growth & Design*, **20** (2020), 4433-4442. https://doi.org/10.1021/acs.cgd.0c00252

IF: 4.089 C: 0

XIII. P. Vass, E. Pantea, **A. Domokos**, E. Hirsch, J. Domján, Á. Németh, M. Molnár, Cs. Fehér, S. K. Andersen, T. Vigh, G. Verreck, I. Csontos, G. Marosi, Zs. K. Nagy, Electrospun Solid Formulation of Anaerobic Gut Microbiome Bacteria, *AAPS PharmSciTech*, **21**, 214 (2020). https://doi.org/10.1208/s12249-020-01769-y

IF: 2.401 C: 0

Oral presentations (in English):

XIV.   **A. Domokos**, A. Balogh, B. Farkas, B. Démuth, H. Pataki, Zs. K. Nagy, G. Marosi, Coupling flow synthesis and formulation by electrospinning, 18AIChE Annual Meeting, Pittsburgh, USA, 2018.10.28.-11.02.

XV.   **A. Domokos**, B. Nagy, K. Tacsi, G. Marosi, Z. K. Nagy, Zs. K. Nagy, Integration of continuous filtration into a continuous pharmaceutical production line, The 12th Edition of the Biopharmacy-Pharmacokinetics & Industrial Pharmacy Symposium, Cluj-Napoca, Romania, 2019.11.08.

Oral presentations (in Hungarian):

XVI.   **Domokos A.**, Balogh A., Nagy Zs. K., Rapi Z., Marosi G. Acetilszalicilsav teljesen folyamatos szintézise és formulációja elektrosztatikus szálképzés alkalmazásával, XXXVIII. Kémiai Előadói Napok, Szeged, 2016.10.17-19.

XVII.   **Domokos A.**, Balogh A., Rapi Z., Nagy Zs. K., Marosi G., Folyamatos áramlásos reaktor és elektrosztatikus szálképzés összekapcsolhatóságának vizsgálata, Kristályosítási és Gyógyszerformulálási Szakosztály 10. Kerekasztal Konferenciája, Balatonszemes, 2017.05.19-20.

Poster presentations:

XVIII.   T. Sohajda, **A. Domokos**, A. Darcsi, I. Fejős, S. Béni, É. Fenyvesi, L. Szente, Cucurbiturils and Cyclodextrins: Comparison of Complexation Behavior and Analytical Characterization, 4th European Conference on Cyclodextrins - Euro CD 2015, Lille, 2015.10.6-9.

XIX.   **A. Domokos**, A. Balogh, B. Farkas, Z. Rapi, P. Tóth, E. Juhász, G. Marosi, Zs. K. Nagy; The investigation of the connectability of continuous flow reactors and electrospinning, 7th BBBB Conference on Pharmaceutical Sciences, Balatonfüred, 2017.10.5-7.

8   References

[1]   A. Adamo, R.L. Beingessner, M. Behnam, J. Chen, T.F. Jamison, K.F. Jensen, J.-C.M. Monbaliu, A.S. Myerson, E.M. Revalor, D.R. Snead, T. Stelzer, N. Weeranoppanant, S.Y. Wong, P. Zhang, On-Demand Continuous-Flow Production of Pharmaceuticals in a Compact Reconfigurable System, *Science*. **352** (2016) 61–67. https://doi.org/10.1126/science.aaf1337.

[2]   J.S. Srai, C. Badman, M. Krumme, M. Futran, C. Johnston, Future supply chains enabled by continuous processing-opportunities and challenges May 20-21, 2014 continuous manufacturing symposium, *J. Pharm. Sci.* **104** (2015) 840–849. https://doi.org/10.1002/jps.24343.

[3]   C. Badman, B.L. Trout, Achieving Continuous Manufacturing May 20–21 2014 Continuous Manufacturing Symposium, *J. Pharm. Sci.* **104** (2015) 779–780. https://doi.org/10.1002/jps.24246.

[4]   K. Plumb, Continuous Processing in the Pharmaceutical Industry: Changing the Mind Set, *Chem. Eng. Res. Des.* **83** (2005) 730–738. https://doi.org/10.1205/cherd.04359.

[5]   N. Shah, Pharmaceutical supply chains: Key issues and strategies for optimisation, in: Comput. Chem. Eng., Pergamon, 2004: pp. 929–941. https://doi.org/10.1016/j.compchemeng.2003.09.022.

[6]   J.S. Srai, T. Harrington, L. Alinaghian, M. Phillips, Evaluating the Potential for the Continuous Processing of Pharmaceutical Products - A Supply Network Perspective, *Chem. Eng. Process. Process Intensif.* **97** (2015) 248–258. https://doi.org/10.1016/j.cep.2015.07.018.

[7]   L.X. Yu, Pharmaceutical Quality by Design: Product and Process Development, Understanding, and Control, *Pharm. Res.* **25** (2008) 781–791. https://doi.org/10.1007/s11095-007-9511-1.

[8]   M. Teżyk, B. Milanowski, A. Ernst, J. Lulek, Recent progress in continuous and semi-continuous processing of solid oral dosage forms: a review, *Drug Dev. Ind. Pharm.* **42** (2016) 1195–1214. https://doi.org/10.3109/03639045.2015.1122607.

[9]   S. Mascia, P.L. Heider, H. Zhang, R. Lakerveld, B. Benyahia, P.I. Barton, R.D. Braatz, C.L. Cooney, J.M.B. Evans, T.F. Jamison, K.F. Jensen, A.S. Myerson, B.L. Trout, End-to-end continuous manufacturing of pharmaceuticals: Integrated synthesis, purification, and final dosage formation, *Angew. Chemie*. **125** (2013) 12585–12589. https://doi.org/10.1002/ange.201305429.

[10]   P. Suresh, P.K. Basu, Improving Pharmaceutical Product Development and Manufacturing: Impact on Cost of Drug Development and Cost of Goods Sold of Pharmaceuticals, *J. Pharm. Innov.* **3** (2008) 175–187. https://doi.org/10.1007/s12247-008-9043-1.

[11]   Food and Drug Administration, Guidance for Industry Changes to an Approved NDA or ANDA, *FDA Off. Doc.* (2004) 1–40. https://www.fda.gov/media/71846/download.

[12]   J. Rantanen, J. Khinast, The Future of Pharmaceutical Manufacturing Sciences, *J. Pharm. Sci.* **104** (2015) 3612–3638. https://doi.org/10.1002/jps.24594.

[13] Q. Su, S. Ganesh, M. Moreno, Y. Bommireddy, M. Gonzalez, G. V. Reklaitis, Z.K. Nagy, A perspective on Quality-by-Control (QbC) in pharmaceutical continuous manufacturing, *Comput. Chem. Eng.* **125** (2019) 216–231. https://doi.org/10.1016/j.compchemeng.2019.03.001.

[14] S.L. Lee, T.F. O'Connor, X. Yang, C.N. Cruz, S. Chatterjee, R.D. Madurawe, C.M. V Moore, L.X. Yu, J. Woodcock, Modernizing Pharmaceutical Manufacturing: from Batch to Continuous Production, *J. Pharm. Innov.* **10** (2015) 191–199. https://doi.org/10.1007/s12247-015-9215-8.

[15] Food and Drug Administration, Drug Shortages: Root Causes and Potential Solutions, *FDA Off. Doc.* (2019).

[16] Food and Drug Administration, Report on Drug Shortages for Calendar Year 2018, *FDA Off. Doc.* (2018).

[17] J.A. DiMasi, H.G. Grabowski, R.W. Hansen, Innovation in the pharmaceutical industry: New estimates of R&D costs, *J. Health Econ.* **47** (2016) 20–33. https://doi.org/10.1016/j.jhealeco.2016.01.012.

[18] M.M. Nasr, M. Krumme, Y. Matsuda, B.L. Trout, C. Badman, S. Mascia, C.L. Cooney, K.D. Jensen, A. Florence, C. Johnston, K. Konstantinov, S.L. Lee, Regulatory Perspectives on Continuous Pharmaceutical Manufacturing: Moving From Theory to Practice: September 26-27, 2016, International Symposium on the Continuous Manufacturing of Pharmaceuticals, in: J. Pharm. Sci., Elsevier, 2017: pp. 3199–3206. https://doi.org/10.1016/j.xphs.2017.06.015.

[19] S. Byrn, M. Futran, H. Thomas, E. Jayjock, N. Maron, R.F. Meyer, A.S. Myerson, M.P. Thien, B.L. Trout, Achieving Continuous Manufacturing for Final Dosage Formation: Challenges and How to Meet Them May 20–21 2014 Continuous Manufacturing Symposium, *J. Pharm. Sci.* **104** (2015) 792–802. https://doi.org/10.1002/jps.24247.

[20] I.R. Baxendale, R.D. Braatz, B.K. Hodnett, K.F. Jensen, M.D. Johnson, P. Sharratt, J.-P. Sherlock, A.J. Florence, Achieving Continuous Manufacturing: Technologies and Approaches for Synthesis, Workup, and Isolation of Drug Substance May 20–21, 2014 Continuous Manufacturing Symposium, *J. Pharm. Sci.* **104** (2015) 781–791. https://doi.org/10.1002/jps.24252.

[21] G. Allison, Y.T. Cain, C. Cooney, T. Garcia, T.G. Bizjak, O. Holte, N. Jagota, B. Komas, E. Korakianiti, D. Kourti, R. Madurawe, E. Morefield, F. Montgomery, M. Nasr, W. Randolph, J.-L. Robert, D. Rudd, D. Zezza, Regulatory and Quality Considerations for Continuous Manufacturing May 20–21, 2014 Continuous Manufacturing Symposium, *J. Pharm. Sci.* **104** (2015) 803–812. https://doi.org/10.1002/jps.24324.

[22] S.D. Schaber, D.I. Gerogiorgis, R. Ramachandran, J.M.B. Evans, P.I. Barton, B.L. Trout, Economic Analysis of Integrated Continuous and Batch Pharmaceutical Manufacturing: A Case Study, *Ind. Eng. Chem. Res.* **50** (2011) 10083–10092. https://doi.org/10.1021/ie2006752.

[23] L.L. Simon, A.A. Kiss, J. Cornevin, R. Gani, Process engineering advances in pharmaceutical and chemical industries: digital process design, advanced rectification, and continuous filtration, *Curr. Opin. Chem. Eng.* **25** (2019) 114–121. https://doi.org/10.1016/j.coche.2019.02.005.

[24] V. Vanhoorne, C. Vervaet, Recent progress in continuous manufacturing of oral solid

dosage forms, *Int. J. Pharm.* **579** (2020) 119194. https://doi.org/10.1016/j.ijpharm.2020.119194.

[25] American Chemical Society, ACS GCI Roundtable, (2005). https://www.acs.org/content/acs/en/greenchemistry/industry-roundtables/pharmaceutical.html.

[26] P. Poechlauer, J. Manley, R. Broxterman, B. Gregertsen, M. Ridemark, Continuous processing in the manufacture of active pharmaceutical ingredients and finished dosage forms: An industry perspective, *Org. Process Res. Dev.* **16** (2012) 1586–1590. https://doi.org/10.1021/op300159y.

[27] P. Poechlauer, J. Colberg, E. Fisher, M. Jansen, M.D. Johnson, S.G. Koenig, M. Lawler, T. Laporte, J. Manley, B. Martin, A. O'Kearney-McMullan, Pharmaceutical Roundtable Study Demonstrates the Value of Continuous Manufacturing in the Design of Greener Processes, *Org. Process Res. Dev.* **17** (2013) 1472–1478. https://doi.org/10.1021/op400245s.

[28] Food and Drug Administration, Guidance for Industry PAT: A Framework for Innovative Pharmaceutical Development, Manufacuring, and Quality Assurance, *FDA Off. Doc.* (2004) 16.

[29] L.L. Simon, H. Pataki, G. Marosi, F. Meemken, K. Hungerbühler, A. Baiker, S. Tummala, B. Glennon, M. Kuentz, G. Steele, H.J.M. Kramer, J.W. Rydzak, Z. Chen, J. Morris, F. Kjell, R. Singh, R. Gani, K. V. Gernaey, M. Louhi-Kultanen, J. Oreilly, N. Sandler, O. Antikainen, J. Yliruusi, P. Frohberg, J. Ulrich, R.D. Braatz, T. Leyssens, M. von Stosch, R. Oliveira, R.B.H. Tan, H. Wu, M. Khan, D. Ogrady, A. Pandey, R. Westra, E. Delle-Case, D. Pape, D. Angelosante, Y. Maret, O. Steiger, M. Lenner, K. Abbou-Oucherif, Z.K. Nagy, J.D. Litster, V.K. Kamaraju, M. Sen Chiu, Assessment of Recent Process Analytical Technology (PAT) Trends: A Multiauthor Review, *Org. Process Res. Dev.* **19** (2015). https://doi.org/10.1021/op500261y.

[30] Food and Drug Administration, Quality considerations for continuous manufacturing Guidance for industry, *FDA Off. Doc.* (2019).

[31] International Council for Harmonization, ICH Q8: Pharmaceutical Development, 2009.

[32] International Council for Harmonization, ICH Q9: Quality Risk Management, 2005.

[33] International Council for Harmonization, ICH Q10: Pharmaceutical Quality System, 2008.

[34] International Council for Harmonization, ICH Q11: Development and Manufacture of Drug Substances (Chemical Entities and Biotechnological/Biological Entities), 2012.

[35] International Council for Harmonization, ICH Q13: Continuous Manufacturing of Drug Substances and Drug Products, 2018. http://www.ich.org (accessed February 19, 2020).

[36] N. Mihokovic, Continuous manufacturing - EMA perspective and experience, in: Eng. Conf. Int., 2017.

[37] L.X. Yu, G. Amidon, M.A. Khan, S.W. Hoag, J. Polli, G.K. Raju, J. Woodcock, Understanding pharmaceutical quality by design, *AAPS J.* **16** (2014) 771–783. https://doi.org/10.1208/s12248-014-9598-3.

[38] Food and Drug Administration, FDA statement on FDA's modern approach to advanced

pharmaceutical manufacturing, (2019). https://www.fda.gov/news-events/press-announcements/fda-statement-fdas-modern-approach-advanced-pharmaceutical-manufacturing?platform=hootsuite.

[39] C. Badman, C.L. Cooney, A. Florence, K. Konstantinov, M. Krumme, S. Mascia, M. Nasr, B.L. Trout, Why We Need Continuous Pharmaceutical Manufacturing and How to Make It Happen, *J. Pharm. Sci.* **108** (2019) 3521–3523. https://doi.org/10.1016/j.xphs.2019.07.016.

[40] P. McKenzie, S. Kiang, J. Tom, A.E. Rubin, M. Futran, Can pharmaceutical process development become high tech?, *AIChE J.* **52** (2006) 3990–3994. https://doi.org/10.1002/aic.11022.

[41] E. Palmer, FDA Urges Companies to Get On Board with Continuous Manufacturing, *FiercePharma*. (2016). https://www.fiercepharma.com/manufacturing/fda-urges-companies-to-get-on-board-continuous-manufacturing.

[42] J.D. Orr, G.L. Reid, Process Analytical Technology: Meeting FDA's Aspirational Guidance In Continuous Manufacturing, *Pharm. Online*. (2018). https://www.pharmaceuticalonline.com/doc/process-analytical-technology-meeting-fda-s-aspirational-guidance-in-continuous-manufacturing-0001.

[43] I.R. Baxendale, R.D. Braatz, B.K. Hodnett, K.F. Jensen, M.D. Johnson, P. Sharratt, J.-P. Sherlock, A.J. Florence, Achieving Continuous Manufacturing: Technologies and Approaches for Synthesis, Workup, and Isolation of Drug Substance May 20–21, 2014 Continuous Manufacturing Symposium, *J. Pharm. Sci.* **104** (2015) 781–791. https://doi.org/10.1002/jps.24252.

[44] K. Nepveux, J.P. Sherlock, M. Futran, M. Thien, M. Krumme, How development and manufacturing will need to be structured-heads of development/manufacturing May 20-21, 2014 continuous manufacturing symposium, *J. Pharm. Sci.* **104** (2015) 850–864. https://doi.org/10.1002/jps.24286.

[45] H. Leuenberger, New trends in the production of pharmaceutical granules: batch versus continuous processing, *Eur. J. Pharm. Biopharm.* **52** (2001) 289–296. https://doi.org/10.1016/S0939-6411(01)00199-0.

[46] C. Vervaet, J.P. Remon, Continuous granulation in the pharmaceutical industry, *Chem. Eng. Sci.* **60** (2005) 3949–3957. https://doi.org/10.1016/j.ces.2005.02.028.

[47] H. Chen, E. Diep, T.A.G. Langrish, B.J. Glasser, Continuous fluidized bed drying: Residence time distribution characterization and effluent moisture content prediction, *AIChE J.* **66** (2020). https://doi.org/10.1002/aic.16902.

[48] D.M. Parikh, ed., Handbook of Pharmaceutical Granulation Technology, CRC Press, 2016. https://doi.org/10.3109/9781616310035.

[49] D. Webb, T.F. Jamison, Continuous flow multi-step organic synthesis, *Chem. Sci.* **1** (2010) 675. https://doi.org/10.1039/c0sc00381f.

[50] M.B. Plutschack, B. Pieber, K. Gilmore, P.H. Seeberger, The Hitchhiker's Guide to Flow Chemistry, *Chem. Rev.* **117** (2017) 11796–11893. https://doi.org/10.1021/acs.chemrev.7b00183.

[51] J.C. Pastre, D.L. Browne, S. V. Ley, Flow chemistry syntheses of natural products, *Chem. Soc. Rev.* **42** (2013) 8849. https://doi.org/10.1039/c3cs60246j.

[52]   P. Bana, R. Örkényi, K. Lövei, Á. Lakó, G.I. Túrós, J. Éles, F. Faigl, I. Greiner, The route from problem to solution in multistep continuous flow synthesis of pharmaceutical compounds, *Bioorg. Med. Chem.* **25** (2017) 6180–6189. https://doi.org/10.1016/j.bmc.2016.12.046.

[53]   R. Munirathinam, J. Huskens, W. Verboom, Supported Catalysis in Continuous-Flow Microreactors, *Adv. Synth. Catal.* **357** (2015) 1093–1123. https://doi.org/10.1002/adsc.201401081.

[54]   C.J. Mallia, I.R. Baxendale, The Use of Gases in Flow Synthesis, *Org. Process Res. Dev.* **20** (2016) 327–360. https://doi.org/10.1021/acs.oprd.5b00222.

[55]   M. Brzozowski, M. O'Brien, S. V. Ley, A. Polyzos, Flow Chemistry: Intelligent Processing of Gas–Liquid Transformations Using a Tube-in-Tube Reactor, *Acc. Chem. Res.* **48** (2015) 349–362. https://doi.org/10.1021/ar500359m.

[56]   R. Porta, M. Benaglia, A. Puglisi, Flow Chemistry: Recent Developments in the Synthesis of Pharmaceutical Products, *Org. Process Res. Dev.* **20** (2016) 2–25. https://doi.org/10.1021/acs.oprd.5b00325.

[57]   D. Cambié, C. Bottecchia, N.J.W. Straathof, V. Hessel, T. Noël, Applications of Continuous-Flow Photochemistry in Organic Synthesis, Material Science, and Water Treatment, *Chem. Rev.* **116** (2016) 10276–10341. https://doi.org/10.1021/acs.chemrev.5b00707.

[58]   A.R. Bogdan, A.W. Dombrowski, Emerging Trends in Flow Chemistry and Applications to the Pharmaceutical Industry, *J. Med. Chem.* **62** (2019) 6422–6468. https://doi.org/10.1021/acs.jmedchem.8b01760.

[59]   F.M. Akwi, P. Watts, Continuous flow chemistry: where are we now? Recent applications, challenges and limitations, *Chem. Commun.* **54** (2018) 13894–13928. https://doi.org/10.1039/C8CC07427E.

[60]   B.J. Deadman, S.G. Collins, A.R. Maguire, Taming Hazardous Chemistry in Flow: The Continuous Processing of Diazo and Diazonium Compounds, *Chem. - A Eur. J.* **21** (2015) 2298–2308. https://doi.org/10.1002/chem.201404348.

[61]   M. Movsisyan, E.I.P. Delbeke, J.K.E.T. Berton, C. Battilocchio, S. V. Ley, C. V. Stevens, Taming hazardous chemistry by continuous flow technology, *Chem. Soc. Rev.* **45** (2016) 4892–4928. https://doi.org/10.1039/C5CS00902B.

[62]   F. Gomollón-Bel, Ten Chemical Innovations That Will Change Our World: IUPAC identifies emerging technologies in Chemistry with potential to make our planet more sustainable, *Chem. Int.* **41** (2019) 12–17. https://doi.org/10.1515/ci-2019-0203.

[63]   B. Gutmann, D. Cantillo, C.O. Kappe, Continuous-Flow Technology-A Tool for the Safe Manufacturing of Active Pharmaceutical Ingredients, *Angew. Chemie Int. Ed.* **54** (2015) 6688–6728. https://doi.org/10.1002/anie.201409318.

[64]   S. V. Ley, D.E. Fitzpatrick, R.J. Ingham, R.M. Myers, Organic Synthesis: March of the Machines, *Angew. Chemie Int. Ed.* **54** (2015) 3449–3464. https://doi.org/10.1002/anie.201410744.

[65]   A. Gioiello, A. Piccinno, A.M. Lozza, B. Cerra, The Medicinal Chemistry in the Era of Machines and Automation: Recent Advances in Continuous Flow Technology, *J. Med. Chem.* **63** (2020) 6624–6647. https://doi.org/10.1021/acs.jmedchem.9b01956.

[66] M. Baumann, T.S. Moody, M. Smyth, S. Wharry, A Perspective on Continuous Flow Chemistry in the Pharmaceutical Industry, *Org. Process Res. Dev.* (2020) acs.oprd.9b00524. https://doi.org/10.1021/acs.oprd.9b00524.

[67] L. Malet-Sanz, F. Susanne, Continuous flow synthesis. a pharma perspective, *J. Med. Chem.* **55** (2012) 4062–4098. https://doi.org/10.1021/jm2006029.

[68] J. Britton, C.L. Raston, Multi-step continuous-flow synthesis, *Chem. Soc. Rev.* **46** (2017) 1250–1271. https://doi.org/10.1039/C6CS00830E.

[69] J. Wegner, S. Ceylan, A. Kirschning, Flow Chemistry – A Key Enabling Technology for (Multistep) Organic Synthesis, *Adv. Synth. Catal.* **354** (2012) 17–57. https://doi.org/10.1002/adsc.201100584.

[70] M. Baumann, I.R. Baxendale, The synthesis of active pharmaceutical ingredients (APIs) using continuous flow chemistry, *Beilstein J. Org. Chem.* **11** (2015) 1194–1219. https://doi.org/10.3762/bjoc.11.134.

[71] B. Pieber, K. Gilmore, P.H. Seeberger, Integrated flow processing — challenges in continuous multistep synthesis, *J. Flow Chem.* **7** (2017) 129–136. https://doi.org/10.1556/1846.2017.00016.

[72] N. Weeranoppanant, A. Adamo, In-Line Purification: A Key Component to Facilitate Drug Synthesis and Process Development in Medicinal Chemistry, *ACS Med. Chem. Lett.* **11** (2020) 9–15. https://doi.org/10.1021/acsmedchemlett.9b00491.

[73] R. Örkényi, J. Éles, F. Faigl, P. Vincze, A. Prechl, Z. Szakács, J. Kóti, I. Greiner, Continuous Synthesis and Purification by Coupling a Multistep Flow Reaction with Centrifugal Partition Chromatography, *Angew. Chemie Int. Ed.* **56** (2017) 8742–8745. https://doi.org/10.1002/anie.201703852.

[74] D.L. Hughes, Applications of Flow Chemistry in Drug Development: Highlights of Recent Patent Literature, *Org. Process Res. Dev.* **22** (2018) 13–20. https://doi.org/10.1021/acs.oprd.7b00363.

[75] A.R. Bogdan, S.L. Poe, D.C. Kubis, S.J. Broadwater, D.T. McQuade, The continuous-flow synthesis of ibuprofen, *Angew. Chemie - Int. Ed.* **48** (2009) 8547–8550. https://doi.org/10.1002/anie.200903055.

[76] M. Viviano, T.N. Glasnov, B. Reichart, G. Tekautz, C.O. Kappe, A Scalable Two-Step Continuous Flow Synthesis of Nabumetone and Related 4-Aryl-2-butanones, *Org. Process Res. Dev.* **15** (2011) 858–870. https://doi.org/10.1021/op2001047.

[77] B. Ahmed-Omer, A.J. Sanderson, Preparation of fluoxetine by multiple flow processing steps, *Org. Biomol. Chem.* **9** (2011) 3854. https://doi.org/10.1039/c0ob00906g.

[78] F. Lévesque, P.H. Seeberger, Continuous-Flow Synthesis of the Anti-Malaria Drug Artemisinin, *Angew. Chemie Int. Ed.* **51** (2012) 1706–1709. https://doi.org/10.1002/anie.201107446.

[79] M.D. Hopkin, I.R. Baxendale, S. V Ley, An expeditious synthesis of imatinib and analogues utilising flow chemistry methods, *Org. Biomol. Chem.* **11** (2013) 1822–1839. https://doi.org/10.1039/C2OB27002A.

[80] P.R.D. Murray, D.L. Browne, J.C. Pastre, C. Butters, D. Guthrie, S. V. Ley, Continuous Flow-Processing of Organometallic Reagents Using an Advanced Peristaltic Pumping

System and the Telescoped Flow Synthesis of (E/Z)-Tamoxifen, *Org. Process Res. Dev.* **17** (2013) 1192–1208. https://doi.org/10.1021/op4001548.

[81] D.R. Snead, T.F. Jamison, End-to-end continuous flow synthesis and purification of diphenhydramine hydrochloride featuring atom economy, in-line separation, and flow of molten ammonium salts, *Chem. Sci.* **4** (2013) 2822. https://doi.org/10.1039/c3sc50859e.

[82] L. Kupracz, A. Kirschning, Multiple Organolithium Generation in the Continuous Flow Synthesis of Amitriptyline, *Adv. Synth. Catal.* **355** (2013) 3375–3380. https://doi.org/10.1002/adsc.201300614.

[83] J. Hartwig, S. Ceylan, L. Kupracz, L. Coutable, A. Kirschning, Heating under High-Frequency Inductive Conditions: Application to the Continuous Synthesis of the Neurolepticum Olanzapine (Zyprexa), *Angew. Chemie Int. Ed.* **52** (2013) 9813–9817. https://doi.org/10.1002/anie.201302239.

[84] P. Zhang, M.G. Russell, T.F. Jamison, Continuous Flow Total Synthesis of Rufinamide, *Org. Process Res. Dev.* **18** (2014) 1567–1570. https://doi.org/10.1021/op500166n.

[85] C.S. Polster, K.P. Cole, C.L. Burcham, B.M. Campbell, A.L. Frederick, M.M. Hansen, M. Harding, M.R. Heller, M.T. Miller, J.L. Phillips, P.M. Pollock, N. Zaborenko, Pilot-scale continuous production of LY2886721: Amide formation and reactive crystallization, *Org. Process Res. Dev.* **18** (2014) 1295–1309. https://doi.org/10.1021/op500204z.

[86] P.L. Heider, S.C. Born, S. Basak, B. Benyahia, R. Lakerveld, H. Zhang, R. Hogan, L. Buchbinder, A. Wolfe, S. Mascia, J.M.B. Evans, T.F. Jamison, K.F. Jensen, Development of a multi-step synthesis and workup sequence for an integrated, continuous manufacturing process of a pharmaceutical, *Org. Process Res. Dev.* **18** (2014) 402–409. https://doi.org/10.1021/op400294z.

[87] C.A. Correia, K. Gilmore, D.T. McQuade, P.H. Seeberger, A Concise Flow Synthesis of Efavirenz, *Angew. Chemie Int. Ed.* **54** (2015) 4945–4948. https://doi.org/10.1002/anie.201411728.

[88] T. Tsubogo, H. Oyamada, S. Kobayashi, Multistep continuous-flow synthesis of (R)- and (S)-rolipram using heterogeneous catalysts, *Nature*. **520** (2015) 329–332. https://doi.org/10.1038/nature14343.

[89] A.D. Martin, A.R. Siamaki, K. Belecki, B.F. Gupton, A flow-based synthesis of telmisartan, *J. Flow Chem.* **5** (2015) 145–147. https://doi.org/10.1556/JFC-D-15-00002.

[90] D.R. Snead, T.F. Jamison, A Three-Minute Synthesis and Purification of Ibuprofen: Pushing the Limits of Continuous-Flow Processing, *Angew. Chemie Int. Ed.* **54** (2015) 983–987. https://doi.org/10.1002/anie.201409093.

[91] L. Pellegatti, A. Hafner, J. Sedelmeier, A two-step continuous-flow procedure towards ribociclib, *J. Flow Chem.* **6** (2016) 198–201. https://doi.org/10.1556/1846.2016.00017.

[92] H. Ishitani, K. Kanai, Y. Saito, T. Tsubogo, S. Kobayashi, Synthesis of (±)-Pregabalin by Utilizing a Three-Step Sequential-Flow System with Heterogeneous Catalysts, *European J. Org. Chem.* **2017** (2017) 6491–6494. https://doi.org/10.1002/ejoc.201700998.

[93] A. Harsanyi, A. Conte, L. Pichon, A. Rabion, S. Grenier, G. Sandford, One-Step Continuous Flow Synthesis of Antifungal WHO Essential Medicine Flucytosine Using

Fluorine, *Org. Process Res. Dev.* **21** (2017) 273–276. https://doi.org/10.1021/acs.oprd.6b00420.

[94] V. De Vitis, F. Dall'Oglio, A. Pinto, C. De Micheli, F. Molinari, P. Conti, D. Romano, L. Tamborini, Chemoenzymatic Synthesis in Flow Reactors: A Rapid and Convenient Preparation of Captopril, *ChemistryOpen*. **6** (2017) 668–673. https://doi.org/10.1002/open.201700082.

[95] K.P. Cole, J.M.C. Groh, M.D. Johnson, C.L. Burcham, B.M. Campbell, W.D. Diseroad, M.R. Heller, J.R. Howell, N.J. Kallman, T.M. Koenig, S.A. May, R.D. Miller, D. Mitchell, D.P. Myers, S.S. Myers, J.L. Phillips, C.S. Polster, T.D. White, J. Cashman, D. Hurley, R. Moylan, P. Sheehan, R.D. Spencer, K. Desmond, P. Desmond, O. Gowran, Kilogram-scale prexasertib monolactate monohydrate synthesis under continuous-flow CGMP conditions, *Science*. **356** (2017) 1144–1151. https://doi.org/10.1126/science.aan0745.

[96] N.C. Neyt, D.L. Riley, Batch–flow hybrid synthesis of the antipsychotic clozapine, *React. Chem. Eng.* **3** (2018) 17–24. https://doi.org/10.1039/C7RE00146K.

[97] E. Yu, H.P.R. Mangunuru, N.S. Telang, C.J. Kong, J. Verghese, S.E. Gilliland III, S. Ahmad, R.N. Dominey, B.F. Gupton, High-yielding continuous-flow synthesis of antimalarial drug hydroxychloroquine, *Beilstein J. Org. Chem.* **14** (2018) 583–592. https://doi.org/10.3762/bjoc.14.45.

[98] R.E. Ziegler, B.K. Desai, J.-A. Jee, B.F. Gupton, T.D. Roper, T.F. Jamison, 7-Step Flow Synthesis of the HIV Integrase Inhibitor Dolutegravir, *Angew. Chemie Int. Ed.* **57** (2018) 7181–7185. https://doi.org/10.1002/anie.201802256.

[99] V. Mancino, B. Cerra, A. Piccinno, A. Gioiello, Continuous Flow Synthesis of 16-Dehydropregnenolone Acetate, a Key Synthon for Natural Steroids and Drugs, *Org. Process Res. Dev.* **22** (2018) 600–607. https://doi.org/10.1021/acs.oprd.8b00038.

[100] P. Zhang, N. Weeranoppanant, D.A. Thomas, K. Tahara, T. Stelzer, M.G. Russell, M. O'Mahony, A.S. Myerson, H. Lin, L.P. Kelly, K.F. Jensen, T.F. Jamison, C. Dai, Y. Cui, N. Briggs, R.L. Beingessner, A. Adamo, Advanced Continuous Flow Platform for On-Demand Pharmaceutical Manufacturing, *Chem. - A Eur. J.* **24** (2018) 2776–2784. https://doi.org/10.1002/chem.201706004.

[101] X. Ma, J. Chen, X. Du, A Continuous Flow Process for the Synthesis of Hymexazol, *Org. Process Res. Dev.* **23** (2019) 1152–1158. https://doi.org/10.1021/acs.oprd.9b00047.

[102] Z. Boros, L. Nagy-Győr, K. Kátai-Fadgyas, I. Kőhegyi, I. Ling, T. Nagy, Z. Iványi, M. Oláh, G. Ruzsics, O. Temesi, B. Volk, Continuous flow production in the final step of vortioxetine synthesis. Piperazine ring formation on a flow platform with a focus on productivity and scalability, *J. Flow Chem.* **9** (2019) 101–113. https://doi.org/10.1007/s41981-019-00036-x.

[103] P. Bana, Á. Szigetvári, J. Kóti, J. Éles, I. Greiner, Flow-oriented synthetic design in the continuous preparation of the aryl piperazine drug flibanserin, *React. Chem. Eng.* **4** (2019) 652–657. https://doi.org/10.1039/C8RE00266E.

[104] W.C. Fu, T.F. Jamison, Modular Continuous Flow Synthesis of Imatinib and Analogues, *Org. Lett.* **21** (2019) 6112–6116. https://doi.org/10.1021/acs.orglett.9b02259.

[105] J. García-Lacuna, G. Domínguez, J. Blanco-Urgoiti, J. Pérez-Castells, Synthesis of

treprostinil: key Claisen rearrangement and catalytic Pauson–Khand reactions in continuous flow, *Org. Biomol. Chem.* **17** (2019) 9489–9501. https://doi.org/10.1039/C9OB02124H.

[106] H. Lee, H. Kim, D. Kim, From p -Xylene to Ibuprofen in Flow: Three-Step Synthesis by a Unified Sequence of Chemoselective C−H Metalations, *Chem. – A Eur. J.* **25** (2019) 11641–11645. https://doi.org/10.1002/chem.201903267.

[107] Z. Jaman, T.J.P. Sobreira, A. Mufti, C.R. Ferreira, R.G. Cooks, D.H. Thompson, Rapid On-Demand Synthesis of Lomustine under Continuous Flow Conditions, *Org. Process Res. Dev.* **23** (2019) 334–341. https://doi.org/10.1021/acs.oprd.8b00387.

[108] M.G. Russell, T.F. Jamison, Seven-Step Continuous Flow Synthesis of Linezolid Without Intermediate Purification, *Angew. Chemie Int. Ed.* **58** (2019) 7678–7681. https://doi.org/10.1002/anie.201901814.

[109] M.C.F.C.B. Damião, H.M. Marçon, J.C. Pastre, Continuous flow synthesis of the URAT1 inhibitor lesinurad, *React. Chem. Eng.* **5** (2020) 865–872. https://doi.org/10.1039/C9RE00483A.

[110] G.J. Lichtenegger, M. Maier, J.G. Khinast, H. Gruber-Wölfler, Continuous Suzuki—Miyaura reactions with novel Ce—Sn—Pd oxides and integrated crystallization as continuous downstream protocol, *J. Flow Chem.* **6** (2016) 244–251. https://doi.org/10.1556/1846.2016.00021.

[111] R.J. Ingham, C. Battilocchio, D.E. Fitzpatrick, E. Sliwinski, J.M. Hawkins, S. V. Ley, A Systems Approach Towards an Intelligent and Self-Controlling Platform for Integrated Continuous Reaction Sequences, *Angew. Chemie - Int. Ed.* **54** (2015) 144–148. https://doi.org/10.1002/anie.201409356.

[112] B. Rimez, J. Septavaux, R. Debuysschère, B. Scheid, The creation and testing of a fully continuous tubular crystallization device suited for incorporation into flow chemistry setups, *J. Flow Chem.* **9** (2019) 237–249. https://doi.org/10.1007/s41981-019-00042-z.

[113] E. Palmer, Lilly commits to continuous manufacturing with Ireland plant, (2016). https://www.fiercepharma.com/manufacturing/lilly-commits-to-continuous-manufacturing-ireland-plant.

[114] M.D. Johnson, S.A. May, J.R. Calvin, J. Remacle, J.R. Stout, W.D. Diseroad, N. Zaborenko, B.D. Haeberle, W.-M. Sun, M.T. Miller, J. Brennan, Development and Scale-Up of a Continuous, High-Pressure, Asymmetric Hydrogenation Reaction, Workup, and Isolation, *Org. Process Res. Dev.* **16** (2012) 1017–1038. https://doi.org/10.1021/op200362h.

[115] J. Chen, B. Sarma, J.M.B. Evans, A.S. Myerson, Pharmaceutical Crystallization, *Cryst. Growth Des.* **11** (2011) 887–895. https://doi.org/10.1021/cg101556s.

[116] T. Wang, H. Lu, J. Wang, Y. Xiao, Y. Zhou, Y. Bao, H. Hao, Recent progress of continuous crystallization, *J. Ind. Eng. Chem.* **54** (2017) 14–29. https://doi.org/10.1016/j.jiec.2017.06.009.

[117] B. Wood, K.P. Girard, C.S. Polster, D.M. Croker, Progress to Date in the Design and Operation of Continuous Crystallization Processes for Pharmaceutical Applications, *Org. Process Res. Dev.* **23** (2019) 122–144. https://doi.org/10.1021/acs.oprd.8b00319.

[118] M. Jiang, R.D. Braatz, Designs of continuous-flow pharmaceutical crystallizers:

developments and practice, *CrystEngComm.* **21** (2019) 3534–3551. https://doi.org/10.1039/C8CE00042E.

[119] Y. Ma, S. Wu, E.G.J. Macaringue, T. Zhang, J. Gong, J. Wang, Recent Progress in Continuous Crystallization of Pharmaceutical Products: Precise Preparation and Control, *Org. Process Res. Dev.* (2020) acs.oprd.9b00362. https://doi.org/10.1021/acs.oprd.9b00362.

[120] D. Zhang, S. Xu, S. Du, J. Wang, J. Gong, Progress of Pharmaceutical Continuous Crystallization, *Engineering.* **3** (2017) 354–364. https://doi.org/10.1016/J.ENG.2017.03.023.

[121] S. Murugesan, P.K. Sharma, J.E. Tabora, Design of Filtration and Drying Operations, in: D.J.A. Ende (Ed.), Chem. Eng. Pharm. Ind., John Wiley & Sons, Inc., Hoboken, NJ, USA, 2010: pp. 315–345. https://doi.org/10.1002/9780470882221.ch17.

[122] S. Ottoboni, C.J. Price, C. Steven, E. Meehan, A. Barton, P. Firth, A. Mitchell, F. Tahir, Development of a Novel Continuous Filtration Unit for Pharmaceutical Process Development and Manufacturing, *J. Pharm. Sci.* **108** (2019) 372–381. https://doi.org/10.1016/j.xphs.2018.07.005.

[123] H. Zhang, J. Quon, A.J. Alvarez, J. Evans, A.S. Myerson, B. Trout, Development of Continuous Anti-Solvent/Cooling Crystallization Process using Cascaded Mixed Suspension, Mixed Product Removal Crystallizers, *Org. Process Res. Dev.* **16** (2012) 915–924. https://doi.org/10.1021/op2002886.

[124] B. Wierzbowska, N. Hutnik, K. Piotrowski, A. Matynia, Continuous Mass Crystallization of Vitamin C in <scp>l</scp> (+)-Ascorbic Acid−Ethanol−Water System: Size-Independent Growth Kinetic Model Approach, *Cryst. Growth Des.* **11** (2011) 1557–1565. https://doi.org/10.1021/cg101521k.

[125] J. Li, T.C. Lai, B.L. Trout, A.S. Myerson, Continuous Crystallization of Cyclosporine: Effect of Operating Conditions on Yield and Purity, *Cryst. Growth Des.* **17** (2017) 1000–1007. https://doi.org/10.1021/acs.cgd.6b01212.

[126] D. Acevedo, D.J. Jarmer, C.L. Burcham, C.S. Polster, Z.K. Nagy, A continuous multi-stage mixed-suspension mixed-product-removal crystallization system with fines dissolution, *Chem. Eng. Res. Des.* **135** (2018) 112–120. https://doi.org/10.1016/j.cherd.2018.05.029.

[127] Y. Yang, L. Song, T. Gao, Z.K. Nagy, Integrated Upstream and Downstream Application of Wet Milling with Continuous Mixed Suspension Mixed Product Removal Crystallization, *Cryst. Growth Des.* **15** (2015) 5879–5885. https://doi.org/10.1021/acs.cgd.5b01290.

[128] G. Hou, G. Power, M. Barrett, B. Glennon, G. Morris, Y. Zhao, Development and Characterization of a Single Stage Mixed-Suspension, Mixed-Product-Removal Crystallization Process with a Novel Transfer Unit, *Cryst. Growth Des.* **14** (2014) 1782–1793. https://doi.org/10.1021/cg401904a.

[129] Y. Cui, M. O'Mahony, J.J. Jaramillo, T. Stelzer, A.S. Myerson, Custom-Built Miniature Continuous Crystallization System with Pressure-Driven Suspension Transfer, *Org. Process Res. Dev.* **20** (2016) 1276–1282. https://doi.org/10.1021/acs.oprd.6b00113.

[130] J.L. Quon, H. Zhang, A. Alvarez, J. Evans, A.S. Myerson, B.L. Trout, Continuous

Crystallization of Aliskiren Hemifumarate, *Cryst. Growth Des.* **12** (2012) 3036–3044. https://doi.org/10.1021/cg300253a.

[131] A.J. Alvarez, A.S. Myerson, Continuous Plug Flow Crystallization of Pharmaceutical Compounds, *Cryst. Growth Des.* **10** (2010) 2219–2228. https://doi.org/10.1021/cg901496s.

[132] A. Majumder, Z.K. Nagy, Fines removal in a continuous plug flow crystallizer by optimal spatial temperature profiles with controlled dissolution, *AIChE J.* **59** (2013) 4582–4594. https://doi.org/10.1002/aic.14196.

[133] M. Furuta, K. Mukai, D. Cork, K. Mae, Continuous crystallization using a sonicated tubular system for controlling particle size in an API manufacturing process, *Chem. Eng. Process. Process Intensif.* **102** (2016) 210–218. https://doi.org/10.1016/j.cep.2016.02.002.

[134] R.J.P. Eder, E.K. Schmitt, J. Grill, S. Radl, H. Gruber-Woelfler, J.G. Khinast, Seed loading effects on the mean crystal size of acetylsalicylic acid in a continuous-flow crystallization device, *Cryst. Res. Technol.* **46** (2011) 227–237. https://doi.org/10.1002/crat.201000634.

[135] R.J.P. Eder, S. Radl, E. Schmitt, S. Innerhofer, M. Maier, H. Gruber-Woelfler, J.G. Khinast, Continuously seeded, continuously operated tubular crystallizer for the production of active pharmaceutical ingredients, *Cryst. Growth Des.* **10** (2010) 2247–2257. https://doi.org/10.1021/cg9015788.

[136] T. McGlone, N.E.B. Briggs, C.A. Clark, C.J. Brown, J. Sefcik, A.J. Florence, Oscillatory Flow Reactors (OFRs) for Continuous Manufacturing and Crystallization, *Org. Process Res. Dev.* **19** (2015) 1186–1202. https://doi.org/10.1021/acs.oprd.5b00225.

[137] R. Pena, J.A. Oliva, C.L. Burcham, D.J. Jarmer, Z.K. Nagy, Process Intensification through Continuous Spherical Crystallization Using an Oscillatory Flow Baffled Crystallizer, *Cryst. Growth Des.* **17** (2017) 4776–4784. https://doi.org/10.1021/acs.cgd.7b00731.

[138] Y.C. Liu, D. Dunn, M. Lipari, A. Barton, P. Firth, J. Speed, D. Wood, Z.K. Nagy, A comparative study of continuous operation between a dynamic baffle crystallizer and a stirred tank crystallizer, *Chem. Eng. J.* **367** (2019) 278–294. https://doi.org/10.1016/j.cej.2019.02.129.

[139] H. McLachlan, X.-W. Ni, On the effect of added impurity on crystal purity of urea in an oscillatory baffled crystallizer and a stirred tank crystallizer, *J. Cryst. Growth.* **442** (2016) 81–88. https://doi.org/10.1016/j.jcrysgro.2016.03.001.

[140] X. Ni, A. Liao, Effects of mixing, seeding, material of baffles and final temperature on solution crystallization of l-glutamic acid in an oscillatory baffled crystallizer, *Chem. Eng. J.* **156** (2010) 226–233. https://doi.org/10.1016/j.cej.2009.10.045.

[141] T. Reynolds, M. Boychyn, T. Sanderson, M. Bulmer, J. More, M. Hoare, Scale-down of continuous filtration for rapid bioprocess design: Recovery and dewatering of protein precipitate suspensions, *Biotechnol. Bioeng.* **83** (2003) 454–464. https://doi.org/10.1002/bit.10687.

[142] G. Foley, A review of factors affecting filter cake properties in dead-end microfiltration of microbial suspensions, *J. Memb. Sci.* **274** (2006) 38–46.

https://doi.org/10.1016/j.memsci.2005.12.008.

[143] M.D.L. de Castro, F. Priego-Capote, Continuous filtration as a separation technique, *Trends Anal. Chem.* **27** (2008) 101–107. https://doi.org/10.1016/j.trac.2007.11.006.

[144] A. Arunkumar, N. Singh, M. Peck, M.C. Borys, Z.J. Li, Investigation of single-pass tangential flow filtration (SPTFF) as an inline concentration step for cell culture harvest, *J. Memb. Sci.* **524** (2017) 20–32. https://doi.org/10.1016/j.memsci.2016.11.007.

[145] L. Song, M. Elimelech, Theory of concentration polarization in crossflow filtration, *J. Chem. Soc. Faraday Trans.* **91** (1995) 3389. https://doi.org/10.1039/ft9959103389.

[146] J. Gursch, R. Hohl, G. Toschkoff, D. Dujmovic, J. Brozio, M. Krumme, N. Rasenack, J. Khinast, Continuous Processing of Active Pharmaceutical Ingredients Suspensions via Dynamic Cross-Flow Filtration, *J. Pharm. Sci.* **104** (2015) 3481–3489. https://doi.org/10.1002/jps.24562.

[147] J. Gursch, R. Hohl, D. Dujmovic, J. Brozio, M. Krumme, N. Rasenack, J. Khinast, Dynamic cross-flow filtration: enhanced continuous small-scale solid-liquid separation, *Drug Dev. Ind. Pharm.* **42** (2016) 977–984. https://doi.org/10.3109/03639045.2015.1100200.

[148] J. Kossik, Operation of a Disposable Rotary Drum Filter, in: AIChE Annu. Meet. Pharm. Biotechnol. Pilot Plants, 2001.

[149] J. Kossik, J.F. Delys, Disposable rotary drum filter, US6336561B1, 2002.

[150] K.W.-S. Wong, Design of a Small-Scale Continuous Linear Motion Pharmaceutical Filtration Module, (2010). https://dspace.mit.edu/handle/1721.1/60210#files-area.

[151] D.J.A. Ende, D. Pfisterer, K. Girard, D.O. Blackwood, E. Plocharczyk, Development of a Continuous Filter-Drier for Lab to Kilo-Lab Scale, in: AIChE, 2011. https://www.researchgate.net/publication/267361532_Development_of_a_%0AContinuous_Filter-Drier_for_Lab_to_Kilo-Lab_Scale.

[152] Indexing belt filter (BF), (2015). https://www.bhs-sonthofen.de/en/products/filtration-technology/indexing-belt-filter.html.

[153] L. Hohmann, L. Löbnitz, C. Menke, B. Santhirakumaran, P. Stier, F. Stenger, F. Dufour, G. Wiese, S. zur zur Horst-Meyer, B. Kusserow, W. Zang, H. Nirschl, N. Kockmann, Continuous Downstream Processing of Amino Acids in a Modular Miniplant, *Chem. Eng. Technol.* **41** (2018) 1152–1164. https://doi.org/10.1002/ceat.201700657.

[154] S.Y. Wong, J. Chen, L.E. Forte, A.S. Myerson, Compact Crystallization, Filtration, and Drying for the Production of Active Pharmaceutical Ingredients, *Org. Process Res. Dev.* **17** (2013) 684–692. https://doi.org/10.1021/op400011s.

[155] S.Y. Wong, A.P. Tatusko, B.L. Trout, A.S. Myerson, Development of Continuous Crystallization Processes Using a Single-Stage Mixed-Suspension, Mixed-Product Removal Crystallizer with Recycle, *Cryst. Growth Des.* **12** (2012) 5701–5707. https://doi.org/10.1021/cg301221q.

[156] S. Ferguson, F. Ortner, J. Quon, L. Peeva, A. Livingston, B.L. Trout, A.S. Myerson, Use of Continuous MSMPR Crystallization with Integrated Nanofiltration Membrane Recycle for Enhanced Yield and Purity in API Crystallization, *Cryst. Growth Des.* **14** (2014) 617–627. https://doi.org/10.1021/cg401491y.

[157] D. Acevedo, R. Peña, Y. Yang, A. Barton, P. Firth, Z.K. Nagy, Evaluation of mixed suspension mixed product removal crystallization processes coupled with a continuous filtration system, *Chem. Eng. Process. Process Intensif.* **108** (2016) 212–219. https://doi.org/10.1016/j.cep.2016.08.006.

[158] G. Capellades, C. Neurohr, M. Azad, D. Brancazio, K. Rapp, G. Hammersmith, A.S. Myerson, A Compact Device for the Integrated Filtration, Drying, and Mechanical Processing of Active Pharmaceutical Ingredients, *J. Pharm. Sci.* **109** (2020) 1365–1372. https://doi.org/10.1016/j.xphs.2019.12.011.

[159] L. Pernenkil, C.L. Cooney, A review on the continuous blending of powders, *Chem. Eng. Sci.* **61** (2006) 720–742. https://doi.org/10.1016/j.ces.2005.06.016.

[160] H. Berthiaux, K. Marikh, C. Gatumel, Continuous mixing of powder mixtures with pharmaceutical process constraints, *Chem. Eng. Process. Process Intensif.* **47** (2008) 2315–2322. https://doi.org/10.1016/j.cep.2008.01.009.

[161] J.C. Williams, Continuous mixing of solids. A review, *Powder Technol.* **15** (1976) 237–243. https://doi.org/10.1016/0032-5910(76)80052-6.

[162] J.G. Osorio, A.U. Vanarase, R.J. Romañach, F.J. Muzzio, Continuous Powder Mixing, in: Pharm. Blending Mix., John Wiley & Sons, Ltd, Chichester, UK, 2015: pp. 101–127. https://doi.org/10.1002/9781118682692.ch6.

[163] M. Ierapetritou, F. Muzzio, G. Reklaitis, Perspectives on the continuous manufacturing of powder-based pharmaceutical processes, *AIChE J.* **62** (2016) 1846–1862. https://doi.org/10.1002/aic.15210.

[164] A.U. Vanarase, F.J. Muzzio, Effect of operating conditions and design parameters in a continuous powder mixer, *Powder Technol.* **208** (2011) 26–36. https://doi.org/10.1016/j.powtec.2010.11.038.

[165] J.G. Osorio, F.J. Muzzio, Effects of processing parameters and blade patterns on continuous pharmaceutical powder mixing, *Chem. Eng. Process. - Process Intensif.* **109** (2016) 59–67. https://doi.org/10.1016/j.cep.2016.07.012.

[166] C.L. Burcham, A.J. Florence, M.D. Johnson, Continuous Manufacturing in Pharmaceutical Process Development and Manufacturing, *Annu. Rev. Chem. Biomol. Eng.* **9** (2018) 253–281. https://doi.org/10.1146/annurev-chembioeng-060817-084355.

[167] M.A. Järvinen, J. Paaso, M. Paavola, K. Leiviskä, M. Juuti, F. Muzzio, K. Järvinen, Continuous direct tablet compression: effects of impeller rotation rate, total feed rate and drug content on the tablet properties and drug release, *Drug Dev. Ind. Pharm.* **39** (2013) 1802–1808. https://doi.org/10.3109/03639045.2012.738681.

[168] B. Wagner, T. Brinz, S. Otterbach, J. Khinast, Rapid automated process development of a continuous capsule-filling process, *Int. J. Pharm.* **546** (2018) 154–165. https://doi.org/10.1016/j.ijpharm.2018.05.009.

[169] S. Chattoraj, C.C. Sun, Crystal and Particle Engineering Strategies for Improving Powder Compression and Flow Properties to Enable Continuous Tablet Manufacturing by Direct Compression, *J. Pharm. Sci.* **107** (2018) 968–974. https://doi.org/10.1016/j.xphs.2017.11.023.

[170] T. Ervasti, S.-P. Simonaho, J. Ketolainen, P. Forsberg, M. Fransson, H. Wikström, S. Folestad, S. Lakio, P. Tajarobi, S. Abrahmsén-Alami, Continuous manufacturing of

extended release tablets via powder mixing and direct compression, *Int. J. Pharm.* **495** (2015) 290–301. https://doi.org/10.1016/j.ijpharm.2015.08.077.

[171] S.-P. Simonaho, J. Ketolainen, T. Ervasti, M. Toiviainen, O. Korhonen, Continuous manufacturing of tablets with PROMIS-line — Introduction and case studies from continuous feeding, blending and tableting, *Eur. J. Pharm. Sci.* **90** (2016) 38–46. https://doi.org/10.1016/j.ejps.2016.02.006.

[172] B. Van Snick, J. Holman, C. Cunningham, A. Kumar, J. Vercruysse, T. De Beer, J.P. Remon, C. Vervaet, Continuous direct compression as manufacturing platform for sustained release tablets, *Int. J. Pharm.* **519** (2017) 390–407. https://doi.org/10.1016/j.ijpharm.2017.01.010.

[173] M.A. Azad, J.G. Osorio, D. Brancazio, G. Hammersmith, D.M. Klee, K. Rapp, A. Myerson, A compact, portable, re-configurable, and automated system for on-demand pharmaceutical tablet manufacturing, *Int. J. Pharm.* **539** (2018) 157–164. https://doi.org/10.1016/j.ijpharm.2018.01.027.

[174] M.A. Azad, J.G. Osorio, A. Wang, D.M. Klee, M.E. Eccles, E. Grela, R. Sloan, G. Hammersmith, K. Rapp, D. Brancazio, A.S. Myerson, On-Demand Manufacturing of Direct Compressible Tablets: Can Formulation Be Simplified?, *Pharm. Res.* **36** (2019) 167. https://doi.org/10.1007/s11095-019-2716-2.

[175] M. Asachi, E. Nourafkan, A. Hassanpour, A review of current techniques for the evaluation of powder mixing, *Adv. Powder Technol.* **29** (2018) 1525–1549. https://doi.org/10.1016/j.apt.2018.03.031.

[176] B. Nagy, A. Farkas, E. Borbás, P. Vass, Z.K. Nagy, G. Marosi, Raman Spectroscopy for Process Analytical Technologies of Pharmaceutical Secondary Manufacturing, *AAPS PharmSciTech.* **20** (2019) 1. https://doi.org/10.1208/s12249-018-1201-2.

[177] A.L. Bowler, S. Bakalis, N.J. Watson, A review of in-line and on-line measurement techniques to monitor industrial mixing processes, *Chem. Eng. Res. Des.* **153** (2020) 463–495. https://doi.org/10.1016/j.cherd.2019.10.045.

[178] A. Crouter, L. Briens, Methods to Assess Mixing of Pharmaceutical Powders, *AAPS PharmSciTech.* **20** (2019) 84. https://doi.org/10.1208/s12249-018-1286-7.

[179] B. Nagy, A. Farkas, M. Gyürkés, S. Komaromy-Hiller, B. Démuth, B. Szabó, D. Nusser, E. Borbás, G. Marosi, Z.K. Nagy, In-line Raman spectroscopic monitoring and feedback control of a continuous twin-screw pharmaceutical powder blending and tableting process, *Int. J. Pharm.* **530** (2017) 21–29. https://doi.org/10.1016/j.ijpharm.2017.07.041.

[180] J. Palmer, G.K. Reynolds, F. Tahir, I.K. Yadav, E. Meehan, J. Holman, G. Bajwa, Mapping key process parameters to the performance of a continuous dry powder blender in a continuous direct compression system, *Powder Technol.* **362** (2020) 659–670. https://doi.org/10.1016/j.powtec.2019.12.028.

[181] M. Fonteyne, J. Vercruysse, F. De Leersnyder, B. Van Snick, C. Vervaet, J.P. Remon, T. De Beer, Process Analytical Technology for continuous manufacturing of solid-dosage forms, *TrAC - Trends Anal. Chem.* **67** (2015) 159–166. https://doi.org/10.1016/j.trac.2015.01.011.

[182] M. Fonteyne, J. Vercruysse, F. De Leersnyder, R. Besseling, A. Gerich, W. Oostra, J.P. Remon, C. Vervaet, T. De Beer, Blend uniformity evaluation during continuous mixing

in a twin screw granulator by in-line NIR using a moving F-test, *Anal. Chim. Acta*. **935** (2016) 213–223. https://doi.org/10.1016/j.aca.2016.07.020.

[183] A.U. Vanarase, M. Alcalà, J.I. Jerez Rozo, F.J. Muzzio, R.J. Romañach, Real-time monitoring of drug concentration in a continuous powder mixing process using NIR spectroscopy, *Chem. Eng. Sci.* **65** (2010) 5728–5733. https://doi.org/10.1016/j.ces.2010.01.036.

[184] N.O. Sierra-Vega, A. Román-Ospino, J. Scicolone, F.J. Muzzio, R.J. Romañach, R. Méndez, Assessment of blend uniformity in a continuous tablet manufacturing process, *Int. J. Pharm.* **560** (2019) 322–333. https://doi.org/10.1016/j.ijpharm.2019.01.073.

[185] B. Van Snick, J. Holman, V. Vanhoorne, A. Kumar, T. De Beer, J.P. Remon, C. Vervaet, Development of a continuous direct compression platform for low-dose drug products, *Int. J. Pharm.* **529** (2017) 329–346. https://doi.org/10.1016/j.ijpharm.2017.07.003.

[186] W. Grymonpré, B. Blahova Prudilova, V. Vanhoorne, B. Van Snick, F. Detobel, J.P. Remon, T. De Beer, C. Vervaet, Downscaling of the tableting process: Feasibility of miniaturized forced feeders on a high-speed rotary tablet press, *Int. J. Pharm.* **550** (2018) 477–485. https://doi.org/10.1016/j.ijpharm.2018.09.006.

[187] K. Matsunami, T. Nagato, K. Hasegawa, H. Sugiyama, A large-scale experimental comparison of batch and continuous technologies in pharmaceutical tablet manufacturing using ethenzamide, *Int. J. Pharm.* **559** (2019) 210–219. https://doi.org/10.1016/j.ijpharm.2019.01.028.

[188] K. Järvinen, W. Hoehe, M. Järvinen, S. Poutiainen, M. Juuti, S. Borchert, In-line monitoring of the drug content of powder mixtures and tablets by near-infrared spectroscopy during the continuous direct compression tableting process, *Eur. J. Pharm. Sci.* **48** (2013) 680–688. https://doi.org/10.1016/j.ejps.2012.12.032.

[189] Z.K. Nagy, A. Balogh, B. Vajna, A. Farkas, G. Patyi, Á. Kramarics, G. Marosi, Comparison of Electrospun and Extruded Soluplus®-Based Solid Dosage Forms of Improved Dissolution, *J. Pharm. Sci.* **101** (2012) 322–332. https://doi.org/10.1002/jps.22731.

[190] E. Szabo, B. Demuth, B. Nagy, K. Molnar, A. Farkas, B. Szabo, A. Balogh, E. Hirsch, B. Nagy, G. Marosi, Z.K. Nagy, Scaled-up preparation of drug-loaded electrospun polymer fibres and investigation of their continuous processing to tablet form, *Express Polym. Lett.* **12** (2018) 436–451. https://doi.org/10.3144/expresspolymlett.2018.37.

[191] D. Li, Y. Xia, Electrospinning of Nanofibers: Reinventing the Wheel?, *Adv. Mater.* **16** (2004) 1151–1170. https://doi.org/10.1002/adma.200400719.

[192] G. Marosi, E. Hirsch, K. Bocz, A. Toldy, B. Szolnoki, B. Bodzay, I. Csontos, A. Farkas, A. Balogh, B. Démuth, Z.K. Nagy, H. Pataki, Pharmaceutical and Macromolecular Technologies in the Spirit of Industry 4.0, *Period. Polytech. Chem. Eng.* **62** (2018) 457–466. https://doi.org/10.3311/PPch.12870.

[193] K. Molnar, C. Voniatis, D. Feher, A. Ferencz, L. Fonyad, L. Reiniger, M. Zrinyi, G. Weber, A. Jedlovszky-Hajdu, Biocompatibility study of poly(vinyl alcohol)-based electrospun scaffold for hernia repair, *Express Polym. Lett.* **12** (2018) 676–687. https://doi.org/10.3144/expresspolymlett.2018.58.

[194] J.-J. Li, Y.-Y. Yang, D.-G. Yu, Q. Du, X.-L. Yang, Fast dissolving drug delivery

membrane based on the ultra-thin shell of electrospun core-shell nanofibers, *Eur. J. Pharm. Sci.* **122** (2018) 195–204. https://doi.org/10.1016/j.ejps.2018.07.002.

[195] T. Potrč, S. Baumgartner, R. Roškar, O. Planinšek, Z. Lavrič, J. Kristl, P. Kocbek, Electrospun polycaprolactone nanofibers as a potential oromucosal delivery system for poorly water-soluble drugs, *Eur. J. Pharm. Sci.* **75** (2015) 101–113. https://doi.org/10.1016/j.ejps.2015.04.004.

[196] U. Paaver, I. Laidmäe, H.A. Santos, J. Yliruusi, J. Aruväli, K. Kogermann, J. Heinämäki, Development of a novel electrospun nanofibrous delivery system for poorly water-soluble β-sitosterol, *Asian J. Pharm. Sci.* **11** (2016) 500–506. https://doi.org/10.1016/j.ajps.2016.04.005.

[197] Q. Wang, D.-G. Yu, L.-L. Zhang, X.-K. Liu, Y.-C. Deng, M. Zhao, Electrospun hypromellose-based hydrophilic composites for rapid dissolution of poorly water-soluble drug, *Carbohydr. Polym.* **174** (2017) 617–625. https://doi.org/10.1016/j.carbpol.2017.06.075.

[198] G.-Z. Yang, J.-J. Li, D.-G. Yu, M.-F. He, J.-H. Yang, G.R. Williams, Nanosized sustained-release drug depots fabricated using modified tri-axial electrospinning, *Acta Biomater.* **53** (2017) 233–241. https://doi.org/10.1016/j.actbio.2017.01.069.

[199] A. Kovács, B. Démuth, A. Meskó, R. Zelkó, Preformulation Studies of Furosemide-Loaded Electrospun Nanofibrous Systems for Buccal Administration, *Polymers.* **9** (2017) 643. https://doi.org/10.3390/polym9120643.

[200] Z.K. Nagy, K. Nyul, I. Wagner, K. Molnar, G. Marosi, Electrospun water soluble polymer mat for ultrafast release of Donepezil HCl, *Express Polym. Lett.* **4** (2010) 763–772. https://doi.org/10.3144/expresspolymlett.2010.92.

[201] P. Vrbata, P. Berka, D. Stránská, P. Doležal, M. Musilová, L. Čižinská, Electrospun drug loaded membranes for sublingual administration of sumatriptan and naproxen, *Int. J. Pharm.* **457** (2013) 168–176. https://doi.org/10.1016/j.ijpharm.2013.08.085.

[202] Z.K. Nagy, A. Balogh, B. Démuth, H. Pataki, T. Vigh, B. Szabó, K. Molnár, B.T. Schmidt, P. Horák, G. Marosi, G. Verreck, I. Van Assche, M.E. Brewster, High speed electrospinning for scaled-up production of amorphous solid dispersion of itraconazole, *Int. J. Pharm.* **480** (2015) 137–142. https://doi.org/10.1016/j.ijpharm.2015.01.025.

[203] P. Vass, E. Szabó, A. Domokos, E. Hirsch, D. Galata, B. Farkas, B. Démuth, S.K. Andersen, T. Vigh, G. Verreck, G. Marosi, Z.K. Nagy, Scale-up of electrospinning technology: Applications in the pharmaceutical industry, *WIREs Nanomedicine and Nanobiotechnology.* **12** (2020). https://doi.org/10.1002/wnan.1611.

[204] B. Démuth, Z.K. Nagy, A. Balogh, T. Vigh, G. Marosi, G. Verreck, I. Van Assche, M.E. Brewster, Downstream processing of polymer-based amorphous solid dispersions to generate tablet formulations, *Int. J. Pharm.* **486** (2015) 268–286. https://doi.org/10.1016/j.ijpharm.2015.03.053.

[205] E. Szabó, B. Démuth, D.L. Galata, P. Vass, E. Hirsch, I. Csontos, G. Marosi, Z.K. Nagy, Continuous Formulation Approaches of Amorphous Solid Dispersions: Significance of Powder Flow Properties and Feeding Performance, *Pharmaceutics.* **11** (2019) 654. https://doi.org/10.3390/pharmaceutics11120654.

[206] H. Zhang, R. Lakerveld, P.L. Heider, M. Tao, M. Su, C.J. Testa, A.N. Dantonio, P.I.

Barton, R.D. Braatz, B.L. Trout, A.S. Myerson, K.F. Jensen, J.M.B. Evans, Application of continuous crystallization in an integrated continuous pharmaceutical pilot plant, *Cryst. Growth Des.* **14** (2014) 2148–2157. https://doi.org/10.1021/cg401571h.

[207] J.C.M. Monbaliu, T. Stelzer, E. Revalor, N. Weeranoppanant, K.F. Jensen, A.S. Myerson, Compact and Integrated Approach for Advanced End-to-End Production, Purification, and Aqueous Formulation of Lidocaine Hydrochloride, *Org. Process Res. Dev.* **20** (2016) 1347–1353. https://doi.org/10.1021/acs.oprd.6b00165.

[208] C. Hu, C.J. Testa, W. Wu, K. Shvedova, D.E. Shen, R. Sayin, B.S. Halkude, F. Casati, P. Hermant, A. Ramnath, S.C. Born, B. Takizawa, T.F. O'Connor, X. Yang, S. Ramanujam, S. Mascia, An automated modular assembly line for drugs in a miniaturized plant, *Chem. Commun.* **56** (2020) 1026–1029. https://doi.org/10.1039/c9cc06945c.

[209] G.D. Hadiwinoto, P.C.L. Kwok, H.H.Y. Tong, S.N. Wong, S.F. Chow, R. Lakerveld, Integrated Continuous Plug-Flow Crystallization and Spray Drying of Pharmaceuticals for Dry Powder Inhalation, *Ind. Eng. Chem. Res.* **58** (2019) 16843–16857. https://doi.org/10.1021/acs.iecr.9b01730.

[210] H. Dreser, Pharmakologisches über Aspirin (Acetylsalicylsäure), *Pflüger, Arch. Für Die Gesammte Physiol. Des Menschen Und Der Thiere.* **76** (1899) 306–318. https://doi.org/10.1007/BF01662127.

[211] H. Weiss, L. Aledort, IMPAIRED PLATELET/CONNECTIVE-TISSUE REACTION IN MAN AFTER ASPIRIN INGESTION, *Lancet.* **290** (1967) 495–497. https://doi.org/10.1016/S0140-6736(67)91658-3.

[212] G. Evans, M.A. Packham, E.E. Nishizawa, J.F. Mustard, E.A. Murphy, THE EFFECT OF ACETYLSALICYLIC ACID ON PLATELET FUNCTION, *J. Exp. Med.* **128** (1968) 877–894. https://doi.org/10.1084/jem.128.5.877.

[213] K. Schrör, Acetylsalicylic acid, Wiley-VCH Verlag, 2016.

[214] T. Loftsson, S.B. Vogensen, C. Desbos, P. Jansook, Carvedilol: Solubilization and Cyclodextrin Complexation: A Technical Note, *AAPS PharmSciTech.* **9** (2008) 425–430. https://doi.org/10.1208/s12249-008-9055-7.

[215] Y.C. Liu, A. Domokos, S. Coleman, P. Firth, Z.K. Nagy, Development of Continuous Filtration in a Novel Continuous Filtration Carousel Integrated with Continuous Crystallization, *Org. Process Res. Dev.* **23** (2019) 2655–2665. https://doi.org/10.1021/acs.oprd.9b00342.

[216] GEA, ConsiGma™ Continuous Direct Compression, (2015). ConsiGma™ Continuous Direct Compression.

[217] V. Pauli, Y. Roggo, L. Pellegatti, N.Q. Nguyen Trung, F. Elbaz, S. Ensslin, P. Kleinebudde, M. Krumme, Process analytical technology for continuous manufacturing tableting processing: A case study, *J. Pharm. Biomed. Anal.* **162** (2019) 101–111. https://doi.org/10.1016/j.jpba.2018.09.016.

[218] J. Fogel, P. Epstein, P. Chen, Simultaneous high-performance liquid chromatography assay of acetylsalicylic acid and salicylic acid in film-coated aspirin tablets, *J. Chromatogr.* **317** (1984) 507–511. https://doi.org/10.1016/S0021-9673(01)91690-5.

[219] A. Balogh, B. Farkas, K. Faragó, A. Farkas, I. Wagner, I. Van assche, G. Verreck, Z.K. Nagy, G. Marosi, Melt-Blown and Electrospun Drug-Loaded Polymer Fiber Mats for

Dissolution Enhancement: A Comparative Study, *J. Pharm. Sci.* **104** (2015) 1767–1776. https://doi.org/10.1002/jps.24399.

[220] V. Garsuch, J. Breitkreutz, Comparative investigations on different polymers for the preparation of fast-dissolving oral films, *J. Pharm. Pharmacol.* **62** (2010) 539–545. https://doi.org/10.1211/jpp.62.04.0018.

[221] M. Irfan, S. Rabel, Q. Bukhtar, M.I. Qadir, F. Jabeen, A. Khan, Orally disintegrating films: A modern expansion in drug delivery system, *Saudi Pharm. J.* **24** (2016) 537–546. https://doi.org/10.1016/j.jsps.2015.02.024.

[222] B.M. Yapo, B. Wathelet, M. Paquot, Comparison of alcohol precipitation and membrane filtration effects on sugar beet pulp pectin chemical features and surface properties, *Food Hydrocoll.* **21** (2007) 245–255. https://doi.org/10.1016/j.foodhyd.2006.03.016.

[223] A.L.. Pearson, W.J. Roush, Handbook of Reagents for Organic Synthesis: Acetylating Agents and Protecting Groups, 1999.

[224] V. Prosapio, I. De Marco, E. Reverchon, PVP/corticosteroid microspheres produced by supercritical antisolvent coprecipitation, *Chem. Eng. J.* **292** (2016) 264–275. https://doi.org/10.1016/j.cej.2016.02.041.

[225] L. Wang, M.-W. Chang, Z. Ahmad, H. Zheng, J.-S. Li, Mass and controlled fabrication of aligned PVP fibers for matrix type antibiotic drug delivery systems, *Chem. Eng. J.* **307** (2017) 661–669. https://doi.org/10.1016/j.cej.2016.08.135.

[226] A. Balogh, R. Cselkó, B. Démuth, G. Verreck, J. Mensch, G. Marosi, Z.K. Nagy, Alternating current electrospinning for preparation of fibrous drug delivery systems, *Int. J. Pharm.* **495** (2015) 75–80. https://doi.org/10.1016/j.ijpharm.2015.08.069.

[227] O. Karatum, M.A. Deshusses, A comparative study of dilute VOCs treatment in a non-thermal plasma reactor, *Chem. Eng. J.* **294** (2016) 308–315. https://doi.org/10.1016/j.cej.2016.03.002.

[228] European Medicines Agency, ICH guideline Q3C (R5) on impurities: Guideline for Residual Solvents, 2019.

[229] A. Farkas, B. Vajna, P.L. Sóti, Z.K. Nagy, H. Pataki, F. Van der Gucht, G. Marosi, Comparison of multivariate linear regression methods in micro-Raman spectrometric quantitative characterization, *J. Raman Spectrosc.* **46** (2015) 566–576. https://doi.org/10.1002/jrs.4672.

[230] B. Démuth, A. Farkas, B. Szabó, A. Balogh, B. Nagy, E. Vágó, T. Vigh, A.P. Tinke, Z. Kazsu, Demeter, J. Bertels, J. Mensch, A. Van Dijck, G. Verreck, I. Van Assche, G. Marosi, Z.K. Nagy, Development and tableting of directly compressible powder from electrospun nanofibrous amorphous solid dispersion, *Adv. Powder Technol.* **28** (2017) 1554–1563. https://doi.org/10.1016/j.apt.2017.03.026.

[231] E. Borbás, A. Balogh, K. Bocz, J. Müller, É. Kiserdei, T. Vigh, B. Sinkó, A. Marosi, A. Halász, Z. Dohányos, L. Szente, G.T. Balogh, Z.K. Nagy, In vitro dissolution–permeation evaluation of an electrospun cyclodextrin-based formulation of aripiprazole using μFlux^{TM}, *Int. J. Pharm.* **491** (2015) 180–189. https://doi.org/10.1016/j.ijpharm.2015.06.019.

[232] A. Balogh, T. Horváthová, Z. Fülöp, T. Loftsson, A.H. Harasztos, G. Marosi, Z.K. Nagy, Electroblowing and electrospinning of fibrous diclofenac sodium-cyclodextrin complex-

based reconstitution injection, *J. Drug Deliv. Sci. Technol.* **26** (2015) 28–34. https://doi.org/10.1016/j.jddst.2015.02.003.

[233] D.J. van Drooge, W.L.J. Hinrichs, M.R. Visser, H.W. Frijlink, Characterization of the molecular distribution of drugs in glassy solid dispersions at the nano-meter scale, using differential scanning calorimetry and gravimetric water vapour sorption techniques, *Int. J. Pharm.* **310** (2006) 220–229. https://doi.org/10.1016/j.ijpharm.2005.12.007.

[234] Q. Xiao, L. Lim, Q. Tong, Properties of pullulan-based blend films as affected by alginate content and relative humidity, *Carbohydr. Polym.* **87** (2012) 227–234. https://doi.org/10.1016/j.carbpol.2011.07.040.

[235] J.A. de Lima, T.C. Paines, M.H. Motta, W.B. Weber, S.S. dos Santos, L. Cruz, C. de B. da Silva, Novel Pemulen/Pullulan blended hydrogel containing clotrimazole-loaded cationic nanocapsules: Evaluation of mucoadhesion and vaginal permeation, *Mater. Sci. Eng. C.* **79** (2017) 886–893. https://doi.org/10.1016/j.msec.2017.05.030.

[236] M.M.D.C. Vila, E.R. Tardelli, M. V Chaud, M. Tubino, V.M. Balcão, Development of a buccal mucoadhesive film for fast dissolution: mathematical rationale, production and physicochemical characterization, *Drug Deliv.* **21** (2014) 530–539. https://doi.org/10.3109/10717544.2013.851301.

[237] D. Kumar, N. Saini, V. Pandit, S. Ali, An Insight To Pullulan: A Biopolymer in Pharmaceutical Approaches, *Int. J. Basic Appl. Sci.* **1** (2012) 202–219. https://doi.org/10.14419/ijbas.v1i3.101.

[238] A. Low, S.L. Kok, Y. Khong, S.Y. Chan, R. Gokhale, Pharmaceutics, Drug Delivery and Pharmaceutical Technology: A New Test Unit for Disintegration End-Point Determination of Orodispersible Films, *J. Pharm. Sci.* **104** (2015) 3893–3903. https://doi.org/10.1002/jps.24609.

[239] Food and Drug Administration, Guidance for Industry Orally Disintegrating Tablets, *FDA Off. Doc.* (2008).

[240] K. Tacsi, H. Pataki, A. Domokos, B. Nagy, I. Csontos, I. Markovits, F. Farkas, Z.K. Nagy, G. Marosi, Direct Processing of a Flow Reaction Mixture Using Continuous Mixed Suspension Mixed Product Removal Crystallizer, *Cryst. Growth Des.* **20** (2020) 4433–4442. https://doi.org/10.1021/acs.cgd.0c00252.

[241] J. Sripui, C. Pradistsuwana, W.L. Kerr, P. Pradipasena, Effects of particle size and its distribution on specific cake resistance during rice wine microfiltration, *J. Food Eng.* **105** (2011) 73–78. https://doi.org/10.1016/j.jfoodeng.2011.01.033.

[242] D. Bourcier, J.P. Féraud, D. Colson, K. Mandrick, D. Ode, E. Brackx, F. Puel, Influence of particle size and shape properties on cake resistance and compressibility during pressure filtration, *Chem. Eng. Sci.* **144** (2016) 176–187. https://doi.org/10.1016/j.ces.2016.01.023.

[243] The United States Pharmacopeial Convention, ⟨905⟩ Uniformity of Dosage Units, (2011).

NYILATKOZAT

Alulírott Domokos András kijelentem, hogy ezt a doktori értekezést magam készítettem és abban csak a megadott forrásokat használtam fel. Minden olyan részt, amelyet szó szerint, vagy azonos tartalomban, de átfogalmazva más forrásból átvettem, egyértelműen, a forrás megadásával megjelöltem.

Budapest,……………………….………

……………………………